The interactions between apoptotic cells and macrophages within the murine omentum and peritoneal cavity

Simon James William Watson

B. Clin. Sci (Hons), MB, ChB (Commendation), MRCP (UK)

Thesis submitted for the degree of Doctor of Philosophy (PhD)

The University of Edinburgh

2007

Declaration

This work contains no material which has been accepted for the award of any other degree or diploma in any university or tertiary institution and, to the best of my knowledge and belief, contains no material previously published or written by another person, except where due reference has been made in the text.

10.12.2007.

Simon James William Watson Dated

Acknowledgments

Dr. Jeremy Hughes, my principal supervisor, whose intellect, breadth and depth of knowledge, patience and above all else, tireless enthusiasm was a constant source inspiration. Jeremy was an outstanding supervisor and a fantastic group leader.

Professor John Savill, my co-supervisor who inspired my interest in Nephrology and inflammation biology. Despite great responsibilities, John provided invaluable guidance during my PhD and I will always be grateful for his strong support throughout my career.

Dr. Jean-Francois Cailhier - my closest collaborator within the Hughes Group. J-F defies adequate description, possessing both a formidable intellect and an insatiable love of life. The time spent with J-F cemented a great friendship as well as, I hope, some great science.

Spike Clay - it's no exaggeration to say that without his unique talents, this project would not have succeeded. Always a pleasure to work with, no matter how unpleasant the work itself might appear!

The Hughes Group - Jeremy Hughes shaped a happy group of scientists motivated not only by personal achievement but the success of the group as a whole. They were Tiina Kipari, Kris Houlberg, Claire Taylor not forgetting J-F, Spike and Jeremy.

The Centre for Inflammation Research - I couldn't have wished for a better place to undertake a PhD. Those who helped me included Dr Adam Lacy-Hulbert, Dr Simone Brown, Dr David Kluth, Dr Andrew Devitt, Dr Lynda Stuart, Dr Jamie Gilmore, Dr Graham Thomas, Dr Carol-Anne Ogden, Shona McCall, Professor Ian Dransfield, Professor Chris Gregory and Professor Chris Haslett and all in the Phagocyte Lab.

The Dept of Renal Medicine, Royal Infirmary of Edinburgh for their support during and after my PhD. Finally, special thanks to Dr Geoffrey Bellingan of University College, London, whose seminal work in peritoneal macrophage emigration paved the way for this project.

Dedication

For Rachael.

Presentations

Keystone Symposium on Leukocyte Trafficking	2005	p[3]
American Society of Nephrologists	2004	o
Renal SpR Club	2004	o
European Renal Cell Study Group	2004	o
UK Renal Association	2004	p
Scottish Society for Experimental Medicine	2004	o
Academy of Medical Sciences Training Fellows Meeting	2004	p[2]
Innate Immunity in Transplantation	2004	o
UK Renal Association	2003	o[1]
American Society of Nephrologists	2003	p
Keystone Symposium (USA)	2003	p
UK Renal Association	2002	p
American Society of Nephrologists	2002	p

p=poster presentation, o=oral presentation

Prizes

[1] Eugene C Butcher Bursary, National Institutes of Health & Keystone Symposia, USA ($1000)
[2] Academy of Medical Sciences Training Fellows Day – Immunology Section prize (£250)
[3] Renal Assocation & Ortho-Biotech Travel Bursary (£700)

Publications

Directly arising from this thesis

The phagocytosis of apoptotic cells directs the emigration of peritoneal macrophages to lymph nodes SJW Watson, A Lacy-Hulbert, T Kipari JF Cailhier, S Clay, J Savill, G Bellingan, J Hughes – advanced stage pre-submission

Other work

Resident pleural macrophages are key orchestrators of neutrophil recruitment in pleural inflammation. Cailhier JF, Sawatzky DA, Kipari T, Houlberg K, Walbaum D, Watson S, Lang RA, Clay S, Kluth D, Savill J, Hughes J. Am J Respir Crit Care Med. 2006 Mar 1;173(5):540-7.

Apoptosis and glomerulonephritis. Watson S, Cailhier JF, Hughes J, Savill J. Curr Dir Autoimmun. 2006;9:188-204

Nitric oxide is an important mediator of renal tubular epithelial cell death in vitro and in murine experimental hydronephrosis Tiina Kipari, Jean-Francois Cailhier, David Ferenbach, Simon Watson, Kris Houlberg, David Walbaum, Spike Clay, John Savill and Jeremy Hughes American Journal of Pathology. 2006;169:388-399

Conditional macrophage ablation demonstrates that resident macrophages initiate acute peritoneal inflammation. Cailhier JF, Partolina M, Vuthoori S, Wu S, Ko K, Watson S, Savill J, Hughes J, Lang RA. J Immunol. 2005 Feb 15;174(4):2336-42.

Abstract

Inflammation is the response of higher multicellular animals to injury and noxious pathogens and is followed by the remodeling of damaged tissues to their previous healthy state. Many specialized cells are recruited to orchestrate the inflammatory response but these cells must be removed to allow the restoration of normal tissue structure and function. Some recruited cells leave inflamed tissues by emigration to lymph nodes whilst others, having served their purpose, die by 'apoptosis' or programmed cell death. Apoptotic 'corpses' are removed by phagocytosis, a process by which cells or similar particles, are captured, engulfed and ingested by other cells. In higher animals, 'professional' phagocytes, such as Macrophages (Mφ), are primarily responsible for the removal of apoptotic cells from inflamed tissues.

The removal of apoptotic cells prevents their inner contents from being released and inflicting secondary damage upon healthy cells. Furthermore, the act of phagocytosis of an apoptotic cell induces an anti-inflammatory, reparative phenotype in Mφ. It has now become clear that human diseases can arise from, or be exacerbated by defective clearance of apoptotic cells by Mφ. The processes by which Mφ remove apoptotic cells is clearly of importance in our understanding of inflammatory disease.

I began this thesis by examining the rate at which Mφ phagocytosed apoptotic cells *in vivo* using the murine peritoneal cavity as a model system. I noted that the number of Mφ recovered from the peritoneal cavity fell dramatically as apoptotic cells were phagocytosed. This disappearance of Mφ was not merely a non-specific effect of manipulating the peritoneal cavity but was a consequence of the phagocytosis of apoptotic cells. The mechanism underlying this 'Macrophage Disappearance Reaction' (MDR) was investigated and two manipulations – the instillation of hyularonidase enzyme or unfractionated heparin – respectively increased or decreased the magnitude of the MDR without affecting the rate of apoptotic cell clearance.

I then turned my attention to the fate of the disappearing Mφ, focusing on the omentum, an organ within the peritoneal membrane highly adapted for the initiation of acute inflammatory reactions and innate immunity. A series of adoptive transfer experiments showed that, after phagocytosing apoptotic cells, intraperitoneal Mφ migrated to specialized coelomic-associated lymphoid tissue (CALT) called 'Milky Spots' within the omentum. Further experiments showed that some Mφ subsequently left the peritoneal cavity and migrated to parathymic lymph nodes, a known destination for inflammatory peritoneal Mφ during the resolution of peritonitis. I then returned to the starting point of this thesis, ie the rate of phagocytosis of apoptotic cells *in vivo*, and developed a powerful new *in vivo* phagocytosis assay using omental milky spots as the experimental model.

This thesis has contributed to a wider and deeper understanding of the clearance of apoptotic cells by Mφ and the fate of phagocytic peritoneal Mφ. The hitherto unrecognized role of the omentum in the clearance of peritoneal apoptotic cells and Mφ emigration should increase the level of general scientific interest in the omentum which I believe to be a true organ of innate immunity.

List of abbreviations

BCG	Bacillus Calmette-Guérin
BSA	Bovine serum albumin
C. elegans	Caenorhabditis elegans
CAD	Caspase-activated DNAse
CALT	Coelom-associated lymphoid tissue
CMFDA	5-chloromethylfluorescein diacetate
CSF	Colony stimulating factor
Cy5	Cyanin 5
DC	Dendritic cell
DED	Death effecter domain
DNA	Deoxyribonucleic acid
EDTA	Ethylenediamine tetraacetic acid
EGF	Epidermal growth factor
FADD	Fas-associated death domain
FITC	fluorescein isothocyanate
FSC	Forward scatter (in flow cytometry)
g	Gram
GFP	Green fluorescent protein
GM-CSF	Granulocyte-monocyte colony stimulating factor
ICAM	Immunglobulin-like adhesion molecule
ICAM-1	Inter-cellular adhesion molecule 1
IFN	Interferon

IL	Interleukin
IP	Intra-peritoneal
l	Litre
LFA-1	Lymphocyte function-associated antigen-1
LPS	Lipopolysaccharide
M	Mole
mAb	Monoclonal antibody
MCP-1	Monocyte chemotactic protein 1
MDR	Macrophage disappearance reaction
mg	Milligram
ml	Millilitre
mM	Millimole
Mφ	Macrophage
NTN	Nephrotoxin nephritis
OLO	Omental lymphoid organ
PBS	Phosphate buffered solution
PE	Phycoerythrin
PMN	Polymorphoneutrophil
PS	Phosphatidylserine
PSR	Phosphatidylserine receptor
RNA	Ribonucleic acid
siRNA	Small inhibitory RNA
SLE	Systemic lupus erythematosis
SRA	Scavenger receptor A

SSC	Side scatter (in flow cytometry)
TGF-β	Transforming growth factor β
TLR	Toll-like receptor
VLA	Very late antigen
μg	Microgram
μl	Microlitre
μM	Micromole

TABLE OF CONTENTS

TABLES

TABLE OF FIGURES

1 CHAPTER 1 INTRODUCTION

1.1 Inflammation

Inflammation is the response of tissues to injury, the classical injury being bacterial infection. There are four cardinal clinical signs of inflammation – reddening, heat, swelling and pain, often Latinised to *rubor, calor, tumor* and *dolor*. These clinical features reflect the typical physiological changes that occur during acute inflammation. An increased blood supply causes reddening and warmth of inflamed tissue. Local vessels also become permeable to leukocytes and plasma which enter the inflamed tissue causing swelling. Noxious chemicals and other molecules stimulate local nerve fibres, causing the sensation of pain.

In the early stages of inflammation vast numbers of blood borne neutrophils (PMNs) enter injured tissue. The vascular endothelium upregulates adhesion molecules – selectins immediately followed by integrins and immunoglobulin-like cell adhesion molecules (ICAMs) - which allow anchorage of PMNs to the endothelium, a process called *tethering*. Marginated PMNs then cross the endothelium and migrate following a chemokine gradient to the nidus of injury. In bacterial infections, PMNs phagocytose pathogens opsonised with complement or antibody. Phagocytosed bacteria are killed by exposure to intracellular granules containing bacteriocidal substances including proteases, myeloperoxidase, hydrolase enzymes, lysozymes and defensins. PMNs may also degranulate releasing their bacteriocidal contents into the injured tissue. Unfortunately, the contents of PMN granules may damage and kill bystander resident cells as well as bacteria. Whilst these bystander cells may be

replaced in time, the tissue's capacity for regeneration may be exceeded by a very large loss of resident cells. In such circumstances, cells may be replaced by acellular scar tissue with a consequent loss of tissue function. Therefore, successful resolution of inflammation demands that PMN activity is limited to that required for pathogen removal with minimal resident cell damage. PMNs do not emigrate from sites of inflammation so they must be deactivated and removed within inflamed tissues. This is effected by a form of programmed cell death called *apoptosis*.

1.2 Apoptosis

The word 'apoptosis' translates from ancient Greek as 'leaves falling from the tree'. Apoptosis was first described by Kerr et al in a seminal 1972 paper (Kerr et al., 1972). The authors' choice of name for their discovery reflected their belief that apoptosis was a physiologically and immunologically silent form of cell death. Over the last three decades, it has become apparent that apoptosis is involved in a wide variety of biological processes in multicellular organisms. During embryogenesis, organ development produces unwanted cells which are removed by apoptosis, the classical example being loss of interdigital web spaces during vertebrate limb development (Zakeri and Ahuja, 1994). Apoptosis is also involved in post-embryonic tissue remodeling, such as regression of the tadpole tail (Kerr et al., 1974) or deletion of autoreactive thymocytes during T cell maturation (Wyllie, 1980). Apoptosis is an important way of deleting irreparably damaged cells too. This is

especially important for the removal of cells which have sustained chromosomal DNA damage and are at risk of malignant transformation (Danilevicius, 1973).

Cells undergo a well-defined sequence of morphological changes during apoptosis (Kerr et al., 1972). The first stage involves the dissociation of the cell from its neighbours. Then specialised organelles become tightly packed together as the cytoplasmic volume decreases. Next come changes in the nucleus. Chromatin condenses to the peripheral region, the nucleolus disintegrates and finally fragments in a process called *karyorrhexis*. Lastly the cytoplasmic membrane loses its connections with the underlying cytoskeleton and apoptotic blebs are formed. These blebs may contain fragments of the nucleus or cell organelles and are potentially autoantigenic (Casciola-Rosen et al., 1994).

Apoptosis is executed by a specialised sequence of biochemical events. The molecular components of these pathways are pre-formed and present within all cells in an inactive state. This allows the swift execution of the apoptotic program following the addition of a death signal or the removal of a survival signal (or both). The key players in apoptosis are a family of enzymes known as the *caspases* (Miura et al., 1993). Caspases are so called as they are cysteine proteases that cleave proteins at sites following aspartate residues (hence c-asp-ase). One particular unusual feature of some caspases is their ability to activate each other when brought into close proximity – the so called 'induced-proximity' phenomenon. This adaptation aids the rapid activation of the apoptotic program following an

appropriate stimulus. Caspases show high evolutionary conservation and most family members play direct roles in apoptosis (Hengartner, 2000).

The initiating pathways can be broadly divided into a 'death receptor' and 'mitochondrial' pathways; both converge on a common execution pathway. The detailed biochemistry of these pathways is complex and further reading is recommended (Hengartner, 2000). What follows is a simplified version of the current biochemical model of apoptosis.

Figure 1. Schematic diagram of Fas-induced apoptosis

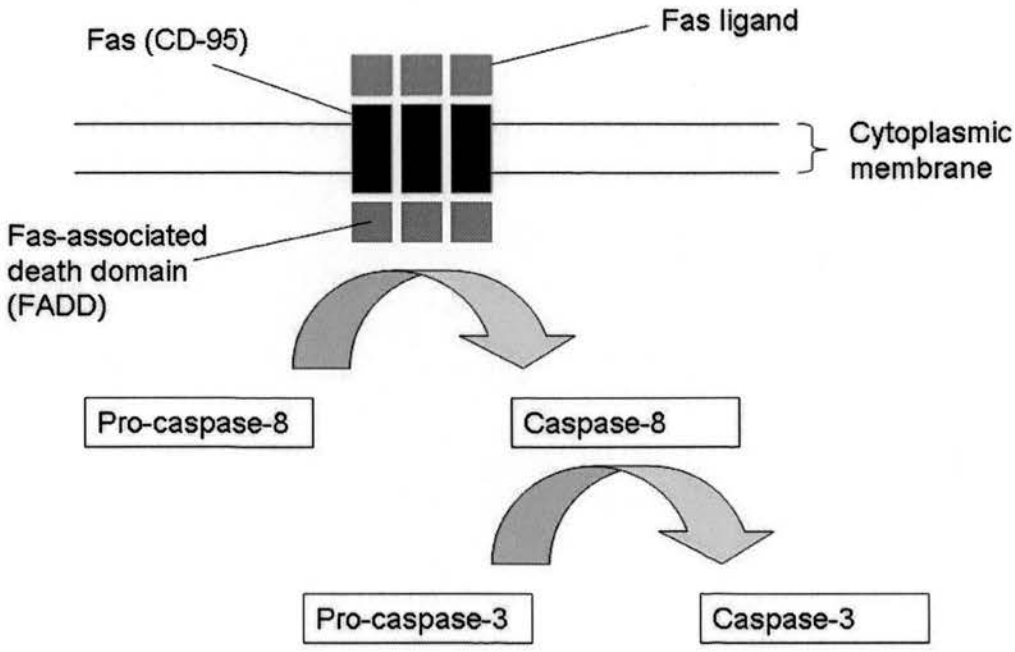

Schematic diagram of Fas-induced apoptosis. Extracellular fas-ligand binds to Fas (CD-95) which associates to form trimers. Fas associated death domains (FADD) are recruited to Fas trimers and they in turn recruit pro-caspase-8 molecules to the FADD death effecter domain (DED). Proximity activation of pro-caspase 8 results in the formation of caspase-8 hetero-tetramers which activate caspase-3, the trigger for the final pathway of apoptosis.

Fas-ligand binds to Fas and promotes the formation of Fas trimers. Fas trimers then recruit Fas associated death domains (FADD) which in turn recruit multiple pro-caspase-8 molecules to the FADD death effector domain (DED). The aggregation of procaspase-8 molecules causes induced proximity activation and the formation of caspase-8 hetero-tetramers. Caspase-8 hetero-tetramers induce the activation of caspase-3 which initiates execution of the final pathway of apoptosis.

The second major pathway which initiates apoptosis is the intracellular mitochondrial pathway. Mitochondria contain pro-apoptotic molecules that, whilst harmless within the mitochondrion, induce apoptosis if released into the cytoplasm. Certain injurious stimuli, including DNA damage, oxidative stress or hypoxia cause mitochondrial membrane pores to open allowing cytochrome c and other pro-apoptotic mediators to enter the cytoplasm. Cytoplasmic cytochrome c associates with pro-caspase-9 and Apaf-1 to form the so-called apoptosome. The apoptosome promotes the conversion of pro-caspase-3 to caspase-3 which then induces the execution phase of apoptosis.

The final execution pathway caspases (3, 7 and 10) cleave specific protein targets within the cell, in some cases destroying them, in other cases causing activation of other enzymes. One of the enzymes activated is the caspase-activated DNAse (CAD) which causes the cleavage of chromosomal DNA; a process long identified as a hallmark of apoptosis (Enari et al., 1998, Wyllie, 1980). Other enzymes cause the breakdown of proteins responsible for cytoskeletal and nuclear structural integrity.

Though the effects of the caspases are observed throughout the cell, it would be a mistake to think they were random or imprecise. Unlike necrosis, cell death resulting from a failure of cell membrane integrity, apoptosis is an ordered and controlled form of cell death.

1.3 Apoptosis, macrophages and phagocytosis

Apoptosis alone does not remove PMNs from inflamed tissue though it does prevent further degranulation (Whyte et al., 1993). However, apoptotic cells can themselves induce inflammation or auto-immunity, a subject covered later in this chapter. PMNs must be removed in order for the successful resolution of inflammation and this removal is achieved by phagocytosis.

Phagocytosis is the process by which cells engulf and digest other cells, cellular debris and other cell-sized particles. Most cells can perform phagocytosis but higher organisms have 'professional phagocytes'; cells specialised for efficient phagocytosis and to effect appropriate immune responses to the material they engulf. In vertebrates these cells are the macrophages (Mφ).

Mφ develop in the bone marrow from CD34+ progenitor cells and enter the circulation as monocytes (Jandl James, 1996). Starting in the later stages of embryonic development, monocyte-derived Mφ take up residence in all tissues where they act as sentinels for infection and injury. The functions of Mφ can be

broadly categorised as phagocytosis, cell killing, cytokine production and antigen presentation. Their defining function in relation to apoptotic cells is phagocytosis however Mφ are also involved in tissue repair. For example, in a carbon tetrachloride (CCl_4) induced reversible model of murine hepatic injury, Mφ persist within scars throughout the recovery phase (Duffield et al., 2005). The changing role of Mφs at different phases of the reparative process was illustrated by Mφ depletion experiments. These experiments used transgenic mice in which Mφ expressed the human heparin binding EGF protein (hb-EGF – the diphtheria toxin receptor) (Duffield et al., 2005, Cailhier et al., 2005). Mφs were selectively depleted following the administration of diphtheria toxin, whereas other murine cells were unharmed by diphtheria toxin. After the induction of CCl_4 hepatic injury, the depletion of Mφ at the height of the injurious phase results in reduced hepatic scarring when compared with Mφ-replete controls (Duffield et al., 2005). Conversely, Mφ depletion during the later recovery phase resulted in failed matrix degradation (Duffield et al., 2005).

Before phagocytosis can occur, a Mφ must come into direct contact with apoptotic cells. Unlike apoptotic cells, Mφ are highly motile and migrate through tissues under the influence of chemokines. Recruited inflammatory Mφ traffic through injured tissues in hours or days (Melnicoff et al., 1989). In contrast, resident tissue Mφ remain in non-inflamed tissue for much longer periods; up to 49 days in the peritoneal cavity (Melnicoff et al., 1988a) and for many months or years in the case of osteoclasts (Vaananen et al., 2000). Chemokines, released by injured or

bystander resident cells or by leukocytes, recruit Mφ to sites of injury. It has recently been shown that apoptotic cells also secrete chemokines. Smooth muscle cells conditionally over-expressing FADD were shown to synthesise and secrete the PMN and monocyte chemokines IL-8 and MCP-1 during apoptosis (Schaub et al., 2000). Following *in vivo* transplantation and the induction of apoptosis, these same smooth muscle cells produced IL-8 and MCP-1 initiating monocyte-derived Mφ and PMN recruitment. Whilst the release of chemokines may exacerbate inflammation, it may also increase the clearance of apoptotic cells via the recruitment of Mφ.

Once Mφ and apoptotic cells are in direct contact, the process of phagocytosis proper can begin. This can be divided into two stages; the tethering of the apoptotic cell and its ingestion and digestion in a phagosome.

Figure 2. Schematic diagram of phagocytosis of an apoptotic cell

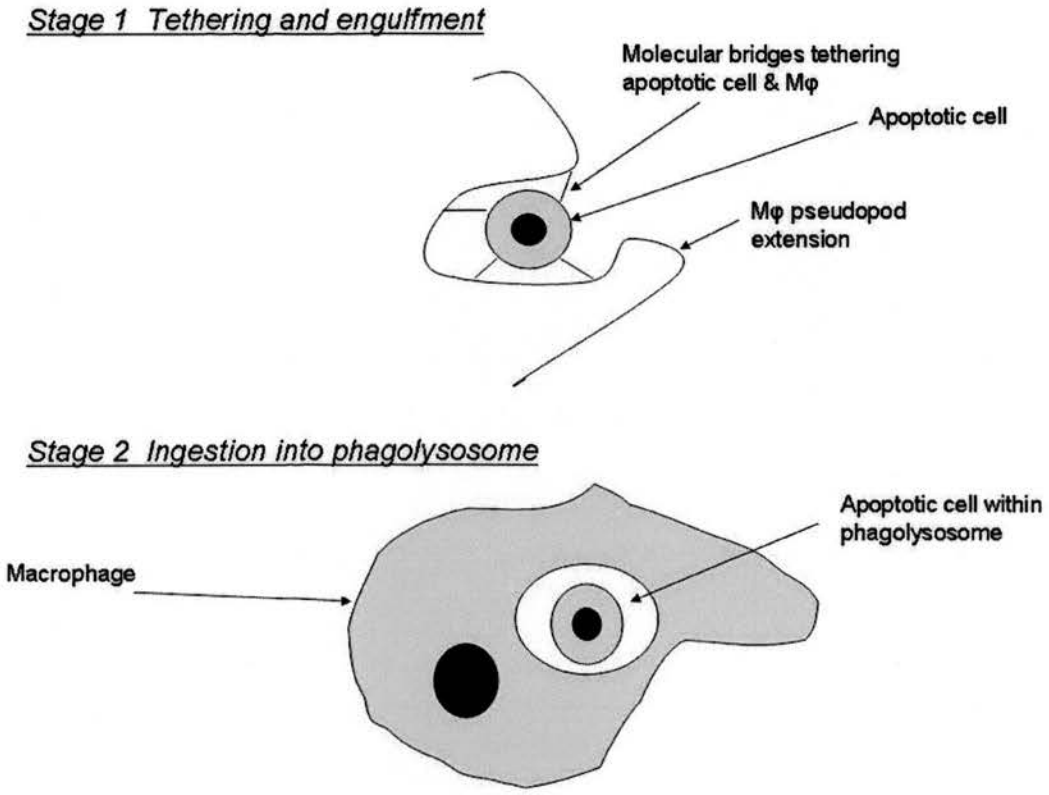

Schematic diagram of phagocytosis. Initial stage involves the tethering of the apoptotic cell within a pseudopodial extension of the Mφ. Tethering is mediated by molecular bridges of apoptotic cell ligands to receptors on the Mφ (upper figure). Cytoskeletal rearrangements within the Mφ result in pseudopodial fusion and the engulfment of the apoptotic cell within a phagolysosome where 'digestion' of the apoptotic cell can occur.

Apoptotic cells display a number of different motifs on their outer cell membrane which are recognised by receptors on the Mφ. These apoptotic cell motifs are sometimes called 'eat me' signals (Savill and Fadok, 2000). One of the most extensively studied of the 'eat me' signals is the aminophospholipid molecule phosphatidylserine (PS). PS is a normal component of the cell membrane but it is usually localised to the inner cell membrane leaflet by the action of the enzyme aminophospholipid translocase (Bretscher, 1972). During apoptosis scramblase enzymes facilitate the translocation of PS to the outer cell membrane leaflet (Fadok et al., 1992b). This appears to be an event unique to apoptosis and occurs *in vivo* in a wide variety of vertebrates and invertebrates (van den Eijnde et al., 1998) and implies a very important role for PS in apoptosis.

A large body of experimental data indicates that PS is a key player in the phagocytosis of apoptotic cells. Early evidence for this came from Fadok, who studied the phagocytosis of apoptotic cells by different populations of Mφ (Fadok et al., 1992a). Fadok demonstrated that the the phagocytosis of apopotic cells by murine peritoneal Mφ was inhibited in the presence of PS liposomes. This implied the existence of a Mφ-borne receptor which recognized PS on the surface of target apoptotic cells. Fadok also observed that bone marrow-derived murine Mφ used a different, PS-independent mechanism to phagocytose apoptotic cells (Fadok et al., 1992a). Further evidence for the role of PS in phagocyte-apopotic cell interaction came from a later observation that annexin V (which binds to and obscures PS on

the surface of apoptotic cells (Koopman et al., 1994)) significantly inhibits the engulfment of apoptotic cells by phagocytes (Krahling et al., 1999).

The identification of the receptor for PS has been the subject of much investigation and controversy. Fadok concluded that 'stimulated' peritoneal Mφ expressed a receptor for PS whereas unstimulated (bone marrow derived) Mφ did not (Fadok et al., 1992a). Fadok then created a monoclonal antibody (mAb 217) which bound to the surface of stimulated Mφ, binding which was inhibited by PS vesicles (Fadok et al., 2000). Furthermore, mAb 217 also inhibited the phagocytosis of apoptotic cells (Fadok et al., 2000). These strands of evidence suggested that the antigenic target of mAb 217 was the PS receptor. Later experiments by the same group offered insights into the function of this putative PS receptor. The presence of PS on the surface of surrogate particles did not affect their tethering to Mφ but was required for later engulfment (Hoffmann et al., 2001). The presence of mAb 217 triggered the phagocytosis of bound, previously unphagocytosed cells (Hoffmann et al., 2001). These observations were interpreted as indicating that the PS receptor was not involved in the tethering of apoptotic cells but instead triggered a signaling cascade resulting in the engulfment of tethered apoptotic cells by Mφ.

Fadok's group then investigated potential antigens for mAb 217 and identified a 47kDa protein as the most likely candidate (known henceforth as the PS receptor (PSR)) (Fadok et al., 2000). Genes encoding the PSR in humans and C. elegans were also identified. Transfection of human or nematode PSR genes into cells lacking

phagocytic capacity conferred a new, albeit inefficient, ability to phagocytose apoptotic cells (Hoffmann et al., 2001, Wang et al., 2003). Furthermore, the transfection of PSR-expressing cells with small inhibitory RNA (siRNA) corresponding to the PSR gene product lead to reduced binding of mAb 217 and reduced phagocytosis of apopotic cells (Hoffmann et al., 2001).

The sum of these data offered compelling evidence that the true PSR had been identified. However, more recent work has cast significant doubt on this. Knock out mice and zebrafish lacking the PSR gene have been created. These animals display similar patterns of abnormal embryonic development with brain, lung (in mice) and cardiovascular development most severely affected (Hong et al., 2004, Bose et al., 2004, Kunisaki et al., 2004). These groups reported contradictory findings with regard to the clearance of apoptotic cells; Kunisaki et al. identified defective phagocytosis whereas Bose et al. did not (Kunisaki et al., 2004, Bose et al., 2004). The mice used to generate these knock out animals had different genetic backgrounds which could have explained the different observations regarding phagocytosis. However Bose et al. also demonstrated identical binding of mAb 217 to Mφ derived from PSR -/- knockout mice and PSR +/+ wildtype controls, strong evidence against a link between the PSR gene and the molecule identified by mAb 217 as the receptor for PS on apoptotic cells (Bose et al., 2004).

The identification of the sub-cellular localization of the PSR gene protein has cast further doubt on its role as the true PS receptor. Cells transfected with genes

encoding PSR linked to GFP produced GFP tagged PSR protein in both a vertebrate cell line (Cui et al., 2004) and invertebrate hydra cells (Cikala et al., 2004). In both cases the GFP-tagged PSR protein clearly localized to the nuclear membrane, not the outer cell membrane. Detailed examination of the DNA sequences of the vertebrate and hydra PSR genes identified five potential nuclear localization signals (Cui et al., 2004, Cikala et al., 2004). Cikala et al. also identified a highly conserved central Jumanji domain within the PSR protein (Cikala et al., 2004). This domain and others indicated that the PRS protein is not a receptor but instead part of a family of transcription factors that includes hypoxia-inducible factor with no known or likely role in the recognition and phagocytosis of apoptotic cells (Hewitson et al., 2002). If the PSR encoded protein really is a transcription factor, not a PS receptor, this could explain the extreme developmental abnormalities and mild or absent defect in phagocytosis of apoptotic cells observed in PSR -/- knock out mice.

This remains a controversial area of research in the field of apoptotic cell clearance. At the present time, there remains little doubt as to the importance of PS in the recognition of apoptotic cells by Mφ. However there are now grave concerns that the product of the PSR gene has been mis-identified as the PS receptor. Investigations that re-evaluate other targets of mAb 217 are eagerly awaited.

Mφ exhibit other receptors that recognise 'eat me' signals on apoptotic cells directly or through bridging molecules, such as C1q (Korb and Ahearn, 1997), mannose binding lectin (Ogden et al., 2001) or milk fat globule-EGF-factor 8 (Hanayama et

al., 2002) that bind eat me signals on the apoptotic cell surface. Some of these receptors, such as the scavenger receptors, are homologues of molecules the nematode *Caenorhabditis elegans (C. elegans)* uses to phagocytose apoptotic cells during embryonic development (Horvitz, 2003). *C. elegans* has a rigid, predictable and well-characterised pattern of development. Newly hatched worms all have 556 cells and fully mature adults 959. During development, 131 cells will die by apoptosis in a highly predictable spatial and temporal fashion. All of this is readily observed by microscopy. Mutations of single genes (known as the central cell death or CED genes) can result in deficient clearance of apoptotic cells from the developing worm (Ellis and Horvitz, 1986). *C. elegans* has proved an ideal model in which to study apoptotic cell clearance and many other aspects of biology (Horvitz, 2003).

Unsurprisingly, phagocytosis of apoptotic cells is more complicated in mammals than *C. elegans*. Many molecules have been shown to participate in the clearance of apoptotic cells *in vitro* (see table 1.3). Confirmatory *in vivo* studies using targeted deletion strategies are ongoing but the evidence to date suggest that there is considerable inbuilt redundancy in mammalian phagocytosis. Targeted deletion of a single gene often produces either no failure of phagocytosis or partial inhibition, often confined to specific tissues. For example, antibody-mediated blockade of scavenger receptor A (SRA) in murine Mφ caused a 50% reduction in the phagocytosis of apoptotic thymocytes *in vitro* (Platt et al., 1996). Many T-lymphocytes undergo apoptosis within the thymus and it was hypothesised that the

absence of SRA would result in defective phagocytosis of T-lymphocytes within the thymus. However this is not the case. Experimental mice in which the SRA gene was deleted showed entirely normal phagocytosis of apoptotic T-lymphocytes (Platt et al., 2000). It was concluded that other mediators of phagocytosis were able to compensate for the absence of SRA, illustrating inbuilt redundancy in mammalian phagocytosis of apoptotic cells.

Table 1 Molecules mediating the phagocytosis of apoptotic cells in C. elegans and humans

C. elegans	*Function*	*Human homologue(s)*	*Function*
CED-1 protein[1]	Unknown	Scavenger receptors (CD-36[2], LOX-1[3], SRA[4])	Bind ox-LDL like sites on apoptotic cells (AC)
CED-2, 5 & 10 proteins[1]	Signalling molecules in cytoskeletal rearrangement	crkII, dock 180 & rac[5]	Signalling molecules in cytoskeletal rearrangement
CED-7 protein[1]	Transmembrane lipid re-arrangement	ABC-1[6]	Transmembrane lipid re-arrangement
		Lectins[3]	Bind sugars on AC
		$\beta_{1,3}$ & $_5$ integrins[7]	Bind bridging thrombospondin (TSP)
		β_2 integrin [8]	Binds phosphatidylserine (PS) on apoptotic cell
Phosphatidylserine	Mediates the engulfment of apoptotic cells	Phosphatidlyserine [9,10]	Mediates the engulfment of apoptotic cells
		Calreticulin [11]	Binds C1q and mannose binding lectin on AC
		β_2 glycoprotein 1 receptor [12]	Binds β2 glycoprotein 1 on AC
		$\alpha_v\beta_3$ integrin[7]	Binds bridging TSP
		$\alpha v\beta_5$ integrin[13]	Binds PS via milk fat globulin epidermal growth factor
		CD-31 [14]	Binds disabled CD-31 on AC
		CD-14	Precise ligand for apoptotic cells not defined. Binds LPS and phospholipids. [15-20]
		Mer receptor tyrosine kinase [21]	Unknown

References

[1](Ellis et al., 1991) [2](Savill et al., 1990) [3] (Oka et al., 1998) [4](Platt et al., 1996) [5](Wu and Horvitz, 1998b) [6](Becq et al., 1997) [7] (Savill et al., 1992) [8](Mevorach et al., 1998) [9-10](Fadok et al., 1992a, Fadok et al., 1993) [11](Ogden et al., 2001) [12](Rovere et al., 1998) [13](Akakura et al., 2004) [14](Brown et al., 2002) [15-20](Gregory et al., 1998, Devitt et al., 1998, Gregory and Devitt, 1999, Moffatt et al., 1999,

Devitt et al., 2003, Devitt et al., 2004) [21](Scott et al., 2001)

C1q, the first component of the classical complement activation pathway, also mediates the phagocytosis of apoptotic cells. Its globular heads bind motifs on the surface of apoptotic cells whilst its stalk binds to calreticulin on Mφ (Ogden et al., 2001). Both *in vitro* and *in vivo* studies demonstrated slower phagocytosis of apoptotic cells by peritoneal Mφ from C1qa knockout mice compared to **wild**-type controls (Taylor et al., 2000). However, *in vivo* phagocytosis of apoptotic cells was delayed, rather than arrested completely, further evidence for inbuilt redundancy in the phagocytosis of apoptotic cells.

Mφ produce pseudopodia which engulf tethered apoptotic cells. Pseudopodia are formed by localised actin rearrangement in the cytoskeleton and changes within the cell membrane itself. The intracellular events resulting in apoptotic cell engulfment are complex and further reading is recommended (Castellano et al., 2001). However, studies on *C. elegans* identified CED 2, 5, 10 and 12 as genes encoding intracellular signaling proteins which modulate the engulfment of apoptotic cells (Wu et al., 2001, Reddien and Horvitz, 2000, Wu and Horvitz, 1998a, Wu and Horvitz, 1998b). Interestingly, these genes were also required for embryonic cell migration. CrkII, dock-180 and rac are mammalian homologues of CED 2, 5 and 10 and it is speculated that they perform similar functions.

Eventually the engulfing pseudopodia fuse and the apoptotic cell is trapped within an intracellular vesicle called a 'phagosome'. The phagosome is moved into the interior of the Mφ where it fuses with endosomes and lysosomes (Iger et al., 1994). This

fusion adds digestive enzymes to the phagosome (now called the phago*lyso*some) causing destruction of the apoptotic cell. The processes occurring within the phagolysosome are poorly understood. However recent studies have provided new insights into the composition and maturation of phagolysosomes (Garin et al., 2001) and further developments in the field are anticipated.

Recently work has shown that healthy, non-apoptotic cells actively inform Mφ of their viability in order to avoid capture and phagocytosis, the previous dogma being that Mφ passively 'ignored' viable cells. This was elegantly demonstrated by Brown and colleagues who used a flow chamber system to assess tethering of viable and apoptotic cells to Mφ or Mφ cell lines (Brown et al., 2002). Both viable and apoptotic cells firmly adhered to Mφ at 20°C under shear force. However, when the temperature was raised to 37°C, only viable cells detached from Mφ whilst apoptotic cells remained firmly attached. The requirement for a physiologically appropriate temperature implied that the detachment of viable cells was dependent upon active, metabolic processes. The precise mechanisms underlying this phenomenon are the subject of ongoing investigations. However, membrane bound CD-31 appears to play a role as CD-31 blocking antibodies inhibited the detachment of viable cells from Mφ. CD-31 is not expressed by all tissues so other mechanisms must be involved in the discrimination of viable cells by Mφ.

1.4 Phagocytosis of apoptotic cells and the modulation of inflammation

Mφ assist the resolution of inflammation by removing apoptotic PMNs from inflamed tissue. The phagocytosis of apoptotic PMNs and other cells by Mφ further contributes to the resolution of inflammation in other ways. Firstly, production of anti-inflammatory cytokines by Mφ, secondly the removal of apoptotic cell derived auto-antigens and finally prevention of phagocytosis by dendritic cells.

The *en masse* apoptosis of PMNs can be seen as the beginning of the resolution phase of acute inflammation. However, at this stage Mφ, which remove the apoptotic PMNs, are producing a variety of pro-inflammatory cytokines. It is now known that the act of phagocytosis of an apoptotic PMN, or apparently any apoptotic cell, will halt the production of pro-inflammatory cytokines and induce a new Mφ phenotype characterised by the production of anti-inflammatory cytokines including transforming growth factor-β1 (TGF-β1), interleukin-10 and prostaglandin-E_2 (Voll et al., 1997, Fadok et al., 1998).

Much attention has been focused on the production of TGF-β1 by Mφ following apoptotic cell phagocytosis. TGF-β1 has several functions including downregulation of the acute inflammatory response (Letterio and Roberts, 1998) and scar formation during wound healing (Border and Noble, 1994). In a seminal paper (Huynh et al., 2002), Huynh and colleagues beautifully demonstrated the link between PS-receptor-

mediated apoptotic cell phagocytosis and TGF-β1 production by Mφ *in vivo*. Apoptotic cells instilled intra-tracheally into inflamed murine lungs were phagocytosed by Mφ. Significantly more TGF-β1 and accelerated resolution of the lung injury was subsequently observed in the lungs of animals receiving apoptotic cells compared to controls. However, these effects were lost when non-PS exposing apoptotic cells (the PLB-985 cell line) were instilled. The increase in TGF-β1 levels seen with PS exposing apoptotic cells was re-established when PLB-985 cells were instilled together *with PS* but not with control phospholipids. Furthermore, the instillation of liposomes bearing PS resulted in accelerated resolution of inflammation and increased Mφ production of TGF-β1. Apoptotic cells opsonised with antibody (hence phagocytosed via Mφ borne Fc receptors rather than the PS-receptor) did not induce TGF-β1 production. Similar results were observed in a second model of inflammation, thioglycollate-induced peritonitis. However, recent work has cast doubt on the role of PS in the phagocytosis of apoptotic cells, as previously discussed (Bose et al., 2004).

Certain autoimmune diseases, such as systemic lupus erythematosis (SLE), are characterised by autoantibodies; antibodies targeted against self antigens. Self antigens targeted by classical SLE autoantibodies have been identified at the exposed surface of apoptotic cells. Keratinocytes undergoing apoptosis display autoantigens concentrated in blebs of cell membrane where they are highly visible to the immune system (Casciola-Rosen et al., 1994). These antigens include Ro, La, nucleosome components and snRPNPs. It is also worth noting that antibodies against

phospholipids such as PS are also common in SLE. Many such antigens found on apoptotic blebs are constituent cell peptides which were altered by caspase and other enzymic degradations during apoptosis. The presentation of 'altered self' is believed to be an important mechanism leading to autoantibody generation. Mφ express Class II MHC and can present antigen to T-cells. It has generally been accepted that Mφ have a lesser ability to present antigen to T-lymphocytes compared to another type of phagocyte, the dendritic cell (DC) (Janeway, 2001c). However, Pozzi et al. recently showed that peptide pulsed Mφ can prime T cells *in vivo* (Pozzi et al., 2005). Furthermore, the abundance of Mφ in inflamed tissue may compensate for their lower antigen presentation capacity. The DC has a lower capacity for phagocytosis than the Mφ but a much greater ability to present antigen and activate T-lymphocytes. However, dendritic cells (DCs) can phagocytose apoptotic cells and then activate T-lymphocytes with apoptotic cell-derived antigens (Albert et al., 1998). This is a somewhat controversial area as other data suggests that DCs that phagocytose apoptotic cells contribute to the maintenance of immunological tolerance (Huang et al., 2000, Ma et al., 2005). Furthermore, other studies suggest that immature DCs which phagocytose apoptotic cells have impaired maturation, defective interleukin-12 production and a lower ability to stimulate T-lymphocytes (Stuart et al., 2002). Clearly further work is needed to establish how the context in which DC phagocytose apoptotic cells alters their immune response.

Whilst the phagocytosis of apoptotic cells is generally considered to have neutral or anti-inflammatory consequences in the modulation of inflammation, the phagocytosis of bacteria and other invading pathogens typically has the opposite effect and initates or exacerbates an inflammatory response. Work by Blander and Medzhitov has shed new light on important differences in the mechanisms used by Mφ and dendritic cells to phagocytose and process apoptotic cells and bacteria (Blander and Medzhitov, 2004).

Phagocytosis is a vital process in host defence against invading microbial pathogens. Microbes are removed by phagocytosis and then killed within phagolysosomes by chemical and enzymic degradation (Janeway, 2001c). The discovery of a novel mechanism by which the innate immune system mounted specific and rapid responses to microbes began with the identification of a new role for the 'Toll' genes (which had known functions in embryonic development) in anti-fungal immunity in *Drosophila melanogaster* (Lemaitre et al., 1996). A human homologue for Toll was soon identified (Taguchi et al., 1996) and a year later it was shown that a human Toll protein could activate inflammation through the NF-κB pathway (Medzhitov et al., 1997). The wide expression of Toll proteins across both invertebrate and vertebrate species and the remarkable conservation of their structure and function suggested key roles in innate immunity. It is now accepted that Toll proteins – commonly referred to as Toll-like Receptors (TLRs) – recognize specific pathogen-associated molecular patterns (PAMPs) not expressed by the host. The TLR identified by Medzhitov and Janeway in 1997 is now designated TLR-4 and is a crucial part of the leukocyte

receptor complex for lipopolysaccharide (LPS), a key player in the endotoxin-mediated toxic shock syndrome (Poltorak et al., 1998).

Recent work from Medzhitov's group has shed new light on the role TLR-4 plays in the processing of phagocytosed bacteria and apoptotic cells. Blander and Medzhitov showed that murine Mφ lacking TLR-4 or its adaptor protein MyD88 phagocytosed bacteria at a slower rate that wild type control Mφ (Blander and Medzhitov, 2004). Furthermore the rate at which phagolysosomes containing bacteria matured to their full killing potential was significantly slower in Mφ lacking TLR-4 or MyD88 (Blander and Medzhitov, 2004). Finally, dendritic cells (DCs) lacking MyD88 demonstrated delayed antigen presentation and T cell activation than wildtype control DCs (Blander and Medzhitov, 2004), presumably a consequence of delayed upstream pathogen processing.

Blander and Medzhitov also studied the effect of TLR-4/MyD88 on the phagocytosis of apoptotic cells (Blander and Medzhitov, 2004). Intriguingly they found no difference in either the rate of engulfment or the rate of phagolysosome maturation following the phagocytosis of apoptotic cells in either TLR-4 or MyD88 deficient Mφ. The overall rate of maturation and processing of ingested apoptotic cells was considerably slower that for bacteria and not altered by the simultaneous phagocytosis of apoptotic cells and bacteria (Blander and Medzhitov, 2004). This suggests that TLR-4 is a key player in directing bacteria and apoptotic cells through distinct processing pathways within phagocytes. This may help to explain some of

the differences in the inflammatory responses that follow the phagocytosis of bacteria or apoptotic cells.

1.5 The consequences of failed apoptotic cell clearance

The presence of so much redundancy is a testament to the importance of phagocytosis of apoptotic cells. The ways in which apoptotic cells might induce or exacerbate inflammation have already been outlined. So what is the evidence that defective phagocytosis of apoptotic cells induces inflammation *in vivo*?

Some of the most compelling evidence comes from the study of humans and experimental animals completely deficient in C1q. C1q is the first component of the classical complement activation pathway which acts as a bridging molecule to effect phagocytosis of apoptotic cells (Ogden et al., 2001). Mφ phagocytosis of apoptotic cells *in vivo* is deficient in the absence of C1q (Taylor et al., 2000).

In humans, homozygous C1q deficiency is the strongest predictor for the development of SLE (Botto and Walport, 2002). Some of the evidence for a link between defective apoptotic cell clearance and SLE is circumstantial, namely the presence of autoantibodies targeting apoptotic cell-derived 'altered self'. More direct evidence for the link comes from animal models of immune mediated inflammatory disease. Mice (and humans) have three genes encoding C1q protein – C1qa, C1qb and C1qc (Petry et al., 1996). Targeted deletion of the C1qa gene resulted in a

viable and fertile mouse completely lacking C1q protein – 'C1qa -/- mice' (Botto et al., 1998). C1qa -/- Mφ exhibit defective phagocytosis of apoptotic cells *in vivo* (Taylor et al., 2000).

Botto and colleagues characterised the autoimmune phenotype of C1qa-/- mice and made the following observations. A significant proportion of C1qa -/- mice spontaneously develop anti-nuclear, anti-histone and anti-sm antibodies typical of those found in SLE. They also developed autoimmune glomerulonephritis (GN), an inflammatory renal injury, with similar histological features to SLE-associated GN. A large number of free apoptotic cells were seen within the inflamed glomeruli implying a failure of Mφ to phagocytose the apoptotic cells.

These autoimmune phenomena were more pronounced when the C1qa -/- mice were bred onto a hybrid 129/Ola x C57BL/6 background rather than either pure 129/Ola or C57BL/6 backgrounds suggesting that other genetic modifiers were influencing the autoimmune phenotype (as is also thought to be the case in humans).

A separate study examined the effect of C1q deficiency in accelerated nephrotoxic nephritis, an experimentally induced immune-mediated form of GN (Robson et al., 2001). Induction of NTN injury resulted in more severe glomerular damage and greater loss of kidney function in C1qa -/- mice compared to control animals. As in spontaneous SLE-like GN, many free apoptotic cells were observed in the inflamed

glomeruli of C1qa -/- mice during NTN. These data suggested that C1q was protective against severe NTN-induced GN.

Mice lacking components of the alternative complement pathway or components of the classical pathway downstream from C1q did not develop the severe GN seen in C1qa-/- mice following the induction of NTN. This indicated that C1q itself, rather than other components of the complement cascade, was preventing the development of a more severe GN following the induction of NTN. C1q also mediates the phagocytosis of apoptotic cells by Mφ independently of other complement molecules *in vivo* (Taylor et al., 2000). Taken as a whole, the data from C1q deficient humans and mice provide the most compelling evidence that failed Mφ phagocytosis of apoptotic cells can induce immune-mediated inflammatory diseases.

Deficiency in the clearance of apoptotic cells from tissues in itself does not necessarily generate inflammatory or autoimmune disease. CD-14 is a pattern recognition receptor expressed on the outer cell membrane of Mφ in mammals including humans and mice. It is perhaps best known as a co-receptor (with Toll-like receptor 4 (TLR-4) and MD-2) for LPS but it also plays an important role in the phagocytosis of apoptotic cells. Apoptotic cells bind to CD-14 on human Mφ and this triggers their phagocytosis (Devitt et al., 1998). Although the precise ligand for this interaction remains unknown, the region of CD-14 that apoptotic cells bind is very closely related to the region which interacts with LPS (Devitt et al., 1998). This is a fascinating observation given that interactions between LPS and the CD-14/TLR-

4/MD-2 receptor trigger a strong pro-inflammatory response (Chow et al., 1999, Kawasaki et al., 2000, Paik et al., 2003) whereas the phagocytosis of apoptotic cells is typically anti-inflammatory (see Chapter 1.4 and 1.5). Later work by Devitt and Gregory has shown that CD-14 -/- mice (completely lacking CD-14) demonstrate defective clearance of apoptotic cells *in vivo* (Devitt et al., 2004). Thymic, splenic, pulmonary and intestinal tissues from normal CD-14 -/- mice all contained significantly more free apoptotic cells than tissues from CD-14 +/+ controls (Devitt et al., 2004). Furthermore, CD-14 -/- mice also showed defective clearance of additional apoptotic cells introduced either by direct injection (peritoneal cavity) or generated indirectly following the systemic administration of dexamethasone (thymus) (Devitt et al., 2004). However, the presence of excess apoptotic cells within tissues of normal CD-14 -/- mice did not result in autoimmunity, as evidenced by normal serum auto-antibody levels and the absence of histological evidence of inflammation. This might be explained by the ability of apoptotic cells to retain their ability to confer an anti-inflammatory phenotype to CD-14 -/- Mφ despite defective phagocytosis (Devitt et al., 2004).

1.6 Macrophage emigration in the resolution of inflammation

The inflammatory response is characterized by the recruitment of inflammatory Mφ as well as PMNs. Inflammatory Mφ initiate and sustain inflammation by the secretion of cytokines, in particular tumour necrosis factor-α (TNF-α), α- and β-interferons (IFN-α and IFN-β), and the interleukins (IL) -1, -6, -10, and -18. These cytokines have a variety of effects on other cells involved in the inflammatory

response which are discussed in detail elsewhere (Janeway, 2001b). In cases of bacterial infection, the primary role of Mφs is to phagocytose bacteria and kill them within phagolysosomes. Mφs also kill non-phagocytosed bacteria by secreting bacteriocidal substances including nitric oxide, various oxygen-containing free radical species and proteases (Albina and Reichner, 1998, Shapiro, 1999). However, these substances not only kill pathogens as resident healthy cells may be inadvertently killed too. For this reason, the successful resolution of inflammation requires the deactivation and removal of inflammatory Mφ as well as PMNs.

Mφ are deactivated in several ways. One is the phagocytosis of apoptotic cells (as outlined in chapter 1.4). Other important deactivating events are the cessation of IFN-γ production by Th1 $CD4^+$ T-lymphocytes and the production of anti-inflammatory cytokines by Th2 CD4+ T-lymphocytes (Janeway, 2001b). Unlike PMNs, the deactivated Mφ do not usually undergo apoptosis within inflamed tissues. As the phagocytosis of apoptotic cells is crucial to their safe disposal, it would make little sense for professional phagocytes to undergo apoptosis *en masse*. The final fate of inflammatory Mφ is poorly understood and some may undergo apoptosis within inflamed tissue (Lan et al., 1997). However, some inflammatory Mφs do leave inflamed tissues and migrate to lymph nodes (Bellingan et al., 1996).

Much of our understanding of Mφ emigration to LNs comes from the investigation of peritoneal Mφ (Bellingan et al., 1996, Bellingan et al., 2002). Peritoneal inflammation in mice can be reliably initiated by the intraperitoneal injection of

brewers thioglycollate (TG) (Melnicoff et al., 1989). TG-induced peritonitis is characterised by an almost immediate influx of PMNs (peaking after 8 hours) and Mφ (peaking after 5 days) (Melnicoff et al., 1989). Intraperitoneally injected phagosome specific dyes, such as PKH-2 (green) and PKH 26 (red) (Melnicoff et al., 1988a), are specifically taken up by peritoneal Mφ and are excellent tracker dyes for these cells (Melnicoff et al., 1988a). By employing PKH-dye labeling, it was shown that inflammatory peritoneal Mφ leave the peritoneal cavity during peritonitis and, over the course of 4 days, emigrate to parathymic lymph nodes (Bellingan et al., 1996). The points of Mφ departure from the peritoneal cavity were identified as milky spots, a type of coelom-associated lymphoid tissue (CALT). Mφ binding to milky spots and subsequent emigration to parathymic lymph nodes were partially mediated by VLA-4 and VLA-5 integrins (Bellingan et al., 2002).

1.7 The Mφ disappearance reaction

Peritoneal Mφ also exhibit a very rapid local migratory or redistribution phenomenon known as the 'Macrophage disappearance reaction' (MDR). Peritoneal Mφ are generally harvested by a lavage procedure involving the intra-peritoneal instillation, agitation and recovery of a physiological solution. The recovered suspension contains many peritoneal leukocytes, including Mφ. In the 1960s, it was noticed that the intraperitoneal injection of Bacillus Calmette-Guérin (BCG) into previously immunised guinea pigs resulted in a dramatic reduction in the number of peritoneal Mφ recoverable by peritoneal lavage (Nelson and Boyden, 1963). Similar

phenomena were described in other animals after a variety of stimuli all of which could be considered pro-inflammatory (see Table 2).

Table 2 Published experimental reports of the MDR

1st Author	*Year*	*Species model*	*Agent inducing MDR*
Nelson	1963	Guinea Pig	BCG
Gillissen	1970	Guinea Pig	Mycobacterium bovis
Bultmann	1971	Rat	Streptococcus
Schimke	1977	Guinea Pig	Bovine IgG
Tomazic	1977	Mouse	Mycobacterium tuberculin
Shannon	1980	Mouse	BCG
Ochiya	1982	Guinea Pig	Mφ migration inhibitory factor
D'Silva	1983	Guinea Pig	Haemocyanin
Ochiya	1983	Guinea Pig	Ovalbumin (IP and intradermal)
Melnicoff	1989	Mouse	Brewers thioglycollate

(Gillissen and Bubenzer, 1970, Bultmann et al., 1971, Schimke et al., 1977, Tomazic et al., 1977, Shannon and Love, 1980, Ochiya et al., 1982, D'Silva et al., 1983, Ochiya et al., 1983, Melnicoff et al., 1989, Nelson and Boyden, 1963)

The MDR has also been observed in the pleural cavity (Sultan et al., 1978). A number of molecules that may mediate the MDR have been suggested including thrombin (Jokay and Karczag, 1973), 'lymphokines' (Sipka et al., 1977), fibrin (Sultan et al., 1978) and hyaluronic acid (Shannon and Love, 1980). It is fair to say that no agreement has been reached upon which, if any, of these molecules is predominant. There is also uncertainty as to whether the MDR represents the beginning of Mφ emigration from the peritoneal cavity or local sequestration of Mφ. One study employed selective labeling to demonstrate that some Mφ reappeared within the peritoneal cavity a week after the induction of a MDR (Haskill and Becker, 1985). It was also suggested that these Mφ had undergone cell division prior to their reappearance. Nonetheless, only a small fraction of the original 'disappeared' population reappeared within the peritoneal cavity.

For the past 30 years, the MDR has remained an immunological curiosity, with no explanation for how, where or why peritoneal Mφ disappear.

1.8 The peritoneal cavity, milky spots and omentum

The peritoneal cavity is a serosal cavity whose main function is to protect the organs contained within from damage by external injury or friction (Mutsaers and Wilkosz, 2007). Single cell thick layers of mesothelial cells form the outer and inner epithelial surfaces of the peritoneal membrane which encloses the peritoneal cavity. Although the mesothelial cells are the most abundant cell type within the peritoneal membrane,

there are also significant numbers of fibroblasts and leukocytes all of which play important roles in peritoneal immunity (Faull, 2000). The fibroblasts are located within the interstitial connective tissue that lies below the mesothelial epithelial layer of cells and the deeper network of capillaries (Faull, 2000). Both fibroblasts and mesothelial cells are able to generate cytokines and chemokines during immune responses (Loghmani et al., 2002, Witowski et al., 2001, Topley et al., 1993). The peritoneal blood circulation arises from the systemic, rather than portal, circulation and mostly comprises capillaries arising from the superior and inferior epigastric vessels. These capillaries are accompanied by lymphatic vessels concentrated within the omentum and sub-diaphragmatic area often accompanying milky spots (Goldsmith et al., 1990). During inflammation a great proliferation of lymphatic vessels and milky spots is seen (Dux et al., 1986).

Bellingan and colleagues identified the milky spots as sites of Mφ emigration from the inflamed peritoneum (Bellingan et al., 1996). Milky spots were first described by the great German pathologist Friedrich Daniel von Recklinghausen who gave them the name 'pus balls' (von Recklinghausen, 1863). However pathologists eventually adopted the more appealing, if less accurate, 'milky spots'.

Milky spots appear to be found in all vertebrates. In humans, they first develop in the middle trimester of gestation (Krist et al., 1997). It is often reported that milky spots are most abundant at birth and their number decreases with increasing age. However, the only study to address this in humans examined diseased omentum and

was possibly confounded by the increasing omental adiposity associated with aging (Shimotsuma et al., 1993). Milky spots are unevenly distributed throughout the peritoneal cavity being most abundant within the omentum but also concentrated on the sub-diaphragmatic and peri-uterine regions of the peritoneal membrane (Shimotsuma et al., 1993). Similar structures are found within the pleural and pericardial membranes (Pereira Ade et al., 1994).

Milky spots are aggregations of leukocytes – mostly Mφ and lymphocytes- surrounding a central blood vessel and often a lymphatic vessel (Lenzi et al., 1996). They arise between the two mesothelial cell layers of the peritoneal membrane. The architectural arrangement of Mφ reflects their maturity. Immature monocyte-derived Mφ are found at the innermost aspect of the milky spot close to the central vessels. Further from the central blood vessel, the maturity of Mφ increases with the outermost layer being the most mature (Krist et al., 1995). It is suspected but not demonstrated that similar principles apply to the arrangement of lymphocytes. Fibroblasts and connective tissue are found between the tightly packed leukocytes (Krist et al., 1995). There is a discontinuation of the peritoneal mesothelial cell lining of the interior of the peritoneal cavity associated with milky spots (Mironov et al., 1979). This affords mature Mφ direct contact with the peritoneal fluid which they continuously sample and survey for pathogens (Krist et al., 1997). The break in the peritoneal membrane also assists the seeding of leukocytes into the peritoneal cavity during peritoneal inflammation (Dux et al., 1986).

Peritoneal milky spots increase dramatically in number and cellularity during peritonitis (Dux et al., 1986, Beelen et al., 1988). This is due to a recruitment of PMNs and monocyte-derived Mφ, facilitated by the production of chemokines including SDF-1 (Pinho Mde et al., 2002) and the proliferation of Mφ under the influence of GM-CSF (Koenen et al., 1996, Zhu et al., 1997). Milky spot Mφ and nearby mesothelial cells upregulate a large number of molecules involved with cell adhesion and migration including LFA-1, Mac-1, VLA-4, ICAM-1 and VCAM-1 further facilitating leukocyte trafficking through milky spots (Cui et al., 2002). Blood vessels within milky spots are fenestrated and have a characteristic high endothelial phenotype, further enhancing leukocyte recruitment (Krist et al., 1995).

Milky spots contain an unusually high proportion of B-1 lymphocytes (Kasaian and Casali, 1993). These evolutionarily primitive lymphocytes produce so-called 'natural' antibodies with a low affinity against many (usually bacterial) antigens (Kasaian and Casali, 1993). They are almost exclusively found within the peritoneal cavity and play an important role in the innate immune response to bacterial infections (Boes, 2000). The low specificity of natural antibodies means that they can bind to self- as well as bacterial antigens. Consequently, natural antibodies have been shown to participate in auto-immune diseases (Bell, 1993).

1.9 The Omentum

Most peritoneal milky spots are found within the omentum. The omentum comprises a double fold of peritoneal mesothelium containing adipose tissue and milky spots. The omentum first appears during the 8th week of gestation, arising from the dorsal mesogastrium (Krist et al., 1997). Milky spots appear later, during the middle trimester. The omentum is found in the right hypochondrial abdominal region of mammals and is attached to the stomach, small intestine and, in mice, the pancreas (Goldsmith et al., 1990). The omentum receives a large blood supply from the gastroepiploic vessels and its lymphatic drainage is to the coeliac lymph nodes. Whilst the basic structure of the omentum is similar amongst all vertebrates, there are species variations. In humans, the omentum is apron-like in appearance with milky spots arranged within a lacy network of adipose-rich tissue. This structure is best appreciated in neonates as with increasing age the milky spots are obscured by adipose tissue. In mice, milky spots are organised within fatty ribbon-like structures called omental lymphoid organs (OLOs) (Dux et al., 1986). An individual mouse may have one or more OLOs and their precise architecture varies between strains (Goldsmith et al., 1990). A branch of the gastro-epiploic vessels run along the length of the OLO sending marginal branches to the milky spots. Lymphatic vessels follow similar routes to the blood vessels and eventually drain into the coeliac, pancreatic and ultimately the parathymic lymph nodes.

The omentum has been known to physicians since ancient times and there have been a number of historical theories regarding its function. Galen performed a partial omentectomy on an injured gladiator who recovered but thereafter was greatly intolerant of cold weather. Galen's report of this gave rise to the popular theory that the omentum's purpose was to warm the intestines. Soothsayers believed that examination of animal omenta could foretell future events. The word omentum is in fact derived from *omen*, reflecting this ancient belief.

The modern view of the omentum as an organ of immunity began in 1896 (reported by Rothenberg and Rosenblatt, 1942) when Stichler placed snails into the peritoneal cavity of dogs and observed their subsequent encasement by the omentum (Rothenberg and Rosenblatt, 1942). The belief that the omentum actively patrolled the peritoneal cavity caused surgeons to nickname the omentum the 'abdominal policeman'. However, in 1926 Florey showed that the movement of the omentum was entirely passive (Florey et al., 1926). Sir Charles Sherrington, Nobel Laureate and George Holt Professor of Physiology at Liverpool University 1895-1913, first pointed out that the 'doubled-up' posture associated the acute abdomen is ideal for moving the omentum to the farthest regions of the lower abdomen.

Significant changes occur within the omentum during peritonitis. Its blood supply dramatically increases and it is the principal site of PMN extravasation during peritonitis (Fukatsu et al., 1996, Doherty et al., 1995). The omentum becomes adherent to sites of inflammation and produces a layer of fibrin which may

eventually organise into a walled off collection (Konturek et al., 1994). The changes occurring within omental milky spots have already been discussed.

These functions of the omentum suggest that it is an important 'engine' of peritonitis. Omentectomy renders experimental animals increasingly susceptibile to fatal peritoneal infections (Agalar et al., 1997). Moreover, peritoneal PMNs harvested from such animals were found to have reduced chemotactic ability. A retrospective study compared 406 human patients who had proctocolectomy with omentectomy with 239 patients who had undergone a proctocolectomy without omentectomy. The rate of post operative sepsis was significantly higher in patients who underwent the additional omentectomy compared to those who had not (10% Vs 4%, $p=0.01$) (Ambroze et al., 1991). A similar increase in peritoneal sepsis requiring re-operation (8% Vs 3%, $p=0.01$) was also observed. These data suggest that the omentum is important but not vital for peritoneal immunity. It is likely that activity in other milky spots compensates in individuals lacking an omentum.

1.10 The murine omentum as a model for Mφ interactions with apoptotic cells in vivo

The peritoneal cavity has many features favorable for the study of Mφ interactions with apoptotic cells. Cells can be readily recovered from the peritoneal cavity by a simple lavage procedure. Apoptotic cells and other phagocytosable particles can be readily injected into mice without the requirement for general anaesthesia. Taylor and others have shown that the *in vivo* rate of phagocytosis of labeled apoptotic cells can be measured within the peritoneum (Taylor et al., 2000, Scott et al., 2001).

However studies to date on the phagocytosis of apoptotic cells within the peritoneal cavity have focused on Mφ that can be recovered by lavage. It seems likely that such an approach will only allow the investigation of the subset of less adherent Mφs. The phagocytosis of large numbers of apoptotic cells *in vivo* is likely to involve the recruitment and emigration of Mφ, phenomena best appreciated within the omentum, the major site of peritoneal leukocyte trafficking.

1.11 Aims of this study

- To determine the influence of the administration of apoptotic cells upon peritoneal and milky spot Mφ.

- To determine whether the omental milky spot Mφ phagocytose intra-peritoneal apoptotic cells.

- To determine the relative contribution the omentum makes to apoptotic cell clearance within the peritoneal cavity.

- To investigate the mechanisms influencing apoptotic cell clearance by milky spots.

- To develop an *in vivo* assay of apoptotic cell phagocytosis based upon the omentum and explore the interaction of the omentum with other bioparticles.

- To investigate whether the phagocytosis of apoptotic cells stimulates the emigration of Mφ from the peritoneal cavity and, if so, which mechanisms govern Mφ emigration.

2 CHAPTER 2 – METHODS

2.1 List of reagents used in experiments and suppliers

Reagent	*Supplier*
2μm fluorescent latex beads	Sigma-Aldrich Co Ltd, UK
CMFDA dyes	Molecular Probes, Netherlands
DMSO	Sigma-Aldrich Co Ltd, UK
FACS Flow sheath solution	BD Biosciences, UK
FACS Lysis solution	BD Biosciences, UK
FITC-Annexin V	Sigma-Aldrich Co Ltd, UK
Flowcheck Microspheres	Beckman-Coulter, UK
Foetal calf serum	Invitrogen, UK
Hanks Buffered Salt Solution	Sigma-Aldrich Co Ltd, UK
Hoescht 33342	Sigma-Aldrich Co Ltd, UK
Human C1q	Advanced Research Technologies, CA, USA
Hyularonidase enzyme	Sigma-Aldrich Co Ltd, UK
Liberase enzyme	Roche, UK
PBS	Sigma-Aldrich Co Ltd, UK
Propidium Iodide	Sigma-Aldrich Co Ltd, UK
Rat anti-mouse B220 antibody	Pharmingen, San Diego, USA
Rat anti-mouse CD3 antibody	Pharmingen, San Diego, USA
Rat anti-mouse GR1 antibody	eBiosciences, UK
Rat-anti-mouse F4/80 antibody	Caltag Medsystems, UK
RPMI 1640 culture medium	Invitrogen, UK
RPMI culture medium	Sigma-Aldrich Co Ltd, UK

2.2 Lavage of peritoneal cells

Mice were sacrificed by cervical dislocation in accordance with the Centre for Inflammation Research and Home Office guidelines for the care of experimental animals. After 45-60 seconds agonal breathing, cardiac and muscle activity ceased and dissection could begin.

Deceased animals were placed in the supine position on a polystyrene dissection board and secure by placing a single securing pin through each of the four limbs into the dissection board. Fur was removed carefully removed from the lower abdomen using close cut electic shaving clippers. The underlying skin was then cleaned by applying 70% ethanol solution with sterile skins wipes; the skin was then allowed to air dry (approximately 15 seconds). The skin was lifted using rat-toothed forceps and a midline incision from just below the xiphisternum to the pubic area was made using dissection scissors. This incision went through the skin and subcutaneous tissues but did not breach the underlying peritoneal membrane. The skin and the underlying parietal peritoneum were separated by careful blunt dissection of the sub-dermal fascia using curved-ended forceps. Transverse incisions through the skin were made and further blunt dissection performed allowing it to be reflected completely away from the underlying peritoneal membrane. With practice, this procedure could be completed in 15-20 seconds.

The peritoneum membrane was carefully lifted with curved forceps and PBS (kept cold by storage in an ice bucket) was injected from a 5ml syringe through a 19 guage needle. The needle breached the peritoneal membrane at the anterior midline in the lower part of the abdomen. The needle was only advanced a few milimetres into the abdominal cavity. Extreme care was take to ensure that the needle did not breach or damage the internal abdominal organs.

The bevel of the needle was positioned above the internal abdominal organs approximately 2-3 mm below the inner peritoneal membrane. With the instilling needle remaining in situ, the lavage fluid was agitated by gentle, rhymic squeezing of the fluid-filled peritoneal cavity for about 10 seconds, taking care not to breach the membrane with the needle tip. The peritoneal lavage fluid was then carefully withdrawn from the cavity into the syringe. Intra-abdominal fluid pressure was maintained during the withdrawal of fluid by applying gentle pressure to the lateral walls of the peritoneal cavity using the thumb and index finger of the hand not holding the syringe (eg right handed experimenters use right hand to handle syringe and left to apply pressure to peritoneal cavity). Particular care was taken to ensure that the opening of the needle was kept clear of underlying fat and mesenteric structures. These structures floated freely within the abdominal cavity and could become caught up or sucked into the needle during aspiration of fluid. This could be avoided by fastidious positioning and handling of the needle within the abdominal cavity. The volume of peritoneal fluid withdrawn was noted and was typically in the range of 4.0-4.5 mls (i.e. 80-90% of that injected). The entire procedure, once

learned correctly, took approximately 60 seconds to perform. Recovered peritoneal fluid was then placed in sealed 15 ml plastic tubes and stored at 4°C until labeled and analysed.

2.3 Development and improvement of the peritoneal lavage technique

The technique used to instill material IP and subsequently recover peritoneal cells by lavage evolved from the method described by Taylor and Thomas (Taylor et al., 2000). Dr Graham Thomas (University of Edinburgh) kindly demonstrated the technique, highlighting important practical points. It soon that the technique was very technically demanding and prone to error, particularly the leakage of IP instilled material, heavily blood stained lavages and recovery low volume lavages.

Refinements and new steps were incorporated into the Taylor and Thomas technique and these lead to the final method described in section 2.2 (above). During this development process, it became clear that the success of the entire technique was largely dependant on the initial IP injection of apoptotic cells or other experimental materials. For this reason, the major methodological refinements focused on improving the initial IP injections; these were:-

- A Pre-loading of all injection and lavage syringes prior to experiment.

- B Use of orange (25 gauge needles) for IP injection instillation of cells or other experimental materials prior to lavage (Taylor and Thomas used 21 gauge green needles).
- C Shaving of fur and cleaning of skin with ethanol soaked wipes prior to initial IP injection
- D Limitation of initial injection of IP cells or other experimental needles to a maximum of 0.5ml (previously 1ml).
- E Use of Vaseline gel to seal IP puncture point
- F Positioning of mice 'head down' during IP injection of apoptotic cells

The combination of acquired experience and technical refinements lead to major improvements in overall performance, demonstrated in figure 3. The top and middle figures show the rates of complications – bloody lavages and leaks of IP injection fluid- as percentages of all the total number of procedures performed in each experiment. The bottom figure shows the mean volume of lavage fluid recovered per experiment (in all cases 5ml were instilled). The data are displayed as Shewhart run chart format with the major protocol changes highlighted with arrows. The letters A-F indicating major changes in technique correspond to those listed in the preceding paragraph.

Figure 3. Improvements in the performance of the peritoneal instillation and lavage technique

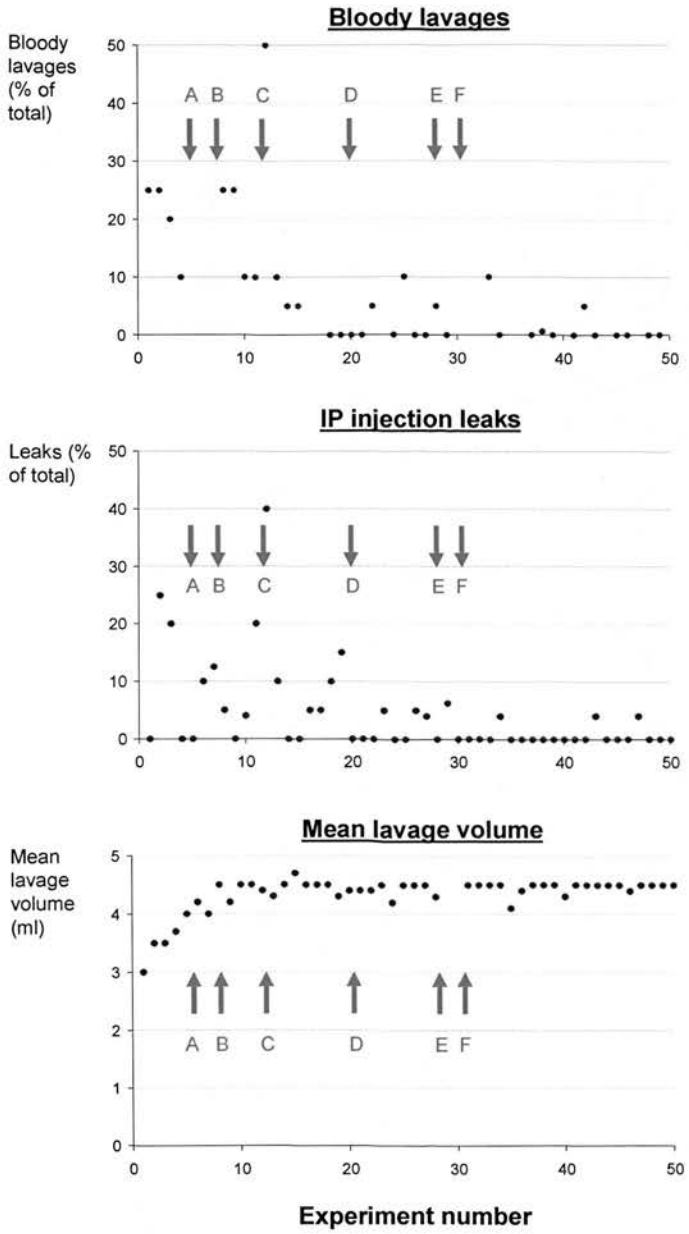

Top figure – Y-axis = blood-stained lavages as a percentage of all lavages performed in the experiment. Middle figure – Y-axis = visible leak of IP injected fluid prior to lavage as a percentage of all IP injections performed in the experiment. Bottom figure – Y-axis = mean volume of instilled peritoneal lavage fluid (5ml) recovered by aspiration. All figures – X-axis=chonological order of experiments, annotated arrows indicate change in experimental protocol (see section 2.3 for key) and experiment in which change was introduced.

Great care was taken to ensure that this was achieved. The accuracy of the time intervals between the initial IP instillation of experimental material and the final lavage of peritoneal cells. All timed lavages were within ± 3 seconds of the time stated in minutes, including those performed 1 minute after the initial IP injection. This was achieved by careful planning and preparation of experiments including a written schedule of desribing the start and finish times for all individual animals. The importance of thorough preparation when performing this technique on multiple animals cannot be over emphasized.

The choice of the number of cells to instill was made after considering both scientific and ethical issues. It was decided at an early stage to use apoptotic murine cells for most experiments. The major reason behind this was to avoid perturbation of the recipient's immune system by cross-species reactivity. The most readily available and reliable source of apoptotic cells were murine thymocytes. The number of apoptotic cells generated by a single murine thymus was approximately $5\text{-}10\text{x}10^6$ depending upon the age of the donor animal and other variables. Empirical data from early developmental work showed that it took approximately 30 minutes for $0.5\text{x}10^6$ apoptotic cells to be cleared from the peritoneal cavity. The technical performance of the peritoneal installation-lavage technique tended to deteriorate if shorter time points were used in experiments involving large numbers of animals. Longer timepoints would have been valid scientifically but would have also demanded larger quantities of apoptotic cell feed. This in turn would have significantly increased the number of experimental animals used per experiment for

no obvious scientific gain. Such an action would have been against the important principal of 'reduction' in *in vivo* experimentation. Therefore, for most experiments that examined the kinetics of intraperitoneal leukocytes, $0.5\text{-}1.0\text{x}10^6$ apoptotic cells were instilled IP and recovered by peritoneal lavage 30 minutes later.

It was clear that large scale experiments in the clearance of apoptotic cells IP could be reliably performed using $0.5\text{-}1.0\text{x}10^6$ apoptotic cells and a 30 minute interval. It was decided that to use longer time intervals and larger cell feeds was unlikely to add significant scientific value but would require larger numbers of animals. As such, this was against the important principle that all experiments involving animals should use the minimum possible number of animals and strive to reduce this number in the future. Hence for most experiments, the 'just right' conditions of 30 minute time intervals from initial IP injection of cells to lavage and $0.5\text{-}1.0\text{x}10^6$ IP injected cells were used.

2.4 Immunolabelling of lavaged peritoneal cells

400µl of well-mixed peritoneal fluid was transferred to a flow cytometry tube using a calibrated pipette and placed in an ice bucket which was covered with aluminium foil to limit unwanted light exposure. 50µl of mouse serum (Serotec) was then added to the tube and the solution thoroughly mixed and left for 30 minutes. 50µl of a mixture of 1µl antibody solution (see below), 9µl mouse serum and 40µl PBS was

then added, thoroughly mixed with the periteonal cell suspension and incubated for a further 30 minutes. Two washing steps were performed in which 2 mls of PBS were added to the tube which was then securely placed in a Sigma centrifuge and spun at 300G for 5 minutes. The excess supernatant fluid was carefully removed by decanting after each centrifugation step and the remaining cell pellett resuspended by 5 seconds of agitation on a bench vortex.

Figure 4. Antibodies used for immunolabeling of peritoneal cells

Name	*Primary peritoneal cell labeled*	*Manufacturer*
Rat anti-mouse F4/80 (conjugated with FITC, PE or PE-Cy5)	Macrophage (low labeling for dendritic cells)	Caltag, UK
Rat anti-mouse B220 (conjugated with PE)	B-lymphocytes (low labeling for macrophages)	Pharmingen, San Diego, CA, USA
Rat anti-mouse CD3 (conjugated with PE)	T-lymphocytes	Pharmingen, San Diego, CA, USA
Rat anti-mouse CD11c	Dendritic cells	Caltag, UK
Rat anti-mouse GR1 (conjugated with PE)	Neutrophils	eBiosciences, UK

2.5 Analysis of lavaged peritoneal cells by flow cytometry (Mφ, neutrophils, lymphocytes)

Suspensions of labeled peritoneal cells were identified by flow cytometry using a Coulter Excel cytometer using Expo 32 software. 200µl of flow cytometry buffered solution was added to each sample and thorough mixing was achieved by repeated use of a 200µl calibrated pipette. A representative FSC/SSC dot plot of lavaged resident peritoneal cells is shown below (Figure 5)

Figure 5. Typical FSC/SSC plot of lavaged peritoneal cells

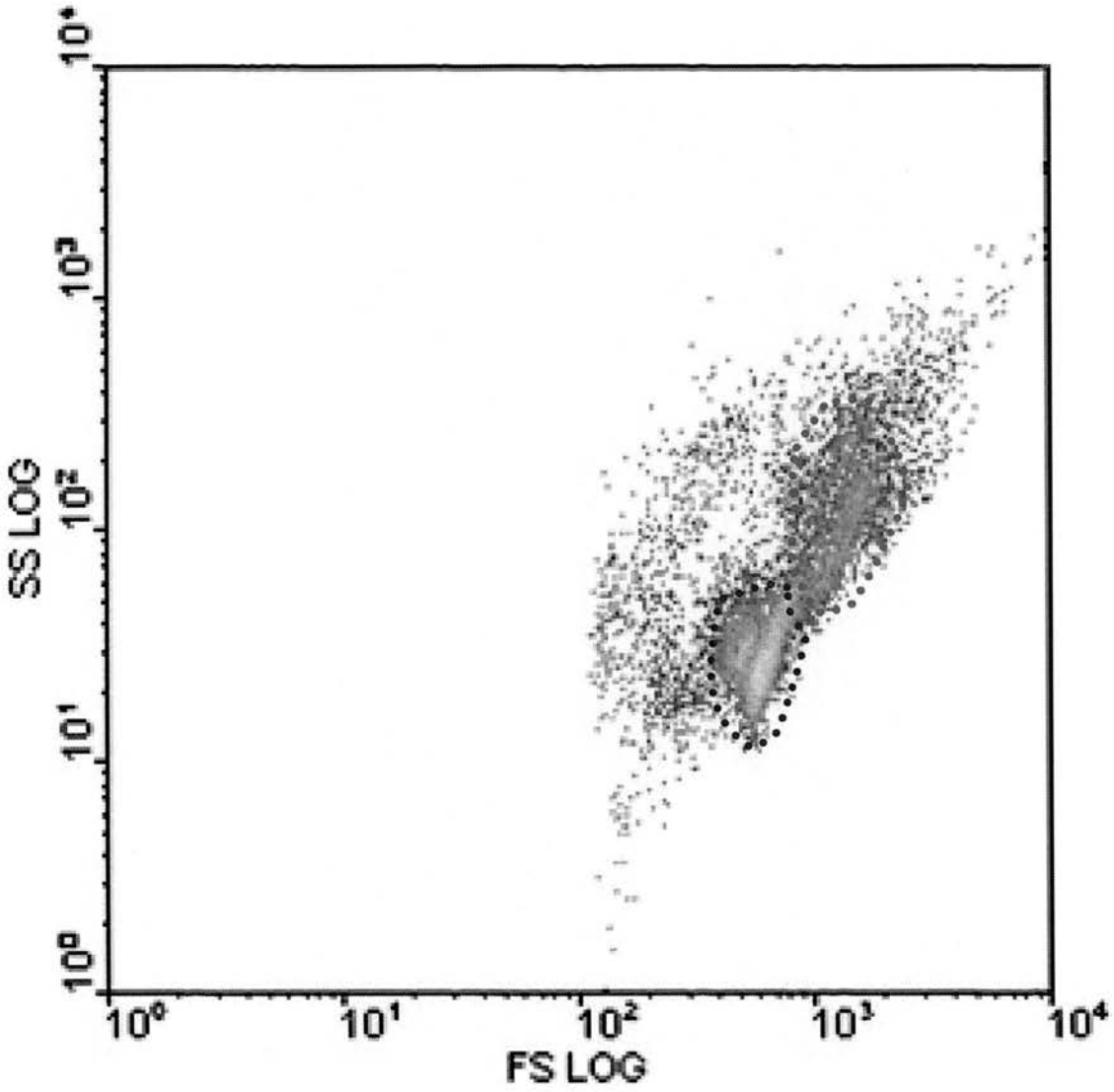

Mφ and monocytes (within red line) are larger and more granulated than lymphocytes (within blue line). This explains the higher FSC & SSC values of Mφ/monocyte populations. Mature Mφ have higher SSC & FSC values than immature Mφ.

For each experiment, fine adjustments to the thresholds for the fluorescent channel detectors were made in order for unlabeled cells to have a peak fluorescence at the midpoint between 10^0 and 10^1 on the logarithmic scale. The FL-3 channel was reserved for Flowcheck™ microspheres, when utilised.

Figure 5. Typical FSC/SSC plot of lavaged peritoneal cells

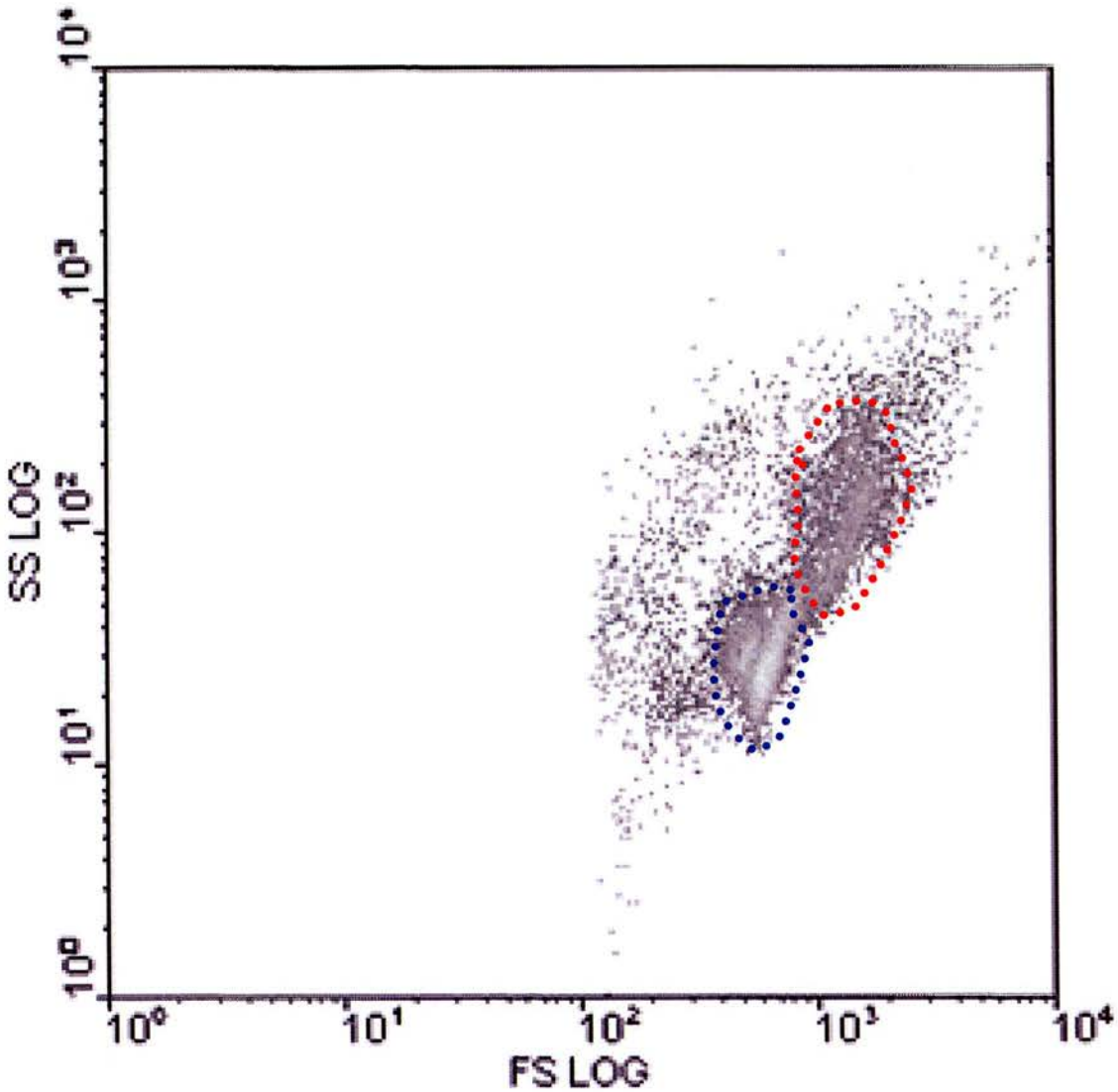

Mφ and monocytes (within red line) are larger and more granulated than lymphocytes (within blue line). This explains the higher FSC & SSC values of Mφ/monocyte populations. Mature Mφ have higher SSC & FSC values than immature Mφ.

2.6 Analysis of flow cytometry data

The LMD files generated by flow cytometry were analysed using WinMDI software (WinMDI 2.8 freeware, Scripps Institute, CA, USA). The most basic data was a 2-dimensional (2D) dot plot of the entire peritoneal cell population show by ungated FSC (Y-axis) and SSC (X-axis). In most experiments, cell populations of interest were identified by immunofluorescent labeling. Furthermore, the cells of interest – primarily Mφs, apoptotic and other lymphocytes – and Flowcheck™ microspheres differed significantly in size. FSC is a recognised surrogate marker for the size of a cell. Therefore, a population of interest was usually identified by plotting a 2D dot plot of FSC (X-axis) with the appropriate fluorescent channel on the Y-axis. Given the specificity of the immunolabeling, it was not strictly necessary to use a 2D plot. However, this was used as a contingency against the theoretical possibility of adherant fluorescent labeling of other particles within a sample. It also made it easier to identify Flowcheck™ microspheres which, by design, were fluorescent in all detector channels.

2.7 Haemocytometry-based counting of peritoneal cells

The number of a particular population of cells within a peritoneal lavage sample could be calculated using a combination of microscopic counting with a

haemocytometer and flow cytometry analysis. Firstly, the absolute number of cells was estimated using a haemocytometer. The mixture was mixed well then a 10μl aliquot removed and placed under a coverslip on a haemocytometer grid. The slide was examined under light microscopy and the total number of cells within a grid counted. The haemocytometer is calibrated such that the concentration of cells per ml of fluid can be calculated by multiplying the number of cells in one large grid by 10^4:-

eg 100 cells per grid = $100x10^4$cells/ml = $1x10^6$ cells/ml.

Then, by separately analysing the sample using flow cytometry, the proportion of a particular cell of interest can be determined as described above. The absolute number of a particular cell type per ml of lavage fluid can thus be easily calculated using the following formula:-

Population A (cells/ml) = Total Concentation (cells/ml) x (percentage A/100)***

*=Measured by haemocytometry **=Measured by flow cytometry

For example, the number of Mφs in 1 ml of lavage fluid can be calculated from the following data set:-

Total cells/ml by haemcytometry = $1x10^7$ cells/ml

Number of flow cytometry events in Mφ gate = 2,500

Total number of flow cytometry events = 15,000

Percentage Mφ events = (2,500/15,000) x 100

= 16.7 %

Macrophages/ml lavage = $1x10^7$ x (16.7/100) cells/ml

= $1.67x10^6$ cells/ml

2.8 Bead-based counting of peritoneal cells by flow cytometry

Whilst the so-called 'dual platform' technique described above is a well-recognised method for determining the absolute cell number within a sample, it has certain drawbacks. Firstly, it is slow and laborious and secondly, for samples containing small numbers of cells, the haemocytometry estimation of total cell number may be inaccurate and thirdly, it is assumed (perhaps incorrectly) that microscopic and flow cytometric analyses identify the same objects as 'cells'. Both microscopy and flow cytometry will mis-identify a small number of non-cellular objects as 'cells'. However, when both microscopy and flow cytometry are used in combination, such errors are combined. Therefore for reasons of speed and accuracy, a robust, flow cytometry based method for counting specific cell populations was desirable. Such a method required a standard reference point from which an exact number of cells within a sample could be determined. This was achieved by 'spiking' each sample

with a known quanitity of Flowcheck™ synthetic polystyrene beads which have a highly uniform size and fluorescence (Flowcheck™ Beckman Coulter ref. 6605359). In each experiment, 25ul of beads from a stock suspension of $1x10^6$ beads per ml were added to each sample (ie $2.5x10^4$ beads). The beads were added immediately before flow cytometric analysis and the sample mixed thoroughly. This was necessary as prolonged co-incubation might have resulted in binding of beads to peritoneal lavage cells – especially Mφs. The fluorescence of the beads was considerably greater than any of the labeled cell populations and they fluoresced in all channels from FL1-FL4. None of the cellular fluorescent labeling techniques required the FL3 channel so this was reserved for the beads. The flow cytometer was adjusted such that the beads had FL3 fluorescence around 10^3 on the log scale. With these settings, other cells had FL3 fluorescence of 10^1 or less and hence could be easily excluded from any analyses.

Figure 7. Flow cytometry plot of flowcheck microspheres

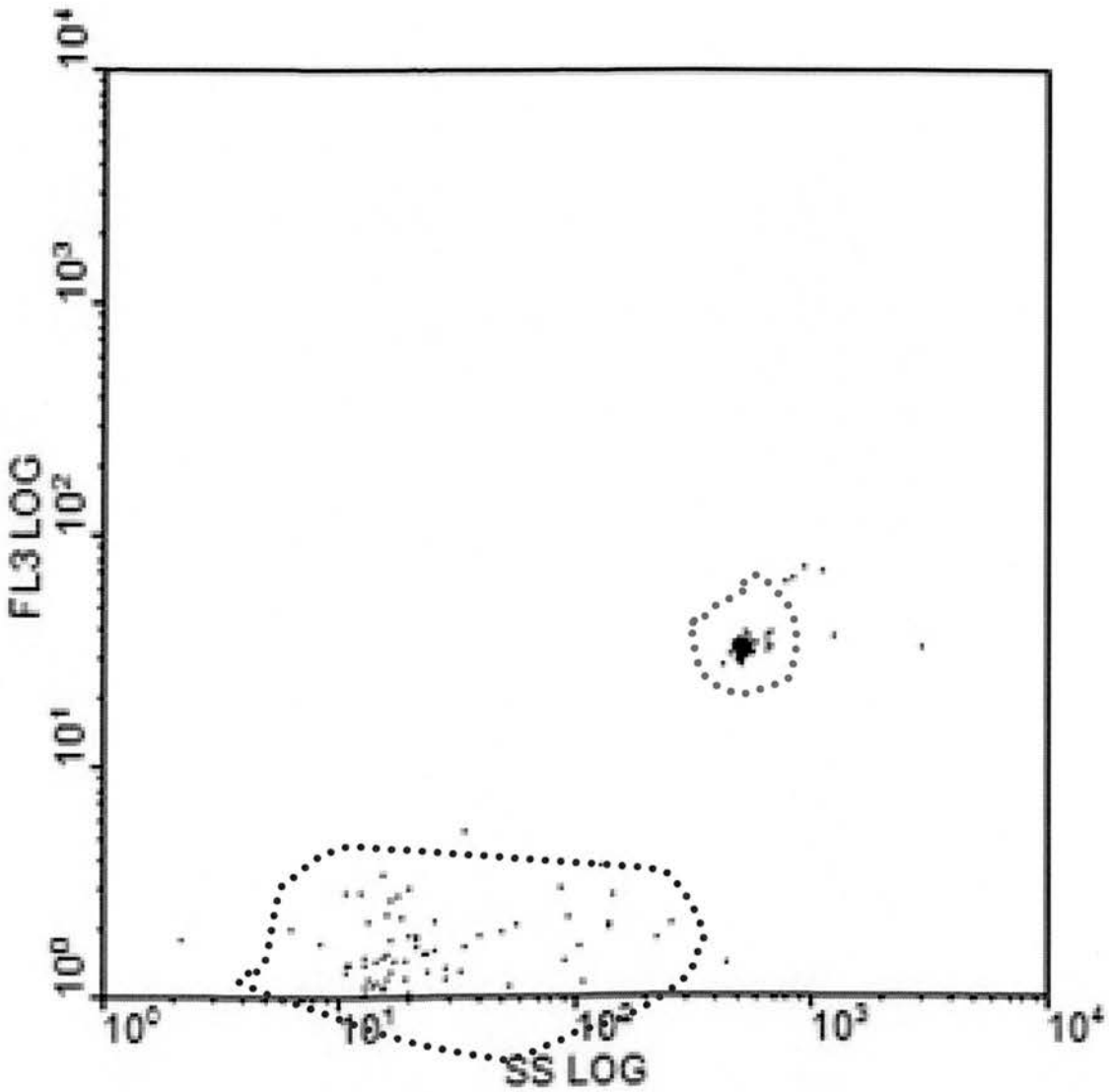

Flow cytometry plot showing Flowcheck ™ microspheres of uniform size with high fluorescence in FL3 channel (points within red line). In contrast, virtually all peritoneal lavage cells (including F4/80-PE/Cy5 labeled Mφ) have virtually no FL3 fluorescence and only a few appear on the positive side of the Y-axis (points within blue line). This demonstrates how effectively Flowcheck™ beads can be separated from peritoneal cells using flow cytometry.

To calculate the number of cells in a particular sample, gates are placed around the cell population of interest and a second gate around the 'spiked' beads. 15000 events are then collected by the flow cytometer. The number of cells per ml is determined using the following equation:-

Cells/ml = (Cell events counted x Number of beads in sample) / (Bead events counted x volume of lavage)

For example,

Cell events counted = 16,000 cells

Bead events counted = 1,000 beads

Number of beads in sample = 25,000 beads

Volume of lavage analysed = 0.4 ml

Cells/ml = (16,000 x 25,000) / (1,000 x 0.4ml)

Cells/ml = 1,000,000 cells/ml

A comparison of the two methods was performed and showed a high degree of correlation between the results obtained. However, the single platform beads-based system proved to be much faster and was used in all experiments unless otherwise stated.

2.9 Intraperitoneal instillation of substances

Substances were instilled IP according to the terms and conditions of the relevant Research Project Licence, my own Personal Licence and the Home Office general guidelines for the use of experimental animals. Unaesthetised animals were scruffed and held in the non-dominant hand and fur was removed from the lower right quadrant of the abdomen using close cutting electric clippers held in the dominant hand. The underlying skin was cleaned by applying 70% ethanol using an anti-septic wipe. The cleaned skin dried within 15 seconds. Then a maximum of 0.5mls of fluid was injected IP using a 21 gauge (orange) needle. During injection the animal was held in a 'head down' position for 5 seconds. Experience showed that this minimized the leakage of IP injected fluid. A small amount of Vaseline was applied to the puncture site whist the needle was being withdrawn to help prevent leakage of fluid after injection - this often required the help of an assistant. The procedure was generally done without general anaesthesia.

2.10 In vivo labeling of peritoneal Mφs with PKH-2 and PKH-26 dyes

The phagocyte-specific dyes PKH-2 and PKH-26 are sold in a kit form complete with instructions. The techniques for PKH-2 and PKH-26 labeling differ only in respect of the dye used and PKH-2 is referred to only in this description. The dyes are equally effective at labeling resident or recruited inflammatory peritoneal Mφs.

In some experiments, PKH dye was injected following the IP injection of brewers thioglycollate.

0.05ml PKH-2 were removed from the kit and mixed thoroughly with 0.95mls of absolute ethanol, providing 50μM working stock dye solution. The metal tab of one diluent bottle was lifted and 0.05ml of the dye into the diluent injected into 10 mls of diluent. The bottle and dye were vigorously mixed and allowed to stand for at least 15 minutes prior to use. 0.5mls of the diluted dye were injected IP into each experimental animal using a fresh needle for each injection. Labeled peritoneal Mφ were harvested 24 hours after IP injection using the peritoneal lavage technique previously described.

2.11 Preparation and labeling of viable thymocytes

Young mice (less than 7 weeks old) were sacrificed by cervical dislocation and the limbs pinned to a polystyrene board as previously described. Fur was removed from the abdominal wall and thorax using close cutting electic clipplers. The skin was cleaned with 70% ethanol solution applied with a sterile wipe. The skin was opened at the midline on the anterior wall at the level of the lower abdomen. A midline incision through the underlying skin and peritoneal membrane was made using dissection scissors. The incision was extended through the thoracic cage to the level of the neck. Extreme care was taken to avoid damage to the underlying blood

vessels, heart and lungs. The thoracic subcutaneous tissue was dissected by lateral thoracotomy scars to expose the internal structures of the thorax. The thorax was opened with lateral thoracotomy incisions and the thoracic cage reflected superiorly. This allowed the passive deflation of the lungs which were not punctured. The thymus was thus exposed and carefully dissected from underlying with a single cut at its root with a sterile scalpel.

Whole thymocytes were then disaggregated by gentle agitation between sterilised frosted glass slides whilst submerged within RMPI 1640 tissue culture medium under sterile conditions within a negative pressure tissue culture hood. For experiments requiring the cells to be labeled with a fluorescent dye, 1µl of CMFDA green or red tracker dye (1ug/ml in DMSO) was added for every $1x10^6$ cells within the suspension and the suspension incubated for 15 minutes at 37°C in a light-proof incubator. Following incubation, 1ml of FCS was added to the suspension to remove any unused dye. The cell suspension was washed by two centrifugations at 4°C, 250G with decanting of supernatant and replacement with fresh PBS.

2.12 Preparation and labeling of apoptotic thymocytes

Thymocytes were harvested from whole thymi and labeled with fluorescent dye as described above. Apoptosis was induced by prolonged serum starvation and exposure to dexamethasone using the following method. A suspension of thymocytes was transferred to a $75cm^2$ tissue culture flask containing RPMI medium,

1μM dexamethasone and 1% FCS. This suspension was then incubated at 37°C for 15 hours. Following incubation, the cell suspension was washed by two centrifugations at 4 °C, 250G with decanting of supernatant and replacement with fresh PBS. Finally, the cells were resuspended to the desired concentration and checked for viability, apoptosis and necrosis as described below.

2.13 Quantification of apoptosis and necrosis in thymocyte suspensions (Annexin V, PI, Hoescht 333342)

The percentage of apoptotic thymocytes in a cell suspension was determined either by a) binding of FITC-conjugated annexin V to the external cell membrane leaflet (demonstrating phosphatidylserine translocation to the outer membrane) or b) pyknotic nuclear morphology (identified by the nuclear dye Hoescht 33342).

2.14 FITC-Annexin V labeling

$1x10^6$ cells were removed from the cell suspension and 1ul of 1:5000 Annexin-V-FITC in (Hanks Balanced Salt Solution with 5μM $CaCl_2$) within a flow cytometry tube. 10ul of the suspension was then placed in a haemocytometer and examined by fluorescence and light microscopy. Annexin-$FITC^+$ cells were apparent by their green fluorescence under fluorescence microscopy; the total number of cells was established by examination under light micrscopy. By dividing the number of

apoptotic cells by the total number of cells in a field the percentage of apoptotic thymocytes within a cell preparation was determined. Typically, a total of 250 cells were counted.

2.15 Hoescht 333342 labeling

The labeling of thymocytes with Hoescht 333342 differs from Annexin-FITC labeling only in the substitution of 1µl of 1:1000 Hoescht 333342 for 1µl Annexin-FITC. Cells were examined under light microscopy to determine the total number of cells in a field as described above. Apoptotic cells were identified by the presence of condensed, pyknotic nuclei, highlighted by Hoescht 333342 which is a DNA-binding nuclear dye. The percentage of apoptotic cells was determined by dividing the number of apoptotic cells by the total number of cells – typically 250 cells were counted in total.

2.16 Propidium iodide (PI) labeling of necrotic cells

PI is a so-called 'vital dye' – ie excluded by cells with proper metabolism and an intact cell membrane. Necrotic cells retain propidium iodide and hence have red fluorescence under fluorescence microscopy. The method for identifying necrotic cells within a sample of thymocytes is identical to that for those for identifying apoptotic cells, as described above. The only difference being the substitution of 1ul of 1:1000 propidium iodide for either annexin-V or Hoescht 333342.

2.17 Preparation and labeling of apoptotic Jurkat T-lymphocytes

The human leukaemic Jurkat T-cell line was maintained in long term culture in 10% FCS/RPMI-1640 medium. Apoptosis was induced and assessed using the methods previously described for apoptotic T-lymphocytes.

2.18 Opsonisation of apoptotic thymocytes with C1q (and BSA)

Apoptotic thymocytes were prepared as previously described. They were then resuspended at $5x10^7$ cells/ml in RMPI culture medium with 10% murine serum from C1qa -/- mice. The cells were then split and either purified human C1q or bovine serum albumin (control) added to a final concentration of 1.5μg/ml. The suspension was then incubated at 37°C for 60 minutes after which the cells were washed twice by centrifugation and resuspension in PBS as previously described.

2.19 Analysis of whole blood for labeled peritoneal Mφs

Experimental mice had previously received IP injections of CMFDA-green labeled apoptotic cells. The peritoneal Mφ which had phagocytosed these cells were thus expected to have acquired the green fluorescent cell tracker dye. 25μl of whole blood was obtained by cardiac puncure and added to 1ml of 3.9% sodium citrate. 100μl of the mixture was aliquoted into flow cytometry tubes. 2 ml of FACSLysis

buffer (BD, UK) was then added to lyse erythrocytes and samples were spun, resuspended and analysed for the presence of green fluorescent apoptotic cell-bearing Mφ using flow cytometry.

2.20 Dissection of the omental lymphoid organ for fluorescence microscopy

Mice were sacrificed by cervical dislocation in accordance with the Centre for Inflammation Research and Home Office guidelines for the care of experimental animals. After 45-60 seconds agonal breathing, cardiac and muscle activity ceased and dissection could begin.

Deceased animals were placed in the supine position on a polystyrene dissection board and secure by placing a single securing pin through each of the four limbs into the dissection board. Fur was removed carefully removed from the lower abdomen using close cut electic shaving clippers. The underlying skin was then cleaned by applying 70% ethanol solution with sterile skins wipes; the skin was then allowed to air dry (approximately 15 seconds). The skin was lifted using rat-toothed forceps and a midline incision from just below the xiphisternum to the pubic area was made using dissection scissors. This incision went through the skin and subcutaneous tissues but did not breach the underlying peritoneal membrane. The skin and the underlying parietal peritoneum were separated by careful blunt dissection of the sub-dermal fascia using curved-ended forceps. Transverse incisions through the skin

were made and further blunt dissection performed allowing it to be reflected completely away from the underlying peritoneal membrane. With practice, this procedure could be completed in 15-20 seconds.

The exposed peritoneal membrane was opened using dissection scissors by means of a longitudinal midline incision. The root of the coeliac mesentary was clamped with a pair of curved forceps and the attached block of tissue comprising the stomach, spleen, part of the small intestine together with the omentum was removed as a single structure by cutting the mesenteric root with dissection scissors. The block was the placed in large petri dish containing cold PBS. Suspension in PBS caused the spleen, stomach and small bowel to sink wheras the omentum floated above these organs, by virtue of it's high fat content. The omentum was then carefully separated from the other organs using dissection scissors and spread on a glass microscope slide. A few drops of PBS were placed over the omentum to assist spreading on the slide and a cover slip placed over the lymphoid organ. Excess fluid was carefully removed with tissue paper and the slide taken for microscopic examination. The process of removing the block of abdominal organs took only 1-2 minutes but the separation of the omentum was an intricate process that took inexperienced operators 10-15 minutes though with experience this operation could be completed within 2-3 minutes.

2.21 Dissection of the omentum for fluorescence microscopy

The abdominal cavity was opened and the omental lymphoid organ and its associated visceral peritoneal membrane recovered as previously described. Other samples of peritoneal membrane were harvested prior to disposal of the carcass. Sections of anterior abdominal wall peritoneal membrane were harvested from the anterior midline region where the abdominal musculature was least abundant. Sub-diaphragmatic peritoneal membrane was removed by careful dissection of the central region of the diaphragm. These samples of peritoneal membrane were mounted on glass slides and covered as described in the previous section. The samples varied somewhat is size but were typically 5x5 mm square sections.

2.22 Quanitification of fluorescent cells within the omental lymphoid organ and other regions of the peritoneal membrane

Labeled cells attached to the omental lymphoid organ were readily seen under fluorescence microscopy. To directly compare the number of labeled apoptotic cells attached to the omental lymphoid organ and other regions of the peritoneal membrane, six randomly selected regions of the lymphoid organ were examined

2.23 Digestion of cells from the omental lymphoid organ and lymph nodes

The omentum or parathymic lymph node was identified, dissected and incubated in 1 ml RPMI 1640 medium with 2.5% liberase (Roche) [1.67 Wunsch U/ml] and 1% DNAse (Roche) for 30 minutes at 37°C. The partially digested lymphoid organ or

lymph node was then disagregated by passed through a 40μm sieve using the plunger from a 1ml sterile syringe. The disagregated cells were resuspended in cold PBS with 5mM EDTA.

2.24 Preparation of a) resident and b) inflammatory Mφs for adoptive transfer

Donor resident peritoneal macrophages were labeled *in situ* with PKH-26PCL dye and peritoneal cells recovered 24 hours later by peritoneal lavage. Peritoneal cells from several donor mice were pooled and resuspended with a macrophage concentration of $1x10^6$ cells/ml. 0.5 ml of donor peritoneal cells were injected into recipients either with $5x10^6$ apoptotic cells (Hoescht 33342 labeled) or PBS. An identical process was followed for the adoptive transfer of inflammatory Mφ except that 0.5 mls of 3% brewers thioglycollate was injected IP 4 days prior to the injection of PKH-26PCL.

The concentration of Mφ was determined by manual counting on a haemocytometer under fluorescent microscopy (red channel). At least 200 cells were counted to determine the final concentration of Mφ.

2.25 Preparation of mixed populations of cells for intraperitoneal injection

Cells of interest were prepared as outlined earlier. Appropriate fluorescent labeling was used to distinguish the populations of cells of interest (as discussed in Results Chapters). Unless otherwise stated, all cells were resuspended to a final concentration of $1x10^{10}$ cells/ml. Cells were differentially labeled to enable identification by microscopy and/or flow cytometry (as discussed in Results Chapters). Equal volumes (and hence equal numbers and concentrations) of cells were mixed to create a 50:50 mixture of cells – no other proportion was used in any experiments. Prior to IP injection, the cells were counted on a haemocytometer to determine a) the presence of fluorescent label and b) the actual mixture of cells in the suspension. An arbitrary tolerance of 50% ± 2% was allowed for each mixture though in fact 50% ± 1% was achieved in practically all experiments. Flow cytometry was used to determine the exact ratio of cells in some early experiments until it became clear that the fluorescence microscopy technique was satisfactory. The following mixtures of cells were used in the work described in this thesis:-

- Viable and apoptotic thymocytes from C57BL/6 mice
- C1q +/+ and C1qa -/- apoptotic thymocytes
- CD-31 +/+ and CD-31 -/- apoptotic thymocytes
- CD-31 +/+ and CD-31 -/- viable thymocytes

2.26 Analysis of data

Experimental data were expressed descriptively as mean values with standard error of mean demonstrated using error bars or preceded by ± symbol. Experimental data were compared using Student's t-test for comparison of two variables. In cases where multiple variables were tested, ANOVA was utilised.

3 CHAPTER 3 – RESULTS SECTION A

3.1 Introduction

The first part of this study involved establishing a murine peritoneal *in vivo* assay for the phagocytosis of apoptotic cells. We took the model employed by Taylor et al. for their work on C1q in the phagocytosis of apoptotic cells (Taylor et al., 2000). This involved the intraperitoneal instillation of apoptotic Jurkat cells – a human T-cell lymphoma derived cell line – which were phagocytosed by either resident or thioglycollate elicited inflammatory Mφ. The rate of phagocytosis of apoptotic cells was determined by measuring the loss of free apoptotic cells and the uptake of apoptotic cells by peritoneal Mφ. We elected to use murine thymocytes as our source of apoptotic cells. These cells die *in vivo* by apoptosis and are cleared by phagocytic Mφ (Surh and Sprent, 1994), though they are not naturally found within the peritoneal cavity. As syngeneic cells, it seemed less likely that they would elicit unwanted immunological or inflammatory responses as a result of cross-species reactivity.

Mφ and apoptotic cells recovered from the peritoneal cavity can be analysed microscopically eg cytospin analysis or by flow cytometry. Flow cytometry has the advantages of speed and objectivity when compared with microscopy and these were the principal reasons why flow cytometry was the preferred method for assessing the phagocytosis of apoptotic cells from peritoneal lavage fluid. Methods to identify Mφ, instilled apoptotic cells and other leukocytes within the peritoneal lavage fluid were developed and validated. This work was then extended to develop a 'single

platform' technique for counting cells within peritoneal lavages using only the flow cytometer, rather than a combination of flow cytometry and microscopy. This required the establishment of an internal standard to convert numbers of flow cytometer recorded events into absolute numbers of target cells per ml of fluid. Fluorescent beads, designed specifically for the calibration of flow cytometers, provided the internal standard required for counting, based on an established technique used to count human blood lymphocyte subpopulations (Nicholson et al., 1997). The assay was then used to determine the kinetics of apoptotic cell clearance from the peritoneal cavity of C57BL/6 mice. A number of genetically manipulated mice lacking genes encoding molecules believed to be important for the phagocytosis of apoptotic cells were bred onto this background and comparative assays were intended to be performed to establish whether knockout mice had *in vivo* defects in the phagocytosis of apoptotic cells.

3.2 Recovery and labeling of peritoneal cells

Peritoneal cells were recovered by the instillation of PBS. The total number of cells recovered from each lavage varied but was typically in the range of 0.5-1.0 $x10^6$ cells/ml in the non-inflamed peritoneal cavity. Flow cytometry with fluorescent immunophenotyping was the principal technique used to identify and quantify peritoneal Mφ. The labels used to identify the principal cell populations within the peritoneal cavity are shown in Figure 8. Representative flow cytometry histogram plots of major peritoneal cell populations are shown in Figure 9. A representative forward versus side scatter dot plot of peritoneal lavage cells is shown in Figure 10.

Figure 8. ***Immunolabeling markers for peritoneal leukocytes***

	Markers[1]	F4/80	B220	CD-3	GR-1	CD11c
Cell types						
Mφ		HI	LO			
B-lymphocyte			HI			
T-lymphocyte				HI		
PMN			LO		HI	
Dendritic cell		LO				HI

HI=highest possible expression of marker; LO=Marker expressed, but at a significantly lower level than HI; Blank box=marker not expressed.

[1](Kishimoto et al., 1997)

Populations of Mφ, B- and T-lymphocytes were all identified amongst cells lavaged from the non-inflamed peritoneal cavity. Neither DCs nor PMNs were found in non-inflamed, resident peritoneal lavages. Bone marrow derived dendritic cells were used as a positive internal control for CD11c.

Figure 9. Flow cytometric analysis of peritoneal leukocytes

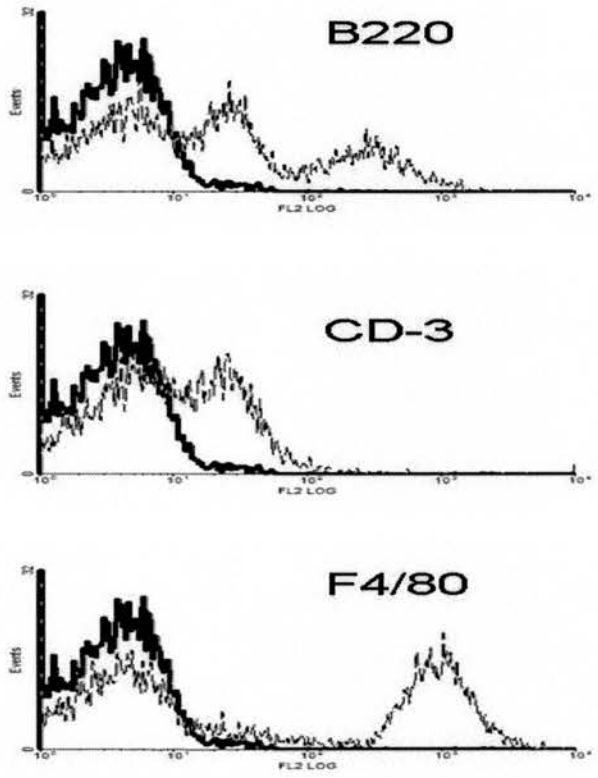

Histograms showing fluorescence in FL2 channel. Faint line represents labeled cells whilst heavy line represents isotype controls. Labels are rat anti-mouse B220-RPE (top), rat anti-mouse CD3-RPE (middle) and rat anti-mouse F4/80-RPE. B220 labeled distinct HI and LO populations. B220-HI are B-1 lymphocytes whereas B220-LO are B-2 lymphocytes and Mφ

Figure 10. Mφ and lymphocytes further defined by distinct forward- and side-scattering properties

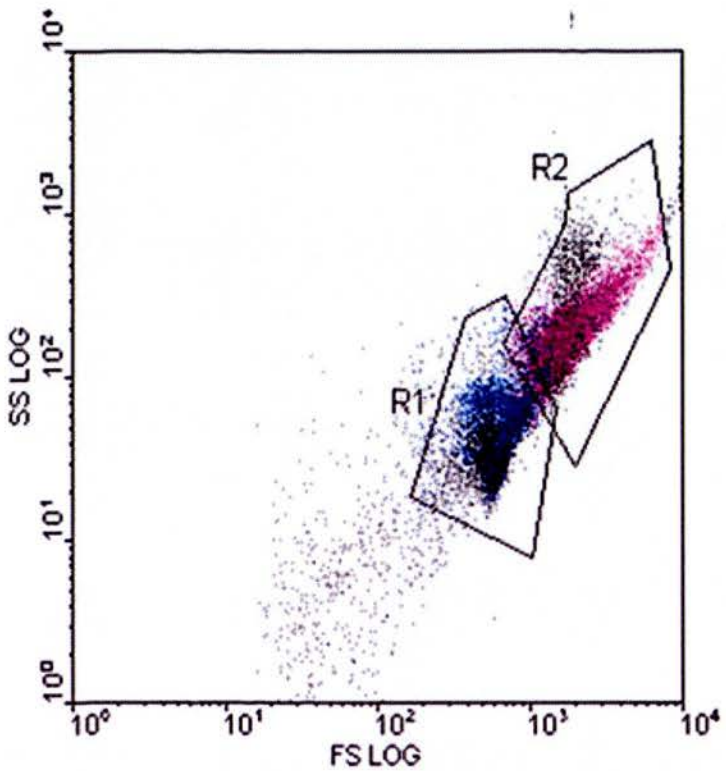

Mφ were clearly and specifically identified by F4/80 fluorescent immunolabeling. Furthermore, applying a coloured gate to F4/80 HI cells identified Mφ as a population of cells with distinct forward (FSC) and side-scattering (SSC) properties (purple events within R2). Similar gating by fluorescence identified lymphocytes within a separate population with lower forward and side scattering properties (blue events within R1). In general terms, forward scatter approximately reflects the size of cells whereas side scatter reflects their granularity. Mφ are larger and more granular than lymphocytes so the relative FSC and SSC properties observed here are appropriate.

3.3 Phagocyte-specific PKH dyes specifically taken up by periteonal Mφ

The fluorescent PKH dyes (PKH-2 and PKH-26) can also be used to label peritoneal Mφ *in vivo* (Melnicoff et al., 1988b). Fluorescent shifts of F4/80-HI Mφ in the FL-1 and FL-2 channels are present 2 hours after the injection of PKH-2 and PKH-26 respectively. Following excitation by a 488nm laser, PKH-2 emits light which is detected in the FL-1 (green) channel. Emitted light from PKH-26 is detected in the FL-2 channel.

Figure 11 below shows peritoneal lavage cells that were either pre-labeled *in vivo* with PKH-2 (green fluorescence, FL-1 channel) or PKH-26 (red fluorescence, FL-2 channel). Peritoneal Mφ were then labeled with F4/80-PE/Cy5 (far-red, FL-4 channel). 99% of the cells which took up the fluorescent PKH dyes were F4/80-HI Mφ. The remaining 1% were F4/80-LO cells and were probably immature monocyte-Mφ.

Figure 11. Peritoneal Mφ specifically take up PKH-2 and PKH-26 fluorescent dyes

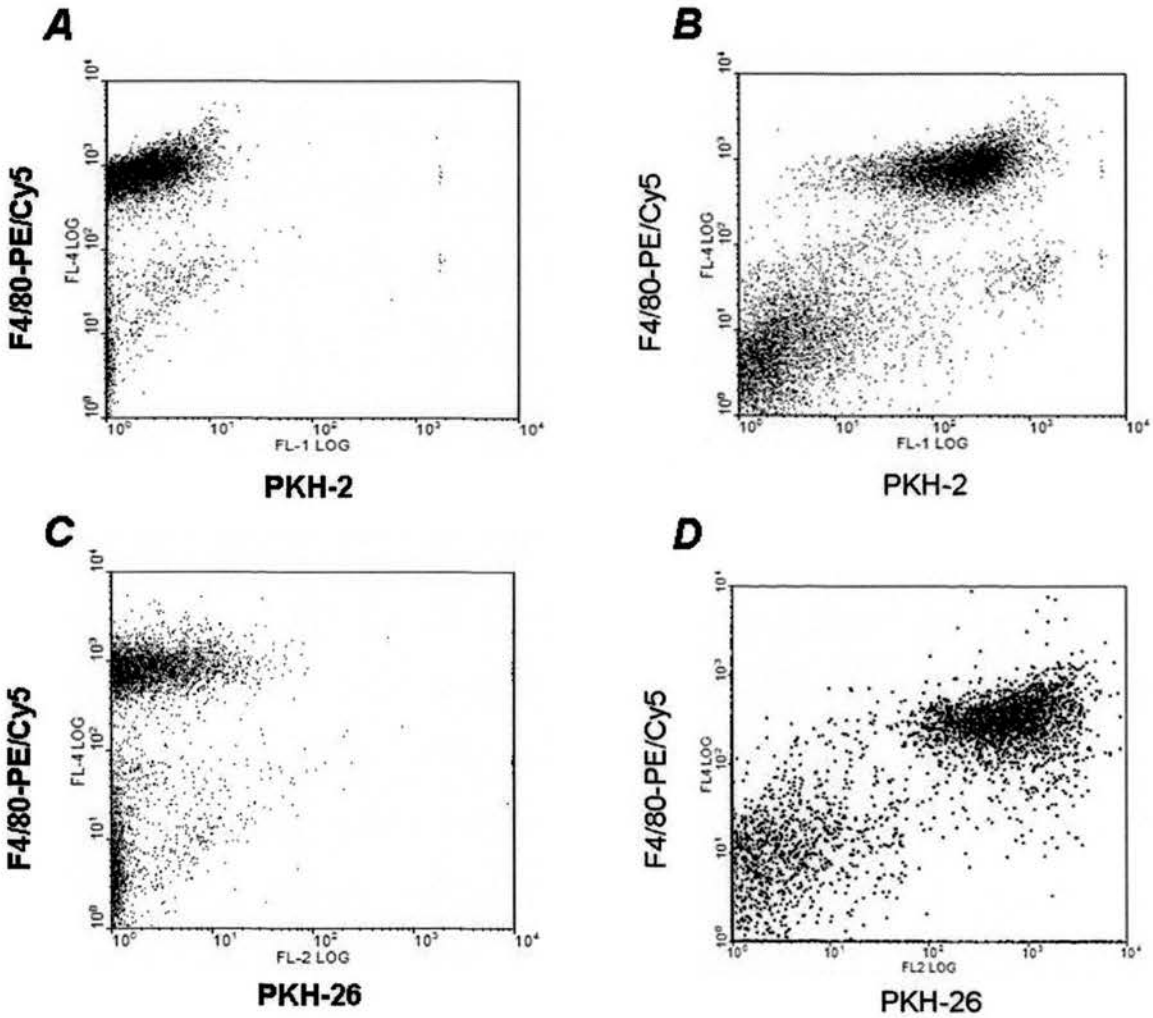

Peritoneal cells from control mice not receiving PKH-2 or PKH-26 have a clear F4/80-HI population (Y-axis) of Mφ with FL-1 and FL-2 fluorescence less that 10^1 units (X-axis) (Panels A and C). The F4/80-HI population acquires FL-1 fluorescence in animals that have received PKH-2 dye (Panel B) and FL-2 fluorescence in those receiving PKH-26 (Panel D). Less than 1% of the PKH+ cells are F4/80-LO.

3.4 Identification of Flowcheck™ microspheres by flow cytometry

Flowcheck microspheres are polystyrene beads of 3 μm diameter that carry fluorophore dyes emitting light detectable in multiple flow cytometer channels. They form a population with very uniform FSC, SSC and fluorescent properties. Their uniform size and fluorescence qualities make these beads ideally suited to the calibration of flow cytometers. They are easy to separate from both the viable and apoptotic cells used in this study.

Figure 12. Flow cytometry FSC/SSC and fluorescent properties of Flowcheck Microspheres

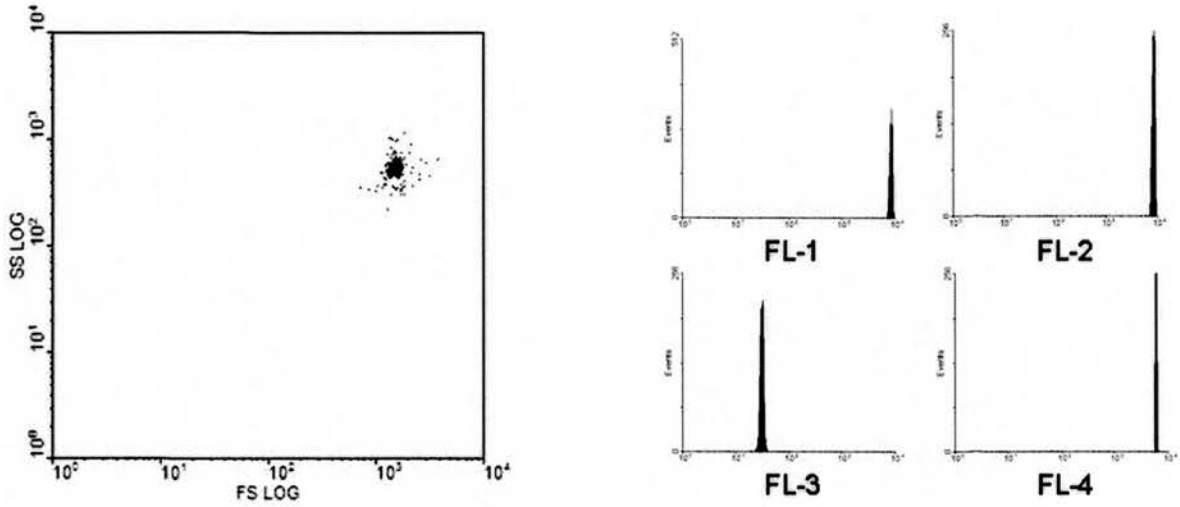

The small degree of variation in the size and shape of Flow-Check® microspheres means that they form a very tight FSC/SSC population (left hand plot). They are polyfluorescent with a very narrow range of emission intensity (right hand panels). These characteristics make it easy to distinguish Flow-Check® microspheres from peritoneal cells by flow cytometry.

3.5 Comparison between single and dual platform enumeration of apoptotic cells

Obtaining the absolute number of cells in a sample by flow cytometry requires the addition of a reference sample of beads to each sample prior to flow cytometry; so-called single-platform counting. By establishing the number of cells of interest per bead, the absolute number of cells per sample can be determined. This method is widely used to precisely define leukocyte subsets in peripheral blood samples (BCSH, 1997). Both single platform and haemocytometer based enumeration of apoptotic thymocytes within peritoneal lavage fluid samples gave extremely similar results (Correlation coefficient=0.96). However, single platform analysis was considerably faster and was unaffected by sample contamination with erythrocytes. For these reasons, single platform analysis was adopted for all subsequent experiments.

Figure 13. Correlation between single and dual platform counting of apoptotic cells from peritoneal lavage fluid

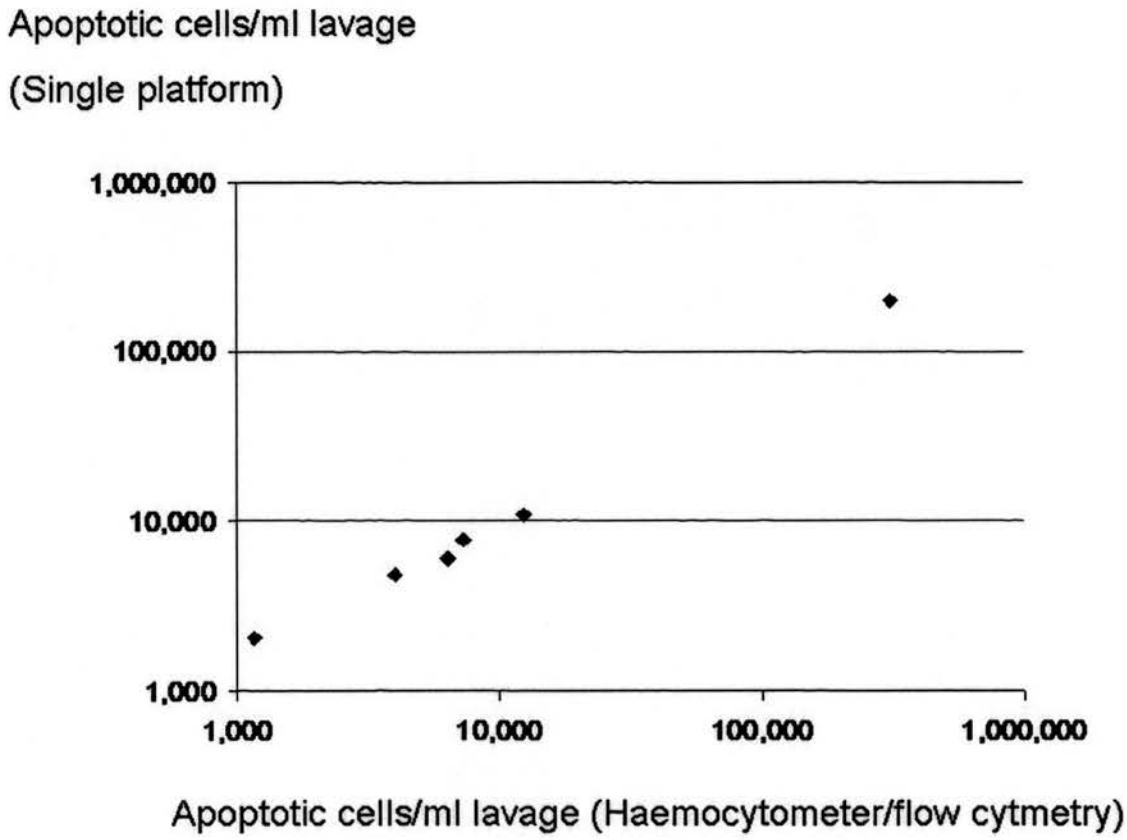

Y-axis shows apoptotic thymocytes counted by the addition of $5x10^4$ Flowcheck™ microspheres into 0.4 mls of various samples of peritoneal lavage fluid. 12,000 events were counted and the number of apoptotic cells/ml lavage fluid calculated as described in 'Methods'. X-axis shows apoptotic cells enumerated by counting total cells/ml by haemocytometry (see methods) and then the number of apoptotic cells within each sample determined by flow cytometry.

3.6 Macrophages phagocytose apoptotic cells

Apoptotic cells are identified within peritoneal lavage samples by flow cytometry. They have the similar FSC and SSC characteristics as lymphocytes. Apoptotic thymocytes have a slightly lower FSC than viable thymocytes as demonstrated below (Figure 14).

Figure 14. Apoptotic thymocytes are annexin-V+

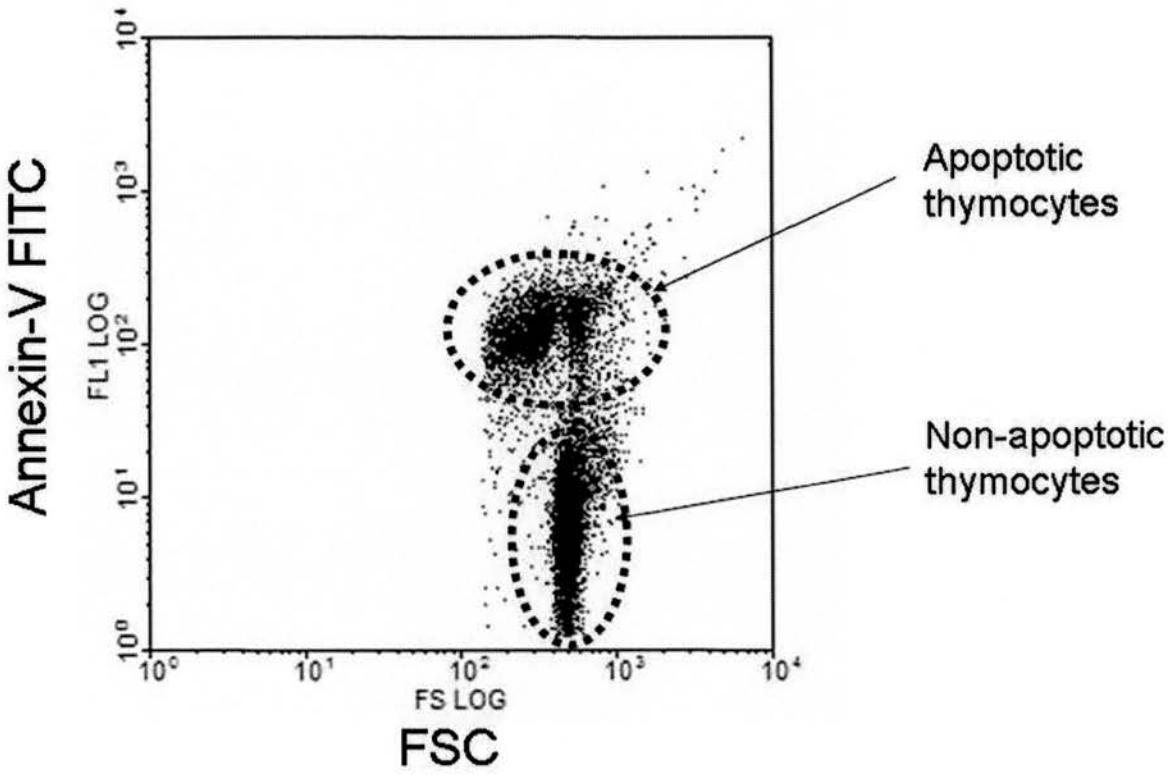

In this sample of thymocytes, approximately half are apoptotic, as defined by annexin-V positivity. The majority of the apoptotic thymocytes have a lower FSC than the non-apoptotic thymocytes. This reflects the loss of cell volume associated with apoptosis.

Figure 15. Flow cytometry plots of peritoneal Mφ phagocytosing apoptotic cells

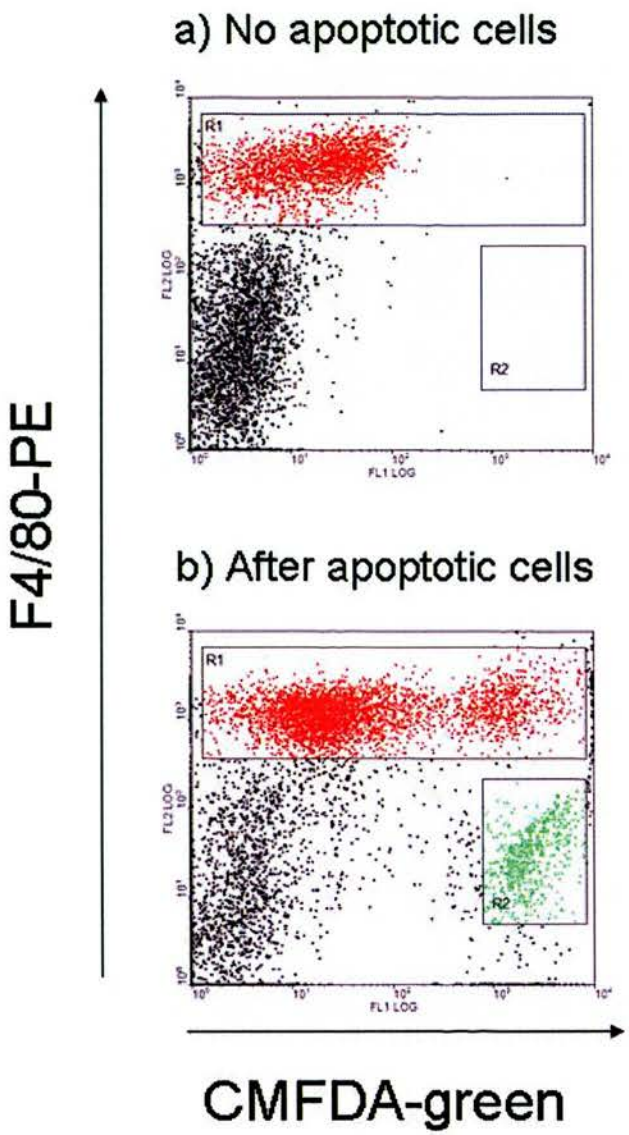

Flow cytometry dot plots of peritoneal lavage cells. Y-axis is F4/80-PE (FL2) and X-axis is CMFDA-Green (FL1). Region 1 (R1) defines Mφ (red); R2 defines apoptotic thymocytes (green). Top panel shows peritoneal lavage cells derived from a non manipulated peritoneum. Bottom panel shows peritoneal lavage cells obtained 15 mins after IP CMFDA-labeled IP apoptotic thymocytes.

Apoptotic thymocytes injected IP are rapidly phagocytosed by peritoneal Mφ. This can be demonstrated by flow cytometry. Apoptotic thymocytes labeled with CMFDA-green were injected IP. After 15 minutes, the peritoneal cells were recovered by lavage. Figure 15 shows recovered peritoneal lavage cells labeled with F4/80-PE (Y-axis, FL-2) from mice which had received CMFDA+ apoptotic thymocytes (panel B) and control mice which received no cells. In control mice receiving no apoptotic cells (panel A), the F4/80-HI Mφ have $<10^2$ units of FL-1 fluorescence (X-axis, FL-1). The Mφ are defined by region 1 (R1). In mice receiving apoptotic thymocytes (panel B), the apoptotic thymocytes form a FL-1 HI, FL-2 LO population (R2). Furthermore, some of the FL-2 HI Mφ in R1 have also become FL-1 HI, indicating phagocytosis of the fluorescent apoptotic cells by Mφ.

3.7 Quantifying the phagocytosis of apoptotic cells in vivo by flow cytometry

Taylor et al. established two methods for quantifying phagocytosis of apoptotic cells within the murine peritoneum by flow cytometry (Taylor et al., 2000). These were to measure (i) the acquisition of apoptotic cell fluorescent marker by peritoneal Mφ phagocytosing labeled apoptotic cells and (ii) the loss of apoptotic cells from the peritoneal cavity over time. Both methods demonstrated delayed peritoneal clearance of apoptotic cells in the C1qa -/- mouse compared to C1q +/+ control animals. However, interpretation of the data from the acquisition of apoptotic cell borne fluorescent label by Mφ was not straightforward.

Figure 16. Phagocytosis of apoptotic Jurkat cells in C1qa -/- and C1q +/+ mice (Taylor et al., 2000)

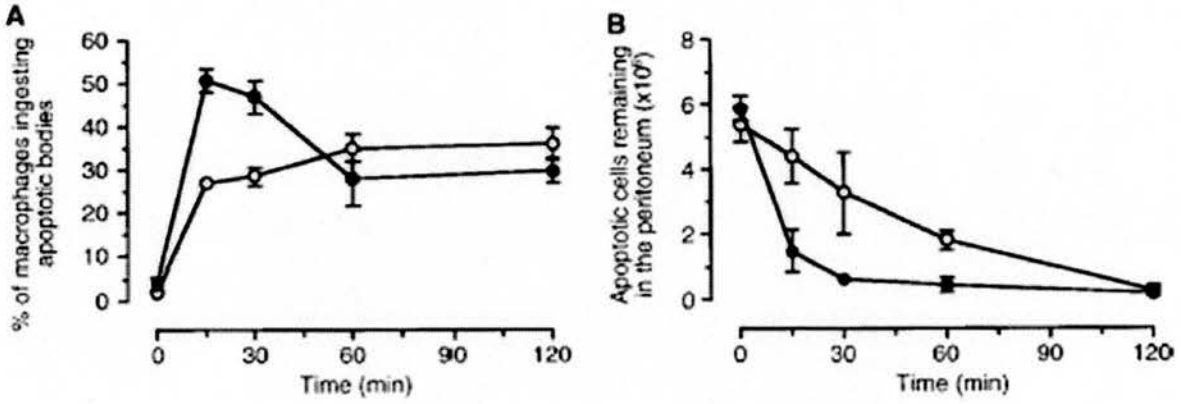

Kinetic assay of fluorescently labeled apoptotic cell (Jurkat cells) peritoneal phagocytosis. Empty circles represent C1qa -/- mice; filled circles represent C1q +/+ control animals. Reproduced from The Journal of Experimental Medicine, 2000, **192,** 359-66 by copyright permission of Rockerfeller University Press (Taylor et al., 2000)

Figure 16A uses the acquisition of fluorescence from phagocytosed apoptotic cells as a surrogate for the percentage of Mφ phagocytosing apoptotic cells. Figure 16B shows the number of apoptotic cells recovered from the peritoneal lavage fluid. In both cases, defective phagocytosis of apoptotic cells within the peritoneal cavity is apparent in Clq -/- mice. Furthermore, the supply of apoptotic cells for phagocytosis appears to have been exhausted after 30 minutes in the wildtype mice (Figure 16B) although the percentage of phagocytic Mφ remains around 30%, significantly above the baseline. If Figure 16A were interpreted in isolation then a misleading conclusion might be reached – that phagocytosis of apoptotic cells continued. Figure 16B seems to give a more straightforward representation of the true state of the system. Therefore the loss of labeled, recoverable apoptotic cells was adopted as the principle quantitative measurement of intraperitoneal apoptotic cell phagocytosis.

3.8 Kinetics of the phagocytosis of apoptotic cells instilled IP into C57BL/6 mice

$5x10^6$ CMFDA-green labeled apoptotic thymocytes in 0.5 mls of PBS were injected intraperitoneally into C57BL/6 mice aged between 8-12 weeks. Peritoneal lavage was performed after 1, 5, 10 and 30 minutes and the recovered cells labeled and counted by flow cytometry as described. The experiment was repeated on 3 occasions with 4-6 animals per time point in each experiment.

The recovery of cells at 1 minute was intended to indicate the proportion of apoptotic cells lost by mechanisms other than phagocytosis; 72.9 ± 1.7 % of injected apoptotic thymocytes were recoverable at this time point.

Figure 17. Intraperitoneal phagocytosis of apoptotic thymocytes in C57BL/6 mice

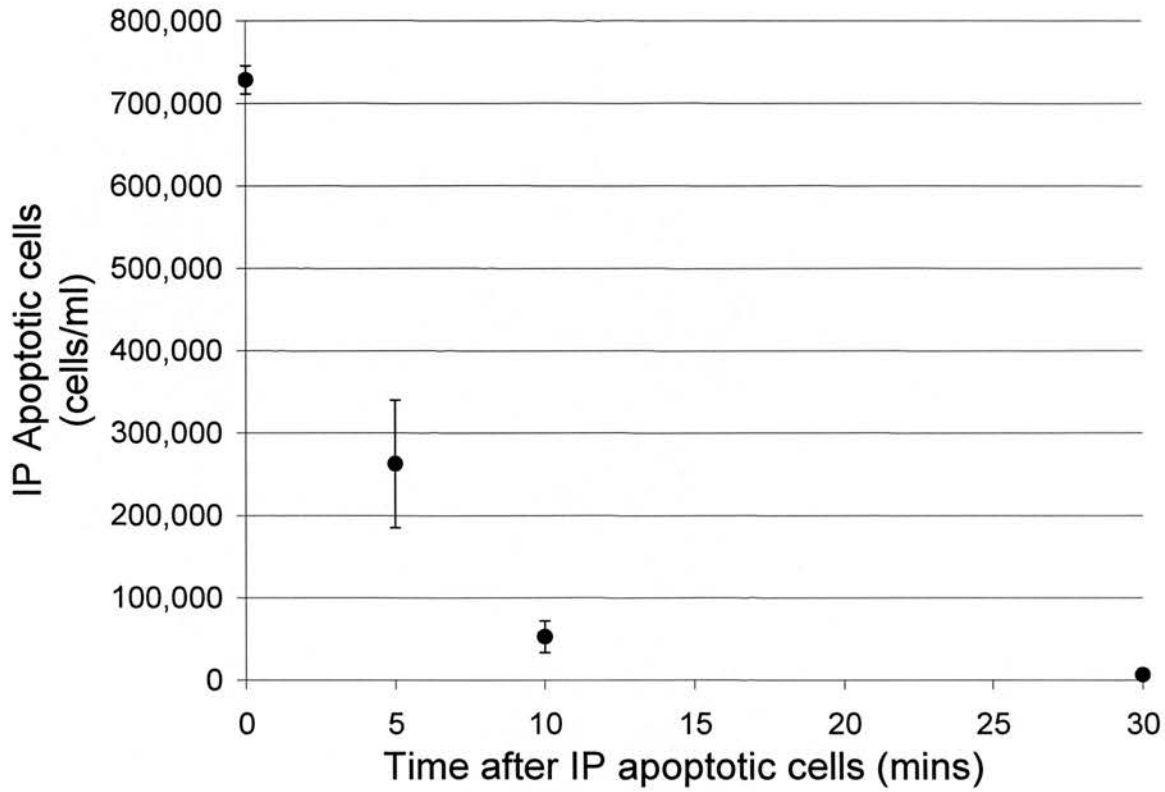

Y-Axis= number of CMFDA-labeled apoptotic thymocytes recovered from C57BL/6 mice at various intervals following their intraperitoneal injection. X-axis = time peritoneal lavage performed following IP injection. N=12 per group; data from 3 experiments.

3.9 'Disappearance' of peritoneal Mφ occurs synchronously with apoptotic cell phagocytosis

Single platform enumeration of apoptotic cells using Flowcheck beads also allowed the quantification of Mφ. Casual observation suggested that the frequency of Mφ 'events' observed by flow cytometry was lower in peritoneal lavages from animals that had received apoptotic thymocytes than those which had not. Formal analysis confirmed that the number of recovered Mφ fell dramatically after IP apoptotic thymocytes (Figure 18).

Figure 18. Mφ disappearance from C57BL/6 peritoneal lavages following IP apoptotic cells

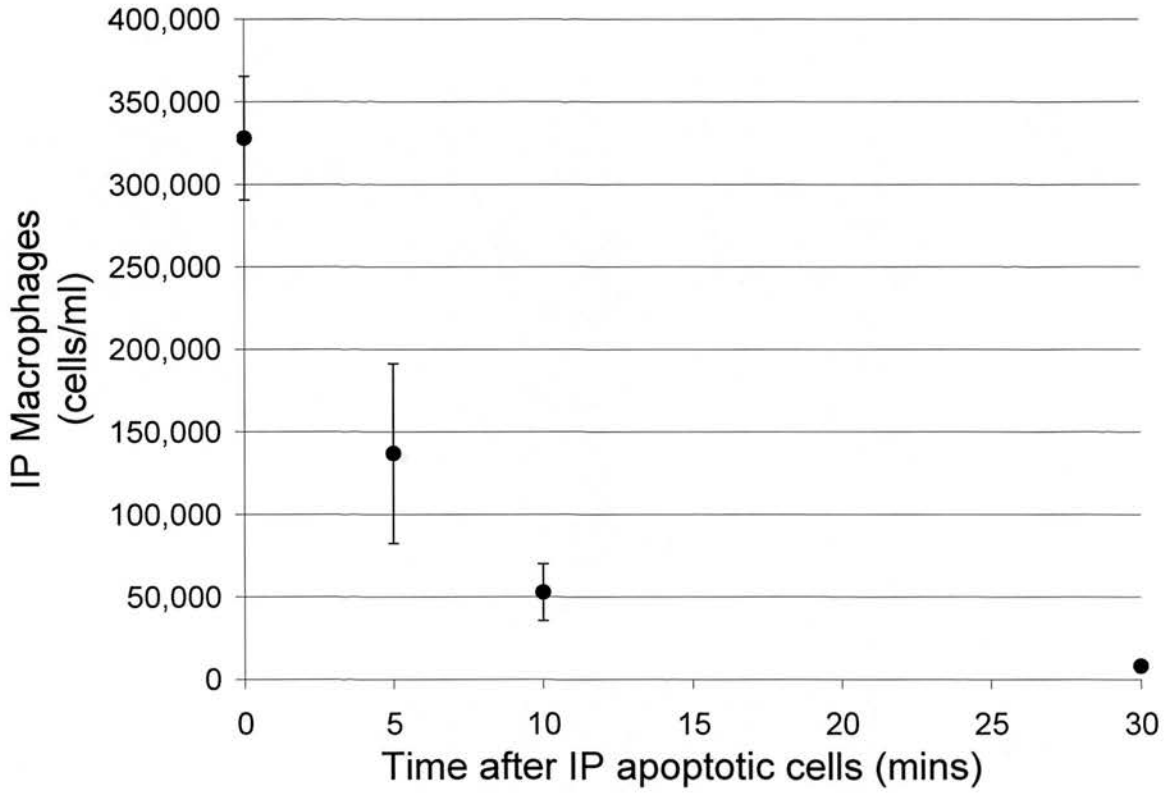

Y-axis = Number of F4/80-labeled peritoneal Mφ recovered from C57BL/6 mice at various time intervals following the IP injection of $5x10^6$ CMFDA-labeled apoptotic cells. X-axis = time that peritoneal lavage was performed following IP apoptotic cells. Time 0 is the 'in-out' lavage of Mφ immediately after the IP injection of apoptotic cells. N=12 per group; data from 3 experiments.

Most striking of all was the high degree of synchronicity observed between the loss of apoptotic cells and the disappearance of peritoneal Mφ. When plotted on the same graph, the rate of apoptotic cell and Mφ disappearance are almost identical (Fig. 20). Analysis of the peritoneal phagocytosis assay data (excluding 1 minute lavages) showed a correlation between Mφ and apoptotic thymocyte recovery of +0.95 (Spearman's Rank Correlation). No significant correlation was seen in lavages taken 1 minute after the instillation of apoptotic cells, supporting the notion that this was a time-dependent phenomenon.

The striking synchronicity of apoptotic cell clearance and Mφ disappearance from the peritoneal cavity raised the possibility of a link between these two processes, meriting further investigation. Moreover the nature of the peritoneal Mφ 'disappearance' was unclear. Both phenomena merited further investigation.

Figure 19. Correlation between apoptotic cell phagocytosis and Mφ disappearance from the peritoneal cavity

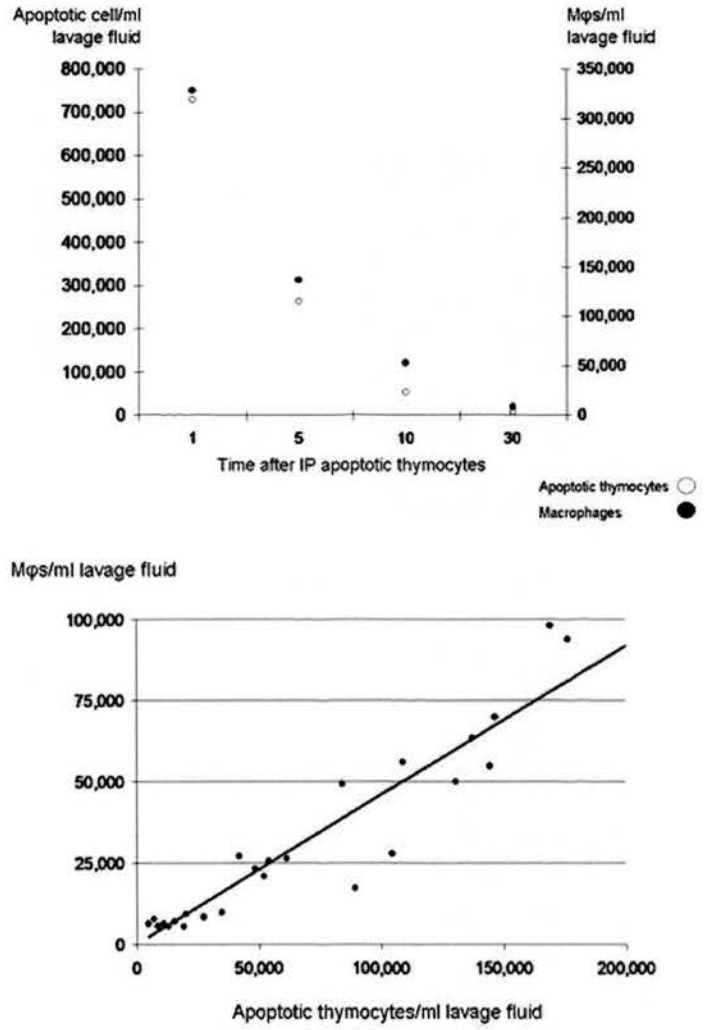

Upper figure –Y axis (left) - Mφ recovered per ml of lavage fluid; Y axis (right) - apoptotic cells recovered per ml of lavage fluid. Values shown are means. X-axis is time after IP injection of apoptotic cells at which peritoneal lavages were performed.

Lower figure – same data set shown as scatter plot. Line of best fit displayed illustrating high degree of correlation between Mφ and apoptotic cell recovery. Spearman's rank correlation coefficient = +0.95. N=12 per group; data from 3 experiments.

3.10 Summary

- Intra-peritoneal cells can be recovered by lavage, identified by immunofluorescent labelling and counted by flow cytometry.

- Peritoneal lavage cells can be counted using a single platform flow cytometry technique with Flowcheck™ microspheres as an internal control.

- Apoptotic thymocytes are rapidly phagocytosed by peritoneal Mφ.

- A profound loss of recoverable peritoneal Mφ occurs in synchrony with the phagocytosis of apoptotic cells – a 'Macrophage Disappearance Reaction (MDR).

3.11 Questions

- Where do the apoptotic cells and Mφ go following the MDR?
- Is the MDR a *consequence* of the phagocytosis of apoptotic cells?
- Can other bioparticles induce a MDR?
- What is the mechanism or mechanisms that drive the apoptotic cell induced MDR?

4 CHAPTER 4 RESULTS SECTION B

4.1 Mφ disappearance reaction is neither caused by sham injection nor injection of PBS

It was necessary to establish that the disappearance of peritoneal Mφ that followed the injection of apoptotic cells was due to the apoptotic cells rather than some other aspect of intraperitoneal injection. To that end, various control experiments were undertaken. The MDR is known to follow the injection of killed bacteria (Haskill and Becker, 1985) and pro-inflammatory substances such as thioglycollate (Melnicoff et al., 1989). The risk that bacteria within the fur of experimental mice might be transferred to the peritoneal cavity and induce a MDR was a potential confounding factor in our previous observations. This was addressed in a number of ways. Firstly, all reagents used in experiments were sterile and manufactured free of lipopolysaccharide (LPS). Secondly, all preparation of substances for intraperitoneal injection was performed in a negative pressure sterile tissue culture hood. Thirdly, polymyxin B, which binds and deactivates LPS was added to all substances for intraperitoneal injection. Fourthly, fur was shaved from the peritoneal injection site and the underlying skin cleaned with a sterile wipe prior to injection. Finally control experiments were performed to determine whether the MDR observed following apoptotic cell injection was caused by the apoptotic cells or some other factor in the injection.

Groups of mice were injected with a variety of control substances to test the specificity of apoptotic cells as a causative agent of the MDR. In the following experiment, mice were divided into the following groups:

- No intraperitoneal injection,
- Sham injection (i.e. skin breeched but NO intraperitoneal injection),
- 0.5ml PBS/polymyxin B (50μg/ml),
- $5x10^6$ thymocytes, 80% viable (PI negative), 20% apoptotic in 0.5 mls PBS/polymyxin (50μg/ml)
- $5x10^6$ thymocytes, 20% viable, 80% apoptotic in 0.5 mls PBS/polymyxin

30 minutes after these intraperitoneal injections, mice were sacrificed and peritoneal cells recovered by a 5ml lavage. Mφ were labeled with F4/80-PE and counted by flow cytometry as previously described.

Neither a sham injection nor the injection of 0.5 mls PBS/polymyxin B induced a MDR. However, IP cells exhibiting either a low or high level of apoptosis induced the disappearance of 59.5% and 82.8% of peritoneal Mφ ($p=0.00004$ and $p=0.000002$ respectively). The MDR induced by highly apoptotic cells was significantly greater than that induced by cells exhibiting a low level of apoptosis ($p=0.01$) (Figure 20).

Figure 20. ***IP Apoptotic cells cause a significant MDR compared to control injections***

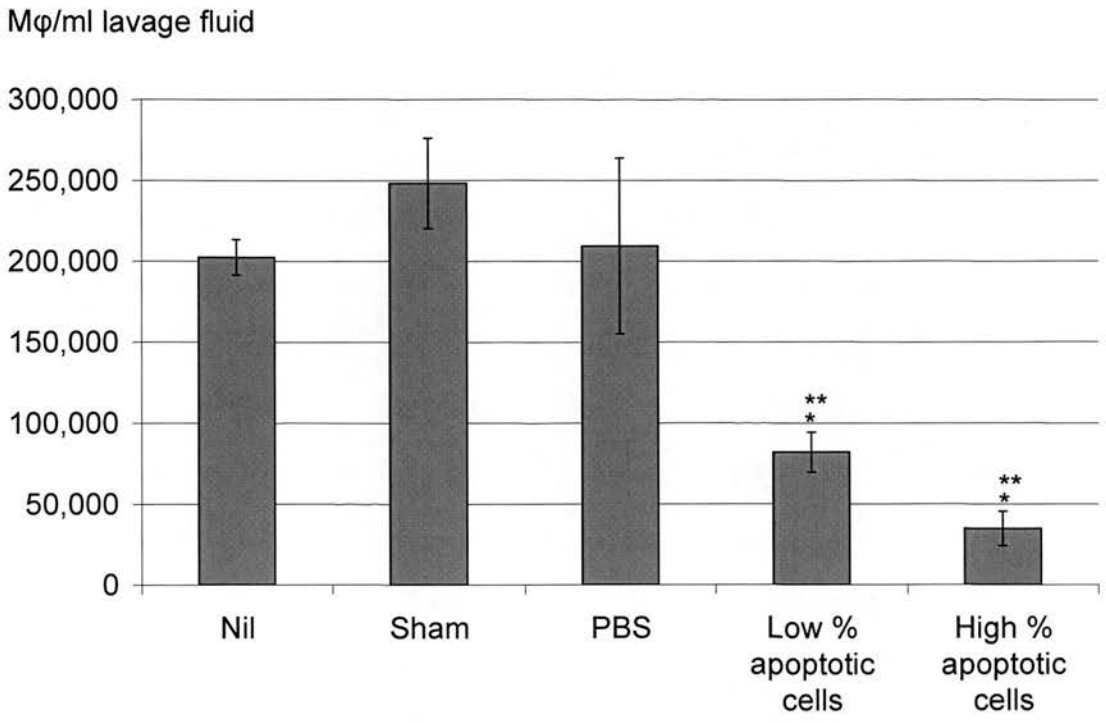

Y-axis = Number of peritoneal Mφ recovered by peritoneal lavage 30 minutes after various intraperitoneal injections. X-axis = nature of peritoneal lavage. N=5 per group; 2 experiments*=statistically significant reduction in the number of Mφ recovered after the injection of either low or high apoptotic cells compared to no IP injection. **=statistically significant reduction in the number of Mφ recovered after IP high % apoptotic cells compared to low % apoptotic cells. N=5 per group; 2 experiments.

LPS is not mediating the apoptotic cell-induced MDR

Lipopolysaccharide (LPS) is a pro-inflammatory substance which may induce a MDR, though this has not been proven. Furthermore, LPS is produced by a wide variety of bacteria and contamination of experimental reagents is often hard to avoid. Experiments were therefore performed to determine whether LPS was entirely or partially mediating the MDR. These employed polymyxin B, a powerful antagonist of LPS (Jacobs and Morrison, 1977), and CD-14 knockout mice which are resistant to LPS (Haziot et al., 1995).

CMFDA-labeled apoptotic thymocytes were prepared using the standard method and resuspended at a concentration of $1x10^7$/ml. Half of the apoptotic cells were resuspended in PBS containing 0.5mg/ml polymyxin B and the remainder in PBS without polymyxin B. Groups of C57BL/6 female mice (6 mice per group) received IP injections of apoptotic cells in suspensions with or without polymyxin B. After 30 minutes, the animals were sacrificed, the peritoneal cells lavaged with 5 mls PBS and Mφ labeled with F4/80 as previously described. Female littermates aged less than 10 weeks were used in all experiments.

A MDR was observed in mice receiving apoptotic cells either with or without polymyxin B (Figure 21). Furthermore, similar losses of apoptotic cells were observed in both groups, indicating similar levels of phagocytosis. No statistically significant difference in either the size of the MDR or the loss of apoptotic cells was

seen in mice receiving polymyxin B or PBS control injections. This suggested that LPS was not mediating the apoptotic cell induced MDR.

Figure 21. Polymyxin B does not change the size of the MDR

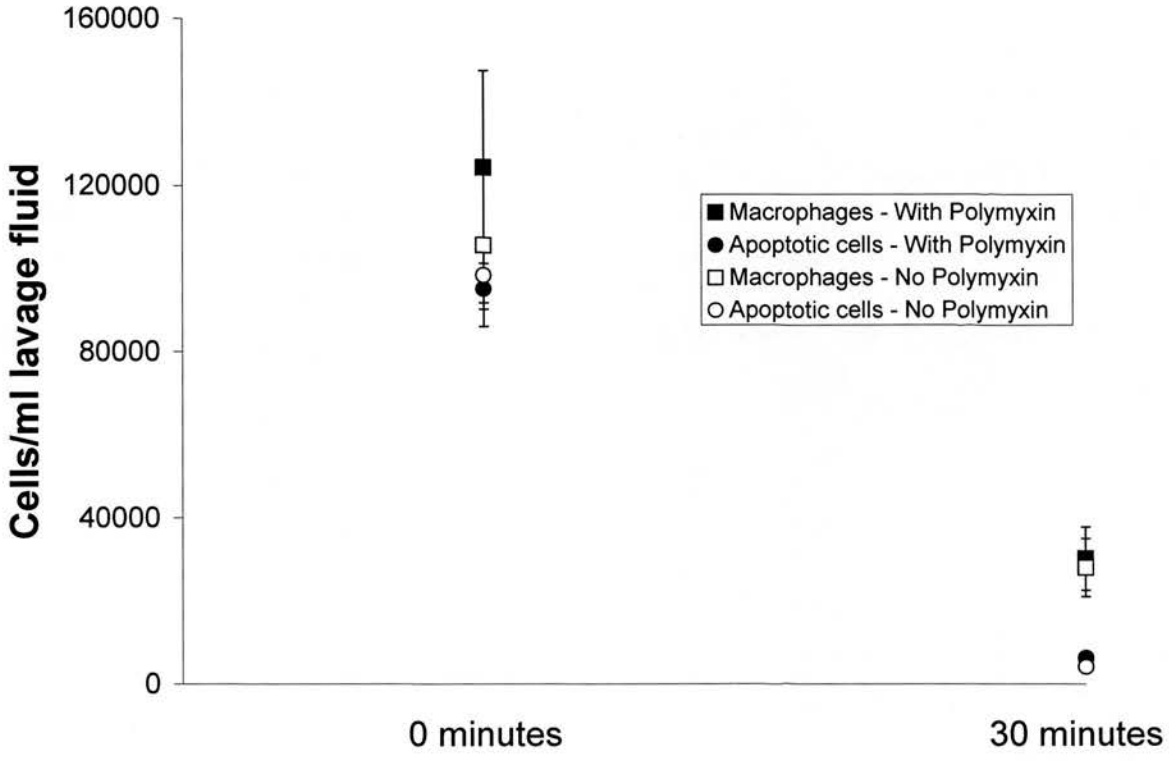

Y-axis = cells (Mφ or apoptotic thymocytes as indicated) recovered by peritoneal lavage after IP injection of apoptotic thymocytes with or without polymyxin. X-axis = time interval between IP injection and peritoneal lavage. N=4 per group; 2 experiments.

To further examine the possibility that LPS was involved in the MDR, CD-14 knockout mice were used. These mice are known to be 10,000 times less responsive to LPS than control mice (Haziot et al., 1995). CD-14 has also been reported to play a role in the phagocytosis of apoptotic cells *in vitro* (Devitt et al., 1998). No significant difference was seen between CD-14 knockout and wildtype mice in either the rate of apoptotic thymocyte phagocytosis or the rate of Mφ disappearance (Figure 22). No significant difference was observed in the clearance of apoptotic cells, though there was a trend towards impaired clearance in the CD-14 KO group (WT Vs KO mice $1.36x10^5 \pm 1.78x10^3$ cells/ml Vs $1.18x10^5 \pm 2.38x10^3$ cells/ml, p=NS). The similar MDR in CD-14 wildtype and knockout animals further suggests that the apoptotic cell-induced MDR is not a merely a consequence of LPS contamination.

Figure 22. The MDR is equivalent in LPS-insensitive CD-14 -/- mice and LPS-sensitive controls

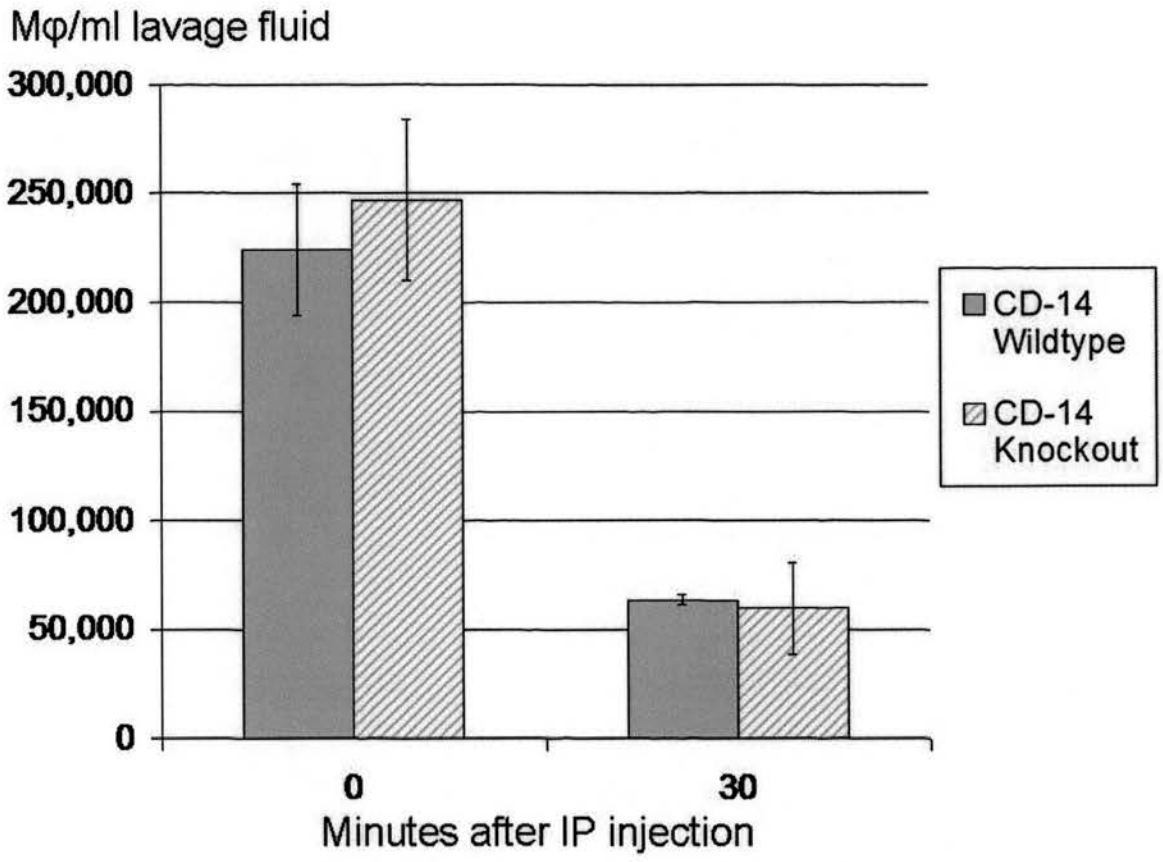

Y-axis=mean number of Mφ recovered per ml lavage fluid. X-axis= time elapsed after the IP injection of $5x10^6$ CMFDA labeled apoptotic thymocytes. N=5 per group; 2 experiments.

4.2 The intraperitoneal administration of apoptotic human cells also cause a MDR

Thus far the MDR had only been observed following the injection of murine apoptotic thymocytes. To determine the generality of the apoptotic cell induced MDR, apoptotic human Jurkat T-cells were injected IP and the effect on the Mφ population was observed. Then $5x10^6$ CMFDA labeled apoptotic Jurkat cells (45.76% apoptotic) were injected IP into female C57/BL6 mice which were sacrificed 30 minutes later. Recovered Mφ and non-phagocytosed Jurkat cells were counted by flow cytometry as previously described.

A MDR was observed following the injection of apoptotic human thymocytes resulting in the disappearance of approximately 60% of the resident Mφ population. An almost identical reduction in the number of apoptotic cells was observed. The magnitude of apoptotic Jurkat cell clearance and the MDR was somewhat less than the equivalent phenomena induced by apoptotic murine thymocytes. This probably was a consequence of the lower proportion of apoptotic cells in the Jurkat cell population (all data – Figure 23).

Figure 23. Intraperitoneal apoptotic Jurkat cells also induce a MDR

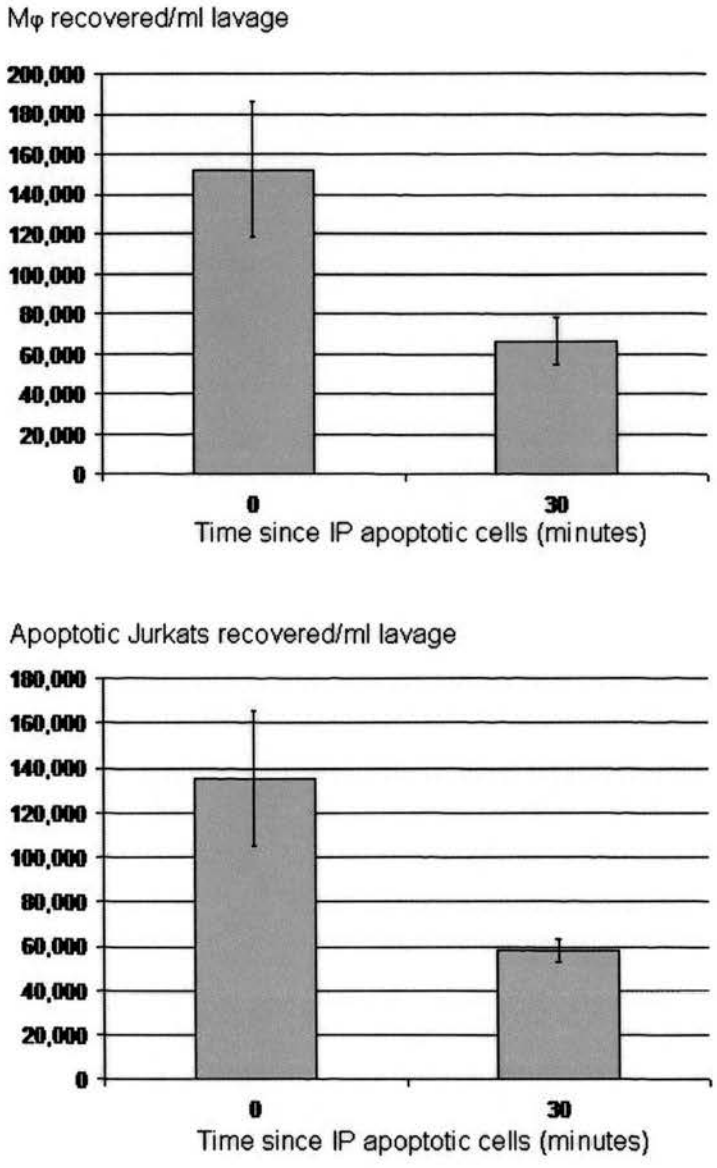

Top figure – Y-axis= mean Mφ recovered/ml lavage fluid; X-axis time interval between apoptotic cell injection and peritoneal lavage

Bottom figure – Y-axis = mean apoptotic Jurkat cells recovered/ml lavage fluid; X-axis same as top figure. N=6 per group; 2 experiments.

4.3 Viable, non-apoptotic jurkat cells do not cause a MDR

The previous experiment had demonstrated that the IP instillation apoptotic human Jurkat T-cells could induce an MDR. The loss of Mφ was smaller than observed with apoptotic murine thymocytes. One possible explanation for this was the presence of a higher proportion of viable cells than was generally present in preparations of apoptotic murine thymocytes. It was decided to determine whether a pure population of viable human Jurkal T-cells would, when instilled IP, cause a MDR.

Viable Jurkat T-cells were taken directly from culture, washed, labeled with CMFDA green and respuspended in PBS at a concentration of 1x106 cells/ml. PI and Hoescht 33342 labelling showed 0.5% necrosis and 1.2% apoptosis respectively. Then $5x10^6$ CMFDA labeled viable Jurkat cells were injected IP into female C57/BL6 mice which were sacrificed 30 minutes later. Recovered Mφ and non-phagocytosed Jurkat cells were counted by flow cytometry as previously described.

Neither a significant MDR nor loss of Jurkat cells was observed 30 minutes after the IP instillation of labeled Jurkat cells (Figure 24). Furthermore, there was little evidence of murine Mφ-jurkat cell interaction seen on flow cytometry (ie few F4/80+ CMDFA + cells). These data suggested that murine Mφ did not phagocytose viable Jurkat T-cells nor did the presence of Jurkat T-cells induce a MDR.

Figure 24. Viable Jurkat cells do not induce a MDR

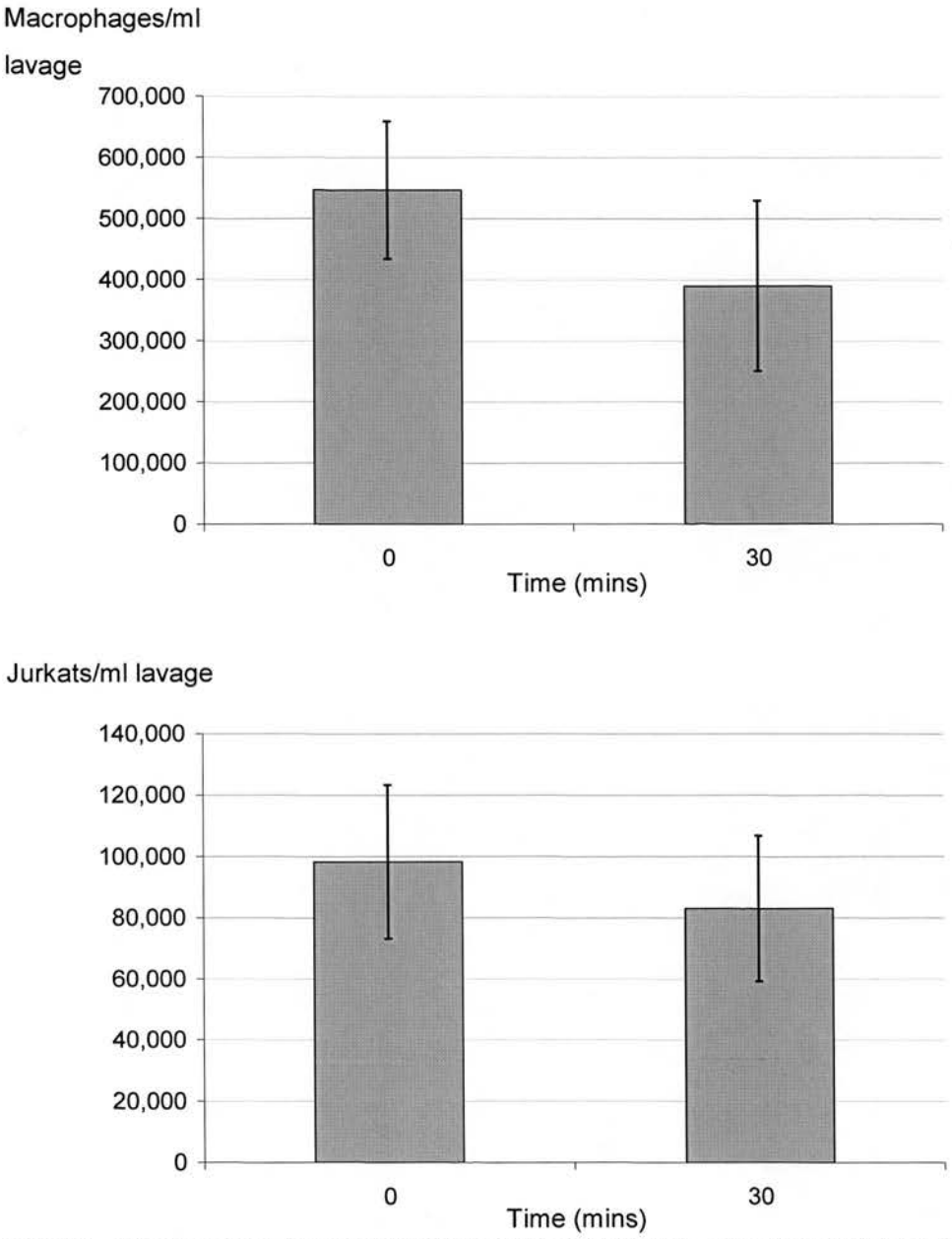

Top figure – Y-axis = mean Mφ recovered/ml lavage fluid; X-axis = time interval between viable cell injection and peritoneal lavage.

Bottom figure – Y-axis = mean viable Jurkat cells recovered/ml lavage fluid; X-axis same as top figure. N=5 per group; 2 experiments.

4.4 Apoptotic human PMNs cause a MDR

Further proof of the generality of the apoptotic cell induced MDR, apoptotic human PMNs were injected IP and the effect PMNs (91% apoptotic) were injected IP into female C57/BL6 mice which were sacrificed 30 minutes later. Recovered Mφ and non-phagocytosed apoptotic PMNs were counted by flow cytometry as previously described.

A very large MDR was observed following the injection of apoptotic human PMNs resulting in the disappearance of 89% of the resident Mφ population. A 91% reduction in the number of recovered apoptotic PMNs was also observed. The magnitude of apoptotic Jurkal cell clearance and the MDR was comparible to that seen when apoptotic murine thymocytes were injected IP, probably reflecting similar high numbers of apoptotic cells instilled (in contrast to the IP injection of apoptotic Jurkat T-cells). This probably was a consequence of the lower proportion of apoptotic cells in the Jurkat cell population. A highly significant MDR was observed following the IP injection of apoptotic cells (0 Vs 30 mins $2.65x10^5 \pm 2.51x10^4$ cells/ml Vs $2.97x10^4 \pm 1.97x10^3$ cells/ml p=0.00003, N=8, data from 2 experiments). A significant loss of apoptotic PMNs was also seen (0 Vs 30 mins $6.93x10^5 \pm 9.60x10^4$ cells/ml Vs $6.29x10^4 \pm 7.00x10^3$ cells/ml p=0.00001, N=8, data from 2 experiments).

Figure 25. Apoptotic human PMNs induces a MDR

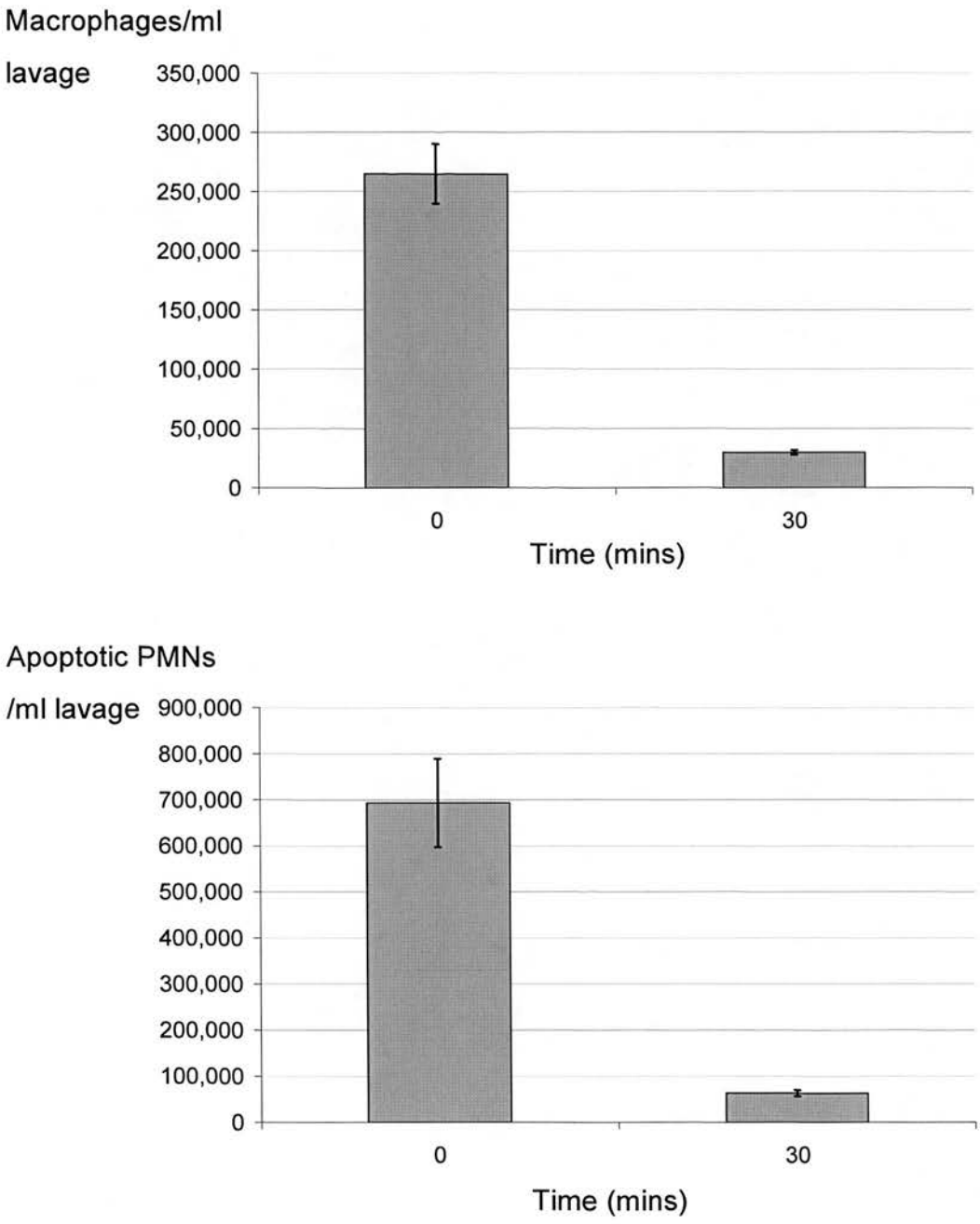

Top figure – Y-axis, mean Mφ recovered/ml lavage fluid; X-axis time interval following apoptotic cell injection.

Bottom figure – Y-axis mean apoptotic human PMNs recovered/ml lavage fluid; X-axis same as top figure. N=8 per group, data from 2 experiments.

4.5 Apoptotic thymocytes induce a greater MDR than latex beads

It was unclear whether the MDR which followed the injection of apoptotic cells was due to the presence of apoptotic cells *per se* or the phagocytosis of apoptotic cells by Mφ. To that end, phagocytosable synthetic beads were injected IP and the subsequent MDR compared with that induced by apoptotic cells. $5x10^6$ 2μm fluorescent polystyrene beads (2 μm latex beads, carboxylate-modified polystyrene, fluorescent yellow-green – Sigma-Aldrich Co. Ltd, UK) were injected IP in 0.5 mls PBS. These beads were known to be readily phagocytosed by Mφ (personal communication Simone Brown). A second group of mice received $5x10^6$ CMFDA labeled apoptotic thymocytes. Mice from both groups were sacrificed after 30 mins, peritoneal lavage performed and the number of recovered Mφ, labeled apoptotic thymocytes or beads counted by flow cytometry. Peritoneal lavage was also performed in a group of uninjected control mice.

The injection of latex beads did induce a significant MDR with a 68% reduction in the number of recoverable Mφ ($p=0.001$). However, a larger MDR (85% Mφ disappearance) was observed following the IP injection of apoptotic thymocytes ($p=0.0001$ – Figure 26). The MDR induced by apoptotic thymocytes was significantly greater than that induced by latex beads ($p=0.01$). More than 98% of beads and apoptotic cells were cleared from the peritoneum during the course of the experiment with no significant difference in the clearance of either particle observed.

Figure 26. Apoptotic thymocytes induce a greater MDR than latex beads despite comparable phagocytic clearance

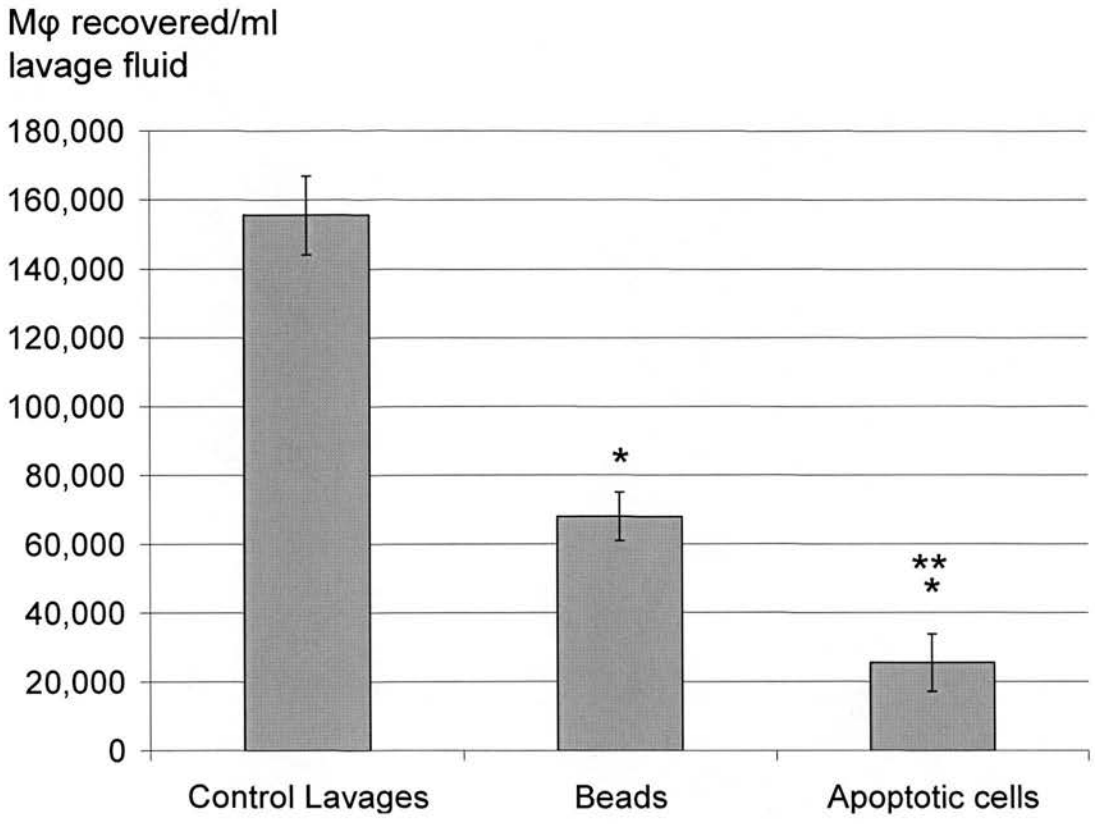

Latex beads and apoptotic thymocytes both induce a significant decrease in the number of recoverable peritoneal Mφ. *=Mφ significantly lower from control ($P<0.05$). **=Mφ significantly lower than beads ($p<0.05$). N= 7 per group; 2 experiments.

4.6 Decreased phagocytosis of apoptotic cells and a decreased MDR are observed in C1qa -/- mice

It has been established that the phagocytic clearance of apoptotic cells is significantly reduced in the C1qa -/- knockout mouse (see Chapter 1) (Taylor et al., 2000). This was manifested most clearly in a delayed removal of fluorescently labeled apoptotic cells from the peritoneal cavity. This previous study used a very similar peritoneal lavage technique to recover and count leukocytes but the number of recovered Mφ was not commented upon. I hypothesised that if the disappearance of Mφ was causally linked to the phagocytosis of apoptotic cells, and this was delayed in the C1qa -/- mouse, the MDR might also be delayed in the C1qa -/- mouse.

The published data suggested that a high number of apoptotic cells would be required to unmask the phagocytosis defect in the C1qa -/- knockout mouse. With this in mind, 10^7 CMFDA-labeled apoptotic thymocytes were injected IP into C1qa -/- knockout mice and age and sex matched wild-type control animals (all females). After 30 minutes, animals were sacrificed, peritoneal cells recovered by lavage, labeled and counted by flow cytometry, as previously described. Lavages of both C1qa -/- knockout and control animals were also performed to establish the number of lavagable peritoneal Mφ for each genotype of mouse.

Approximately four times as many IP apoptotic cells were recovered from the C1qa -/- knockout mice than controls 30 mins after IP apoptotic thymocyte injection

($p=0.007$ – Figure 27A). This demonstrated the expected defect in phagocytosis of apoptotic cells known to exist in C1qa -/- mice (Taylor et al., 2000). There was no significant difference between C1qa -/- knockout and control mice in terms of the baseline number of Mφ. However, whilst a MDR was observed in both the C1qa -/- knockout and control mice 30 minutes after IP apoptotic cells, this was significantly larger in the control mice than C1qa -/- knockout mice ($p=0.0007$ – Figure 27B). This suggested that either C1q itself is actively involved in the MDR or that defective phagocytosis of apoptotic cells is associated with a smaller MDR.

Figure 27. Decreased phagocytosis of apoptotic cells and a decreased MDR are observed in C1qa -/- mice

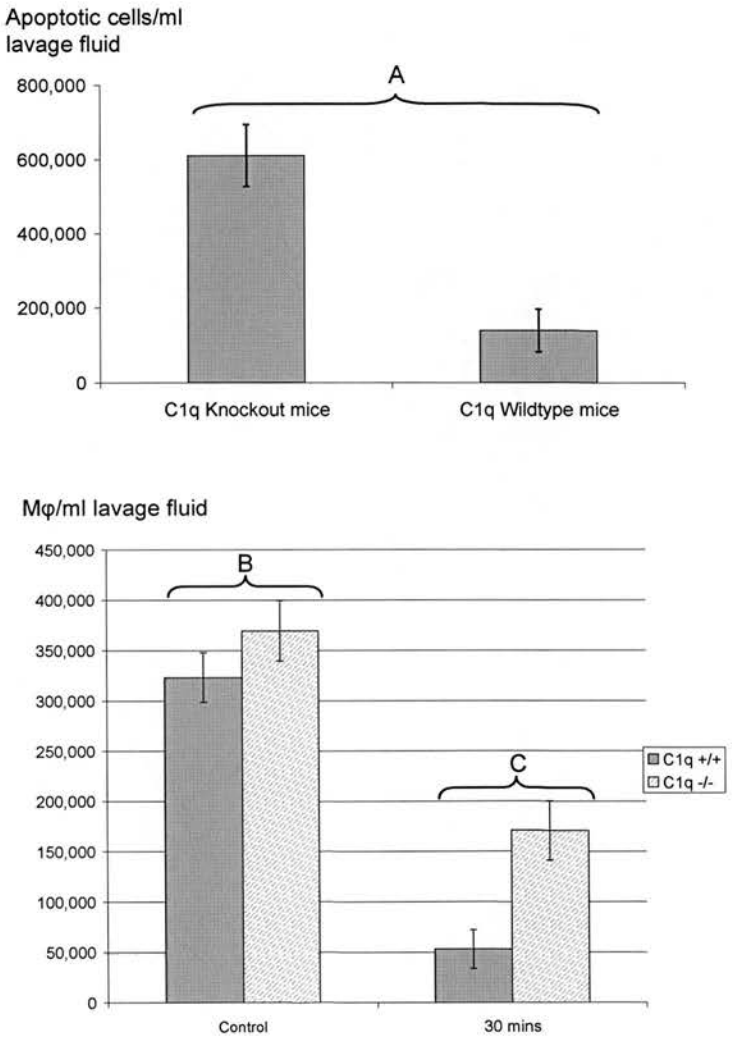

Top panel: non-phagocytosed apoptotic thymocytes remaining 30 minutes after IP injection into either C1qa -/- or +/+ mice or matched controls. **Bottom panel**: peritoneal Mφ recovered from either control non-manipulated C1qa -/- or +/+ mice (i.e. no IP injection) or C1qa -/- mice (hatched bars) and control +/+ animals (solid bars) 30 minutes after the instillation of $10x10^7$ apoptotic thymocytes Marker A - significantly more apoptotic cells were phagocytosed by peritoneal Mφ in C1q +/+ compared with C1qa -/- mice (p=0.007). Marker B - no significant difference between the baseline number of macrophages lavaged from C1qa -/- and +/+ mice at baseline. Marker C – significantly larger MDR seen in C1q +/+ than C1qa -/- mice (p=0.0007). N=7 per group; 2 experiments.

4.7 The effect of exogenous C1q opsonisation on the phagocytosis of apoptotic thymocytes

The defective clearance of apoptotic cells observed in the C1qa knockout mouse is believed to be due to the absence of C1q bridging the surface of apoptotic cells to the Mφ. It follows that fully competent phagocytosis of apoptotic cells could potentially be restored by the opsonisation of apoptotic cells with C1q. To test this, CMFDA-labeled apoptotic thymocytes **from C1qa -/- mice** were opsonised in either 50μg/ml of human recombinant C1q or 50μg/ml BSA in RPMI 1640 plus 10% C1qa knockout mouse serum. After thorough washing, the apoptotic thymocytes were resuspended at $1x10^7$ cells/ml in PBS and injected IP into female C1qa -/- mice (N=6 per group). After 30 mins, peritoneal lavages were performed and Mφ and apoptotic thymocytes remaining were counted. The results were compared against control mice in which no apoptotic cell injection was given.

A significant MDR was observed in mice receiving apoptotic thymocytes opsonised with either C1q or BSA. The MDR was larger when C1q opsonised, rather than BSA treated apoptotic thymocytes were injected. However, this difference did not reach statistical significance (p=0.1 – Figure 28). Similarly, the clearance of C1q-opsonised apoptotic cells was greater than that of BSA-opsonised apoptotic cells but again this did not reach statistical significance (p=0.39). Unfortunately, no information was available regarding the adequacy of opsonisation by this method.

Figure 28. Opsonisation of apoptotic cells with C1q neither increases the phagocytosis of apoptotic cells nor the MDR

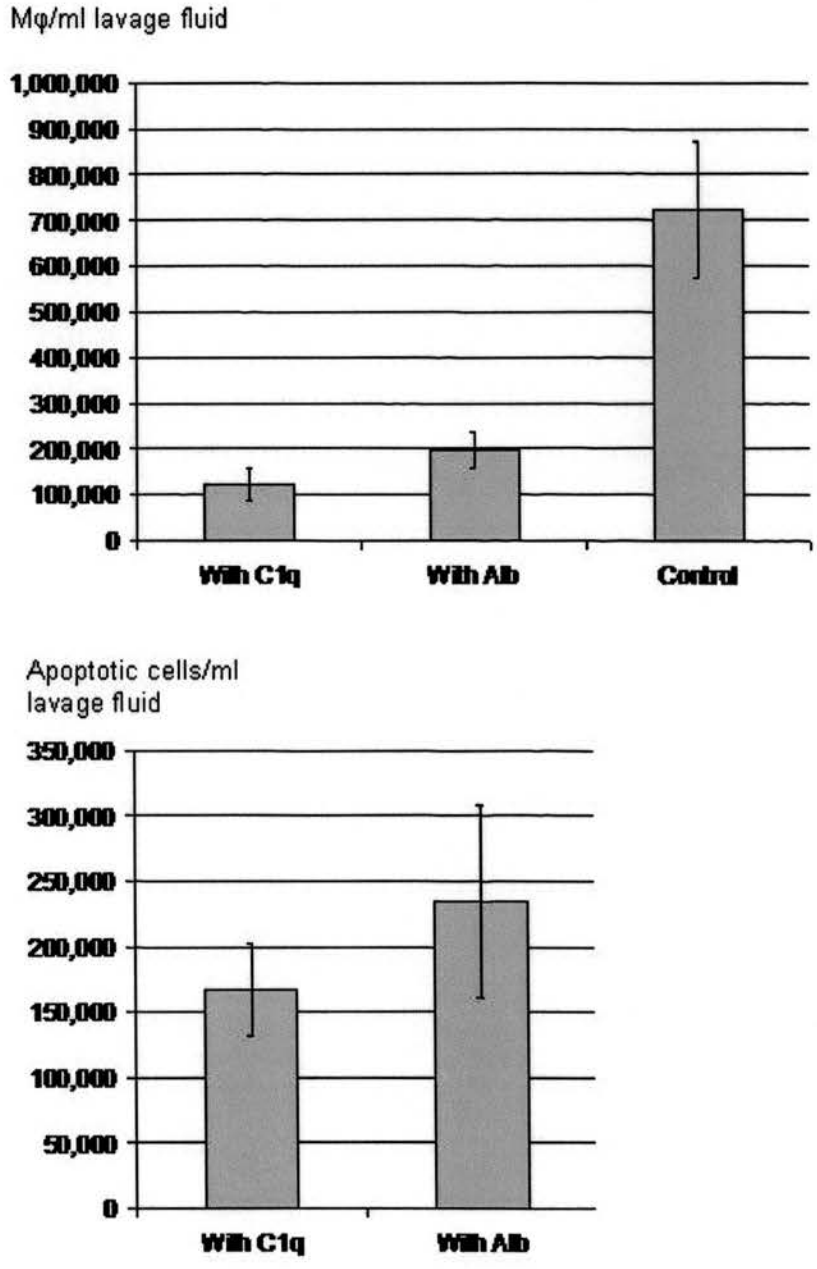

Top panel: Y-axis= Mφ recovered 30 minutes after the injection of apoptotic thymocytes opsonised with C1q, BSA or after no injection (control); X-axis= opsonising agant. Bottom panel: Y-axis= apoptotic thymocytes recovered 30 minutes after IP injection. X-axis= opsonising agent. N=6 per group; 1 experiment.

4.8 The addition of EDTA, but not the absence of Ca^{2+} from IP buffer solution, affects both the phagocytosis of apoptotic cells and the MDR

The question of the possible mechanisms underlying the MDR was then addressed. Extracellular Ca^{2+} is an important modulator of many adhesion molecules including integrins. The effect of extracellular Ca^{2+} was tested by injecting apoptotic thymocytes in PBS either with or without Ca^{2+}. For extra stringency, apoptotic cells were suspended in 5mM EDTA in PBS without calcium and were also injected IP in an attempt to chelate extracellular Ca^{2+} present within the abdomen. As in previous experiments, $5x10^6$ apoptotic thymocytes were injected IP, peritoneal lavage was performed after 30 minutes and labeled cells were counted by flow cytometry.

A significant MDR occurred after apoptotic thymocytes were injected in PBS with or without Ca^{2+} and without Ca^{2+} but with 5mM EDTA. The absence of Ca^{2+} from PBS made no difference to either the magnitude of the MDR or the clearance of apoptotic thymocytes. However, the suspension of apoptotic thymocytes in PBS lacking Ca^{2+} and containing EDTA resulted in a greater MDR than when EDTA was absent which only just failed to reach statistical significance ($p=0.06$). The clearance of apoptotic cells was significantly lower when they were injected with PBS (without Ca^{2+}) containing EDTA than PBS (without Ca^{2+}) alone ($p=0.0002$). These results suggested that removing Ca^{2+} from the extracellular fluid inhibited the clearance of apoptotic thymocytes but not the MDR (Figure 29).

Figure 29. The effect of Ca^{2+} and EDTA containing solutions on the apoptotic cell induced MDR and apoptotic cell clearance

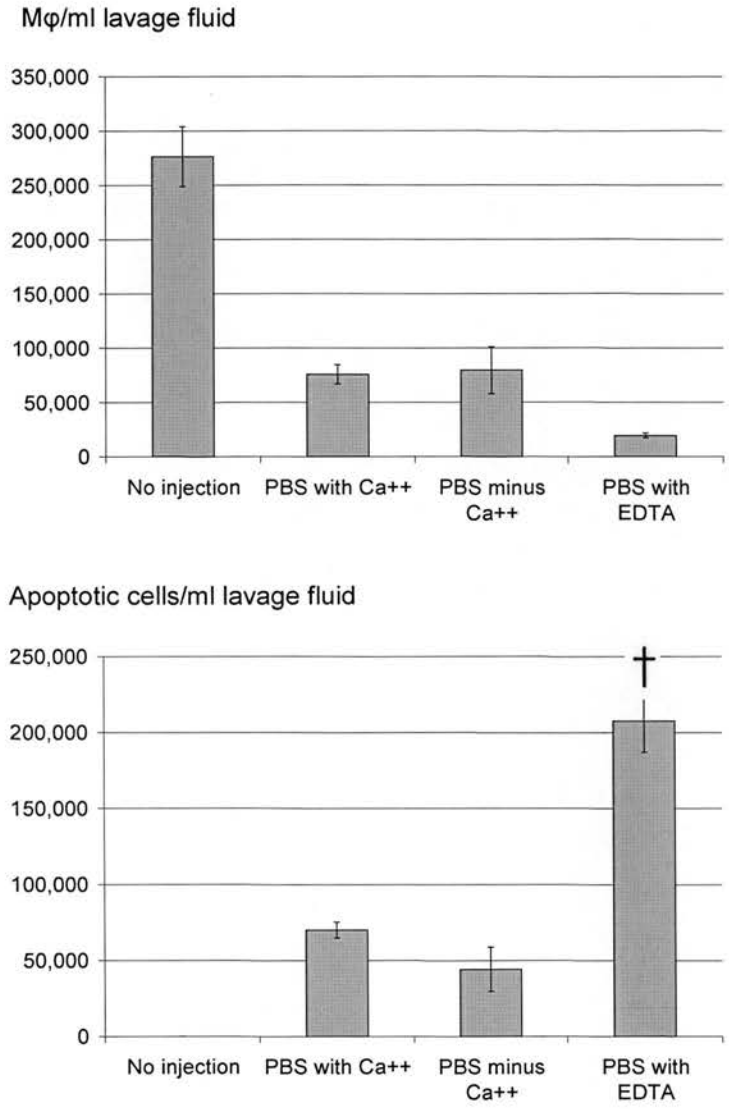

Top figure: Y-axis = Mφ recovered from peritoneal lavage 30 minutes after the IP injection of apoptotic thymocytes in PBS with or without Ca^{2+} or without Ca^{2+} but containing 5mM EDTA; X-axis= nature of vehicle solution for apoptotic cells. **Bottom figure**: Y-axis = apoptotic thymocyte recovery from same experimental conditions. † Significantly more apoptotic cells were recovered when injected with PBS (minus Ca^{2+}) with EDTA compared with PBS (minus Ca++) - p=0.0002. N=6 per group; 1 experiment.

4.9 The addition of Arg-Gly-Asp (RGD) peptide reduces both the MDR and the clearance of apoptotic cells

It has been shown that Mφ emigration to regional lymph nodes is partially mediated by $\alpha_4\beta_1$ and $\alpha_5\beta_1$ integrins (Bellingan et al., 2002). The peptide RGD (Arg-Gly-Asp) blocks the binding of β integrins to their ligands. A role for β_1 integrins in the MDR was investigated by adding RGD peptide to apoptotic thymocyte suspensions prior to their IP injection. The peptide RGE (Arg-Gly-Glu) acted as a non-blocking control peptide. $5x10^6$ CMFDA-labeled apoptotic thymocytes were suspended in either 0.1mM RGD or 0.1mM RGE in PBS. The thymocytes were injected IP and peritoneal lavage performed after 15 minutes. It had become clear that the MDR was a difficult reaction to modulate and previous experiments to completely block it had proved unsuccessful. Focus was shifted to delaying, rather than stopping, the MDR altogether. For this reason, the earlier 15 minute timepoint, midway through the MDR, was chosen. Lavaged cells were labeled and counted by flow cytometry using the standard method.

The MDR that followed the IP injection of apoptotic thymocytes was significantly reduced when thymocytes were injected with RGD peptide than with the RGE control ($p=0.037$). A similar reduction in apoptotic thymocyte clearance was also observed when apoptotic thymocytes were injected with RGD peptide but this was not statistically significant ($p=0.151$). The there was no significant difference in the number of Mφ recovered 30 minutes after the IP injection of RGD or RGE peptide

alone (RGD Vs RGE $6.72x10^4 \pm 8.98x10^3$ Vs $7.30x10^4 \pm 1.20x10^4$. p=NS, N=6 per group, 1 experiment).

Although the difference in apoptotic cell clearance was not statistically significant, these data strongly suggested that RGD was having an effect both on apoptotic thymocyte phagocytosis and the MDR. It was impossible to say whether the RGD effect on the MDR was due to direct inhibition of a β_1-mediated mechanism of Mφ disappearance or due to the inhibition of apoptotic cell phagocytosis.

Figure 30. The effect of RGD and RGE peptides on the MDR and apoptotic cell clearance

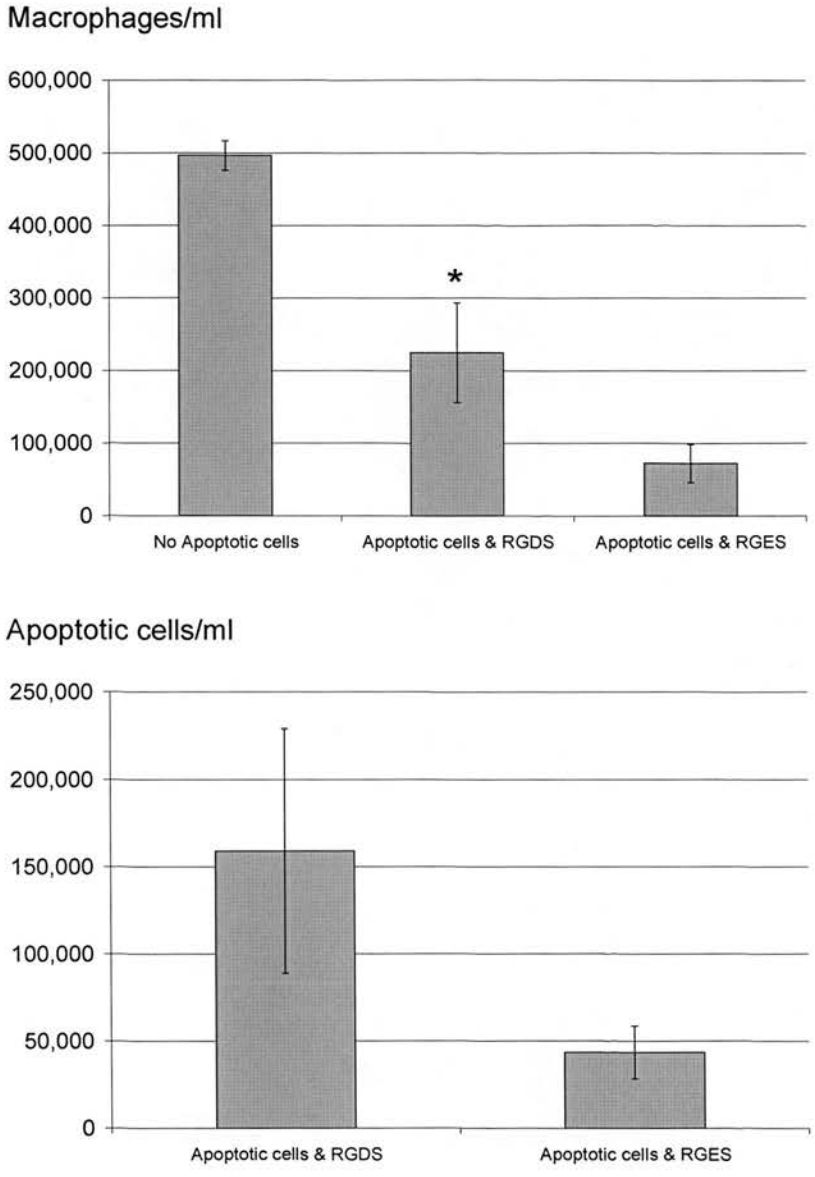

Top figure: Y-axis= Mφ recovery after the IP injection of apoptotic thymocytes with either 0.1mM RGD or 0.1mM RGE peptide X-axis= nature of IP apoptotic cell vehicle solution. (*p=0.037); Bottom figure: Y-axis= Apoptotic cell recovery from same lavage fluid samples. X-axis= as top figure. *p<0.05 when compared with RGES (no significant difference). N=5 per group; 2 experiments.

4.10 Hyaluronidase increases the MDR but has no effect on the phagocytosis of apoptotic cells

Various studies have highlighted a role for hyaluronic acid, a widely-distributed component of the extracellular matrix, in the MDR induced by pro-inflammatory stimuli. In particular, studies in 1980 showed that the MDR induced by IP BCG was reduced by pre-conditioning the peritoneal cavity with IP hyaluronidase and increased by pre-conditioning with IP hyaluronic acid itself (Shannon et al., 1980, Shannon and Love, 1980). The conclusion of these studies was that hyaluronic acid within peritoneal extracellular matrix was acting as a ligand for an unidentified Mφ receptor. Against this background, the effect of hyaluronidase on the MDR was tested.

$5x10^6$ CMFDA-labeled apoptotic thymocytes in 0.5mls PBS were injected IP one hour after an IP injection of either 20 units of streptomyces hyaluronidase (in 0.1ml PBS) or a control injection of 0.1 ml PBS. Previous control experiments had shown that this dose of hyaluronidase would not in itself induce a MDR ($1.23x10^5 \pm 9.40x10^3$ Mφ/ml Vs $1.01x10^5 \pm 1.13x10^4$ Mφ/ml; IP 0.2mg hyularonidase in 100µl PBS Vs 100µl PBS only, lavages performed 30 minutes after injections, N=4 per group, p=NS). Mice receiving no IP injections acted as a control group. The mice were sacrificed 30 minutes after the second IP injection, the peritoneal cavities were lavaged and cells counted by flow cytometry using the standard method.

No difference in the clearance of apoptotic cells was seen following peritoneal pre-conditioning with either PBS or hyaluronic acid ($p=0.65$ – Figure 31). However, a significantly lower number of Mφ were recovered from the mice that had received hyaluronidase than those receiving PBS pre-treatment ($p=0.04$). A substantial MDR nonetheless occurred in both groups of mice.

Figure 31. Hyaluronidase increases the MDR but has no effect on the phagocytosis of apoptotic cells

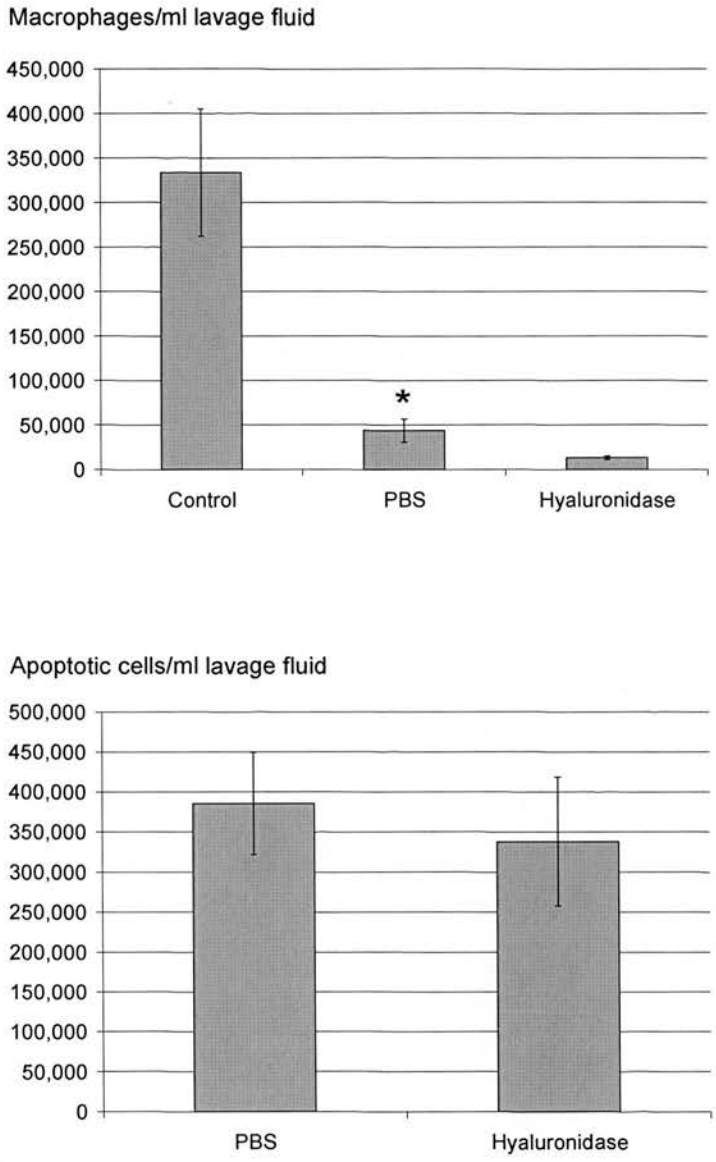

Top panel: Y-axis = the number of Mφ recovered 30 minutes after IP apoptotic thymocytes following peritoneal pre-conditioning with either PBS or hyaluronidase; X-axis=nature of pre-conditioning. Bottom panel: Y-axis = the number of apoptotic thymocytes recovered from the same groups of mice; X-axis= nature of peritoneal pre-conditioning. * $p<0.05$ compared with hyaluronidase. N=5 per group; 1 experiment.

4.11 Unfractionated heparin reduces the MDR but does not affect the phagocytosis of apoptotic cells

Activation of the coagulation system had been shown to mediate the MDR that follows the induction of pleurisy using a number of sterile irritants in rats (Sultan et al., 1978). In these experiments, the coagulation cascade was inhibited *in vivo* by the systemic administration of heparin and warfarin. The use of both these anticoagulants delayed the pleural MDR when compared to controls.

It was decided to inhibit the local coagulation cascade by injecting unfractionated heparin IP together with apoptotic cells and observing the effect on the MDR. $5x10^6$ CMFDA-labeled apoptotic thymocytes were injected IP with either 4 units of unfractionated heparin or PBS into groups of C57BL/6 mice. After 15 minutes, the animals were sacrificed and peritoneal cells recovered by lavage. These cells were labeled and counted by flow cytometry as previously described.

There was no significant difference in the number of apoptotic thymocytes recovered from either the mice receiving PBS or heparin IP ($p=0.81$). A significant MDR was observed after IP apoptotic thymocytes, either with or without heparin. However, almost 3 times as many Mφ were recovered from mice that had received IP heparin with apoptotic cells than those receiving PBS ($p=0.02$ – Figure 32).

Figure 32. Unfractionated heparin reduces the MDR but does not affect the phagocytosis of apoptotic cells

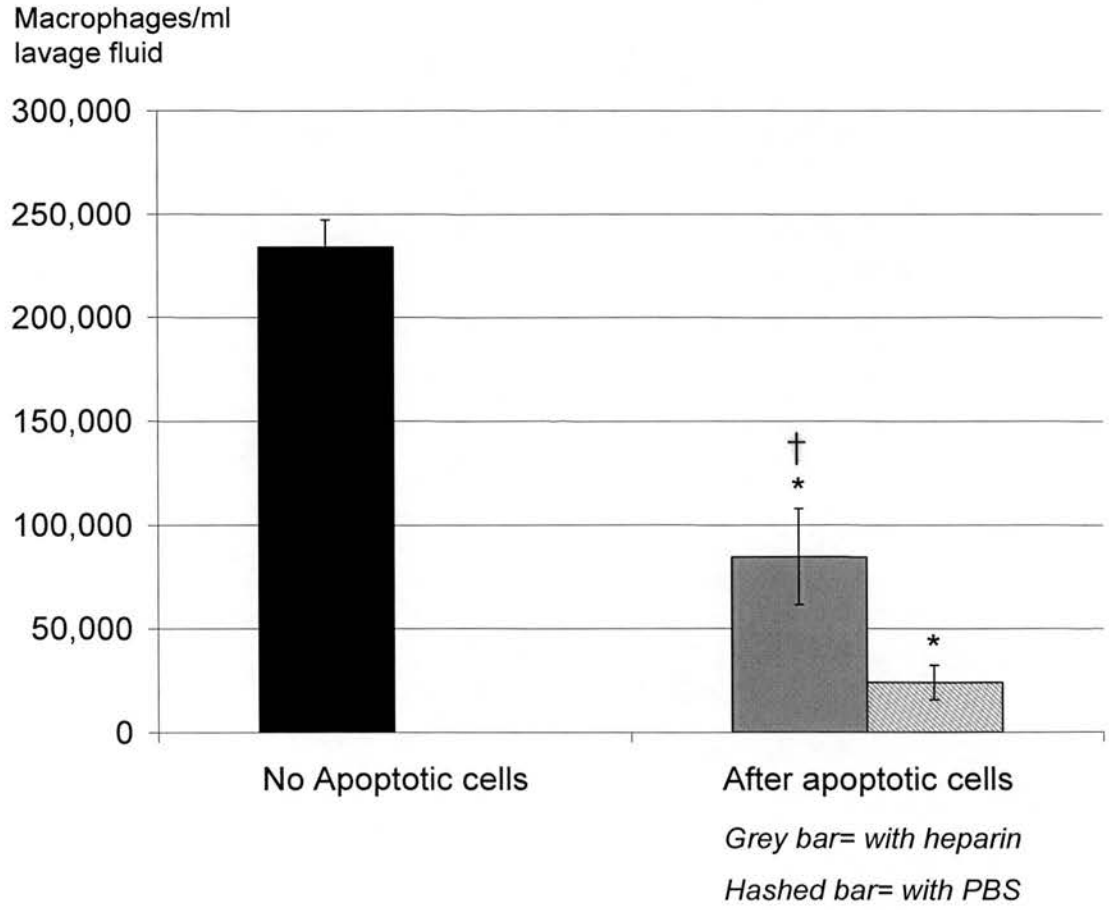

Y-axis = maan number of Mφ recovered from unmanipulated peritoneal cavity (black bar). Mean number of Mφ recovered from peritoneal cavity following IP apoptotic cells either with heparin (grey bar) or with PBS (hashed bar). * $p<0.05$ compared with control; † $p<0.05$ compared with apoptotic cells and PBS. N=5 per group; 2 experiments.

4.12 De-O-sulphated heparin, lacking anticoagulant activity, does not reduce the MDR

The previous experiment had highlighted that heparin inhibited the MDR. Nonetheless, this did not necessarily implicate the coagulation cascade in the apoptotic cell induced MDR. Heparin has many effects on leukocytes that are independent of inhibition of the coagulation system and, in particular, may affect leukocyte migration and the complement system (Ekre et al., 1992). To try and establish whether the reduction in the MDR was due to inhibition of the coagulation cascade, chemically modified heparin (N-Acetyl-de-O-sulfated heparin sodium salt – 'deactivated heparin') which has no anticoagulant properties (Moffat et al., 1991) was compared to standard unfractionated heparin in its effect on the apoptotic cell induced MDR. To that end, $5x10^6$ CMFDA-labeled apoptotic thymocytes in 0.5mls of PBS were injected IP with either 4 units of heparin or 200μg of deactivated heparin. The doses of heparin and its control were based on an approximate equivalence of molarity (approximate as unfractionated heparin is a mixture of different molecules). Control groups of mice received injections of active or deactivated heparin with 0.5 mls PBS only. The mice were sacrificed and peritoneal lavage performed 15 minutes following IP injection. Peritoneal cells were labeled and Mφ counted by the standard method previously described.

There was no difference in the clearance of apoptotic thymocytes between the groups of mice receiving active or deactivated heparin (heparin Vs deactivated heparin

$8.47x10^5 \pm 2.27x10^4$ cells/ml Vs $7.88x10^5 \pm 2.50x10^4$ cells/ml p=0.51). Neither was an MDR observed following the IP injection of either active or deactivated heparin with PBS. However, the injection of deactivated heparin with apoptotic thymocytes resulted in a significant MDR with disappearance of 57% of the original Mφ population (p=0.0015). This MDR induced by apoptotic thymocytes and deactivated heparin was significantly greater than that caused by the administration of apoptotic thymocytes and active heparin (p=0.018). Furthermore, the co-injection of apoptotic cells and 'active' heparin did not cause a significant MDR, reinforcing the previous data showing an inhibitory effect of heparin on the apoptotic cell-induced MDR.

To summarise, the apoptotic cell induced MDR was significantly reduced by administration of IP unfractionated active heparin but not N-Acetyl-de-O-sulfated heparin sodium salt, which lacks anticoagulant properties. These data suggest that the coagulation cascade participates in the apoptotic cell induced MDR.

Figure 33. The effect of active and deactivated heparin on the apoptotic cell-induced MDR

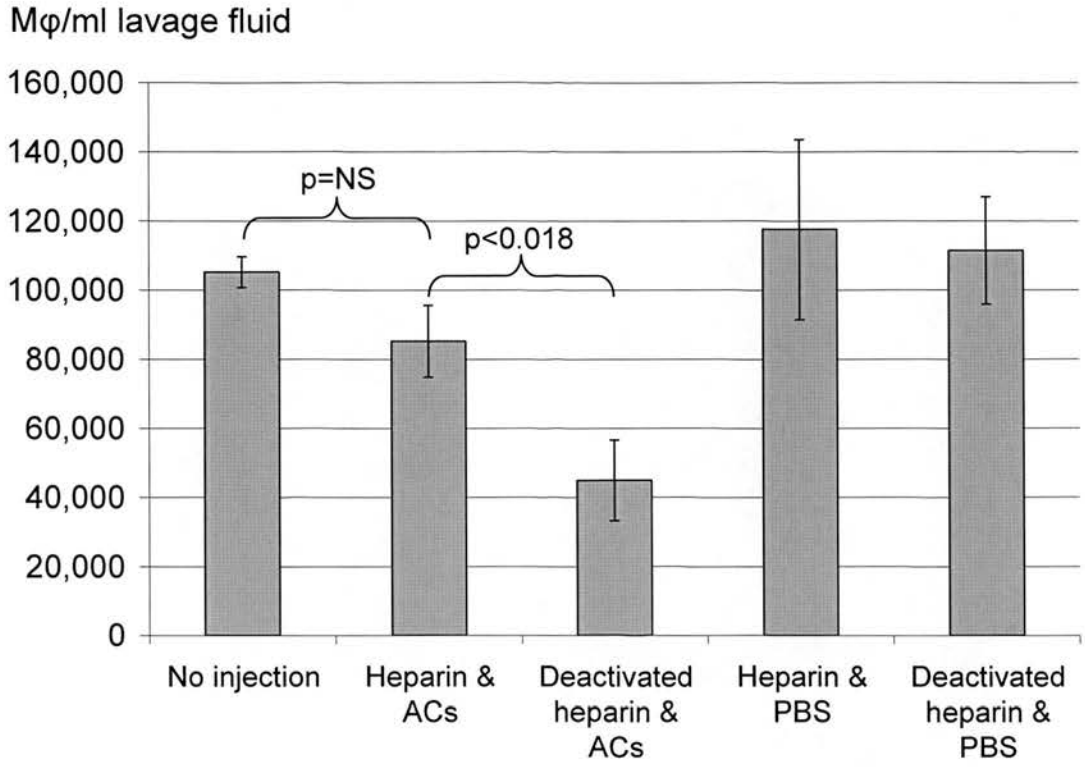

Y-axis= number of Mφ recovered 15 minutes after IP injections of combinations of apoptotic cells, heparin and de-O-sulphated heparin ('deactivated heparin') as indicated by X-axis. N=5 per group; 1 experiment.

4.13 Summary

- The MDR observed following IP apoptotic cells is not caused by LPS contamination
- The IP instillation of apoptotic but not viable human Jurkat T-cells also induced a MDR.
- The IP instillation of apoptotic human PMNs also induced a MDR.
- Phagocytosable latex beads induce an MDR, though of a lesser magnitude than the apoptotic cell induced MDR
- The absence of C1q from apoptotic cells results in both reduced phagocytosis by Mφ and a lesser MDR
- EDTA and the RGD peptide inhibit the phagocytosis of apoptotic cells and the apoptotic cell-induced MDR
- Hyularonidase increases the magnitude of the MDR without affecting the phagocytosis of apoptotic cells
- Unfractionated heparin reduces the magnitude of the MDR without affecting the phagocytosis of apoptotic cells

4.14 Questions

- Where do the disappearing Mφ go following the apoptotic cell-induced MDR?

5 CHAPTER 5 – RESULTS SECTION C

5.1 Introduction

In the previous chapter, various characteristics of the apoptotic cell induced MDR were established. This chapter will address a separate aspect of the MDR, namely what happens to the Mφ following their 'disappearance'. It is worth mentioning that the fate of the Mφ is likely to be intimately linked to the fate of the IP injected apoptotic cells. It has been established in previous studies that Mφ are responsible for the clearance of IP injected apoptotic cells from the peritoneal cavity (Taylor et al., 2000). Flow cytometry data has already been presented in this thesis to show that apoptotic cells are recovered from the peritoneal cavity either in isolation or associated with Mφ (Chapter 2 - Results Section A). Apoptotic cells do not appear to associate with any other cell within the peritoneal cavity. As the IP injected apoptotic cells are fluorescently labeled, it was decided to identify where they went after IP injection. It seemed a reasonable deduction that the disappeared Mφ would be located with the apoptotic cells.

5.2 IP instilled apoptotic cells are not found in the spleen or circulating blood

It was first decided to look for evidence for the emigration of apoptotic cells beyond the peritoneal cavity. $5x10^6$ fluorescently labeled apoptotic thymocytes (labeled with CMFDA green as previously described) in 0.5mls PBS were injected IP into

C57BL/6 mice. Labeling was checked pre-injection and fluorescence was found to be increased by 10^3 in the FL-1 channel when compared to unlabeled apoptotic cells. 0.5 mls of PBS was injected into a separate group of control animals. 30 minutes after the IP injections, the mice were sacrificed by terminal anaesthesia and cardiac puncture, peritoneal lavage and splenectomy performed. The spleen was disaggregated using a combination of physical and enzymic degradation (see methods). Both whole blood and the splenic cell suspension were subjected to hypotonic saline to achieve erythrocyte lysis. The remaining cell suspension was then analysed by flow cytometry to see if there was any evidence of a population of FL-1 HI cells representing either the CMFDA labeled apoptotic cells or Mφ that had phagocytosed these cells (Figure 34).

In fact, there was no evidence of CMFDA Green$^+$ cells in either the blood or spleen. The experiment was repeated including an F4/80-PE labeling step to identify the monocyte-Mφ cell population but even with specific gating on this population, no shift in FL-1 fluorescence was observed. Similarly, no green fluorescent cells were visible by microscopy of the blood and splenocyte cell suspensions.

Figure 34. No FL-1 fluorescent shift apparent in blood or spleen after IP CMFDA Green+ apoptotic thymocytes

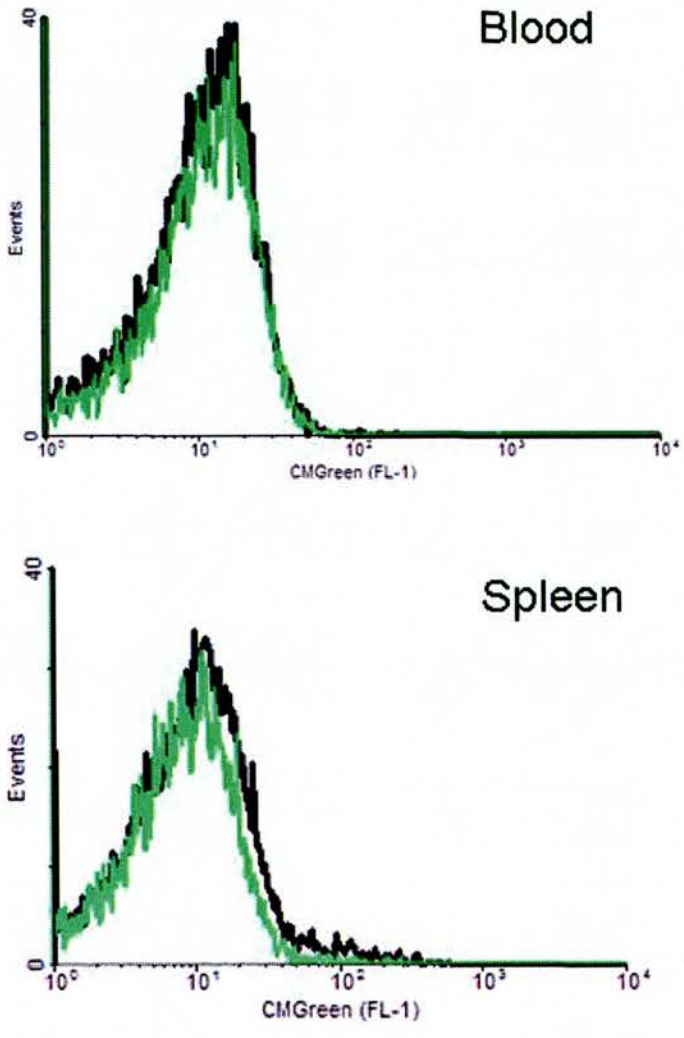

Histograms of FL-1 fluorescence for ungated blood cells (top graph) and splenic cells (bottom graph). In both panels, Y-Axis = number of collected events; X-axis = log measure of FL-1 fluoresence. Black line=cells after IP PBS injection; green line=cells after IP CMFDA-labeled apoptotic thymocytes. Sample of one data set. N=5; 1 experiment.

5.3 IP injected apoptotic cells concentrate within the omental lymphoid organ

Having failed to find the 'disappeared' apoptotic thymocytes in spleen or blood, attention was turned to the peritoneal membrane itself. The majority of the peritoneal membrane is a homogeneous layer of mesothelial cells enclosing a vascularised connective tissue layer. However, there are regions within the peritoneal membrane where Mφ are concentrated in large numbers; the so-called milky spots (see earlier). As previously discussed, the greatest concentration of milky spots is found within the omentum, also a well-established site of peritoneal leukocyte trafficking. For these reasons it was decided to look for apoptotic cell localisation to different regions of the peritoneal membrane, including the omental lymphoid organ, where milky spots are most abundant.

$5x10^6$ apoptotic thymocytes (CMFDA labeled) were injected IP into 6 female C57BL/6 mice. The mice were sacrificed after 30 minutes and their omenta were carefully dissected together with its associated peritoneal membrane. Intact segments of peritoneal membrane were also removed from the anterior abdominal wall and the diaphragm. These tissues were wet mounted on microscopy slides and examined under transmitted or fluorescent microscopy. The number of apoptotic thymocytes per high powered field was counted for all regions of peritoneal membrane.

It was immediately obvious that many more apoptotic thymocytes were present within the omental lymphoid organ than the other regions of peritoneal membrane. Approximately 28 times as many apoptotic cells were counted with the omental lymphoid organ as the other regions of peritoneal membrane ($p=0.00001$ – Figure 35). No significant difference was seen in the number of apoptotic cells binding the other regions of peritoneal membrane examined.

Figure 35. IP injected apoptotic cells concentrate within the omental lymphoid organ

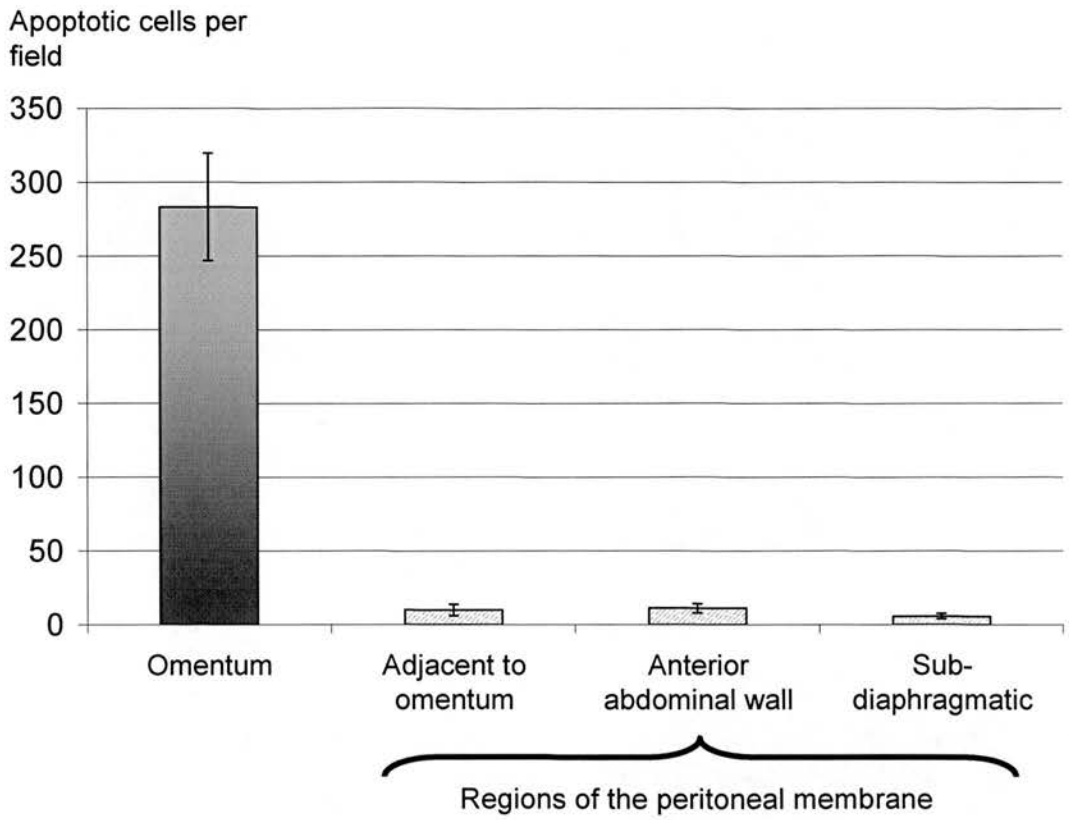

Y-axis = mean number of apoptotic thymocytes counted per high power field. X-axis= sampled region of murine peritoneal membrane (X15 magnification). N=5; 1 experiment.

5.4 IP instilled apoptotic cells concentrate with omental milky spots

Having established a striking localisation of apoptotic cells to the omentum following IP administration, the question of where these apoptotic cells were localised was next addressed. As has been previously discussed, the omentum is an unusual part of the peritoneal membrane in that it contains a very large number of milky spots, specialised Mφ-rich components of the CALT system. It seemed likely that these structures, with their abundance of phagocytic Mφ were the site of apoptotic cell localisation within the omentum.

A phagocyte-specific dye, PKH-26, was used to identify the Mφ within omental milky spots. This dye is known to almost exclusively label Mφ within the uninflamed peritoneal cavity (Melnicoff et al., 1988b), a result confirmed in this study (see Chapter 3 - Results Section A). 0.5 mls of PKH-26 dye in the manufacturer's diluent will label the entire lavageable peritoneal Mφ population within 2-4 hours. When the omenta of mice receiving PKH-26 were dissected and examined under fluorescence microscopy, Mφ-rich milky spots were readily discernable (Figure 36).

Figure 36. PKH-26 (red) fluorescent Mφ visible within omental lymphoid organ milky spots

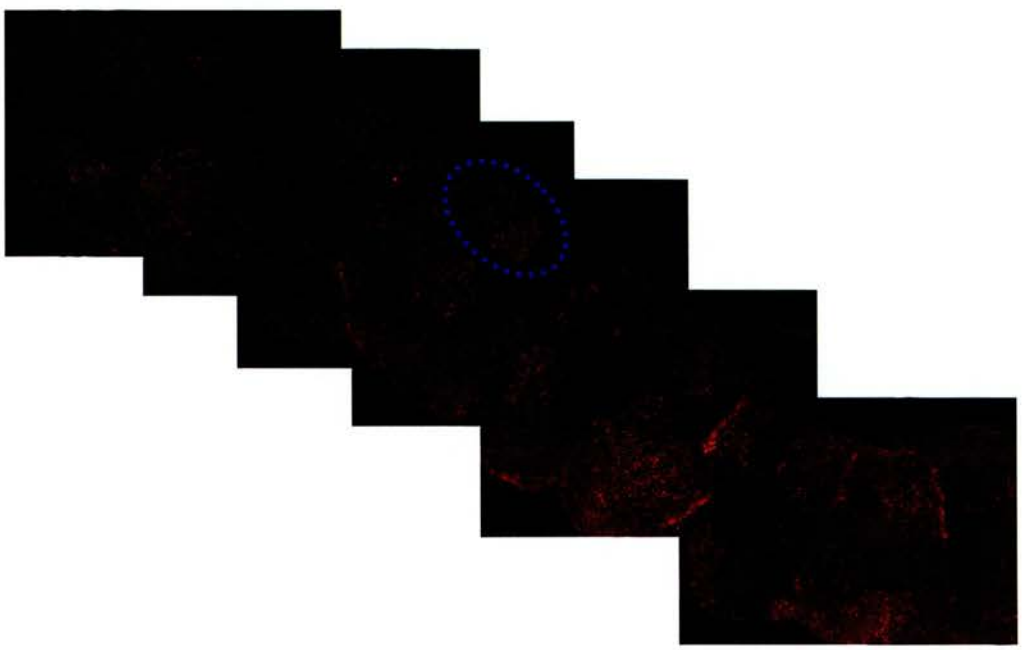

Composite of six transmitted-light fluorescence microscopy images of an omental lymphoid organ following IP PKH-26 dye. Aggregations of red fluorescently-labeled Mφ can be seen along the lateral aspects of the organ. A representative milky spot is highlighted with a blue circle. Magnification x15.

Although the PKH-26 dye readily identified the milky spots, it was also possible to identify these structures by transmitted light microscopy (Figures 36 & 37). As their name suggests, the milky spots have a milky white colour and finer texture than the surrounding cells, which are predominantly adipocytes. The finer texture of the milky spots is a consequence of the smaller size of the leukocytes within the milky spot when compared to the larger surrounding adipocytes. This allowed milky spots to be identified without necessitating the use of pre-labeling with PKH dyes.

Figure 37. Unlabeled milky spot viewed under transmitted light microscopy

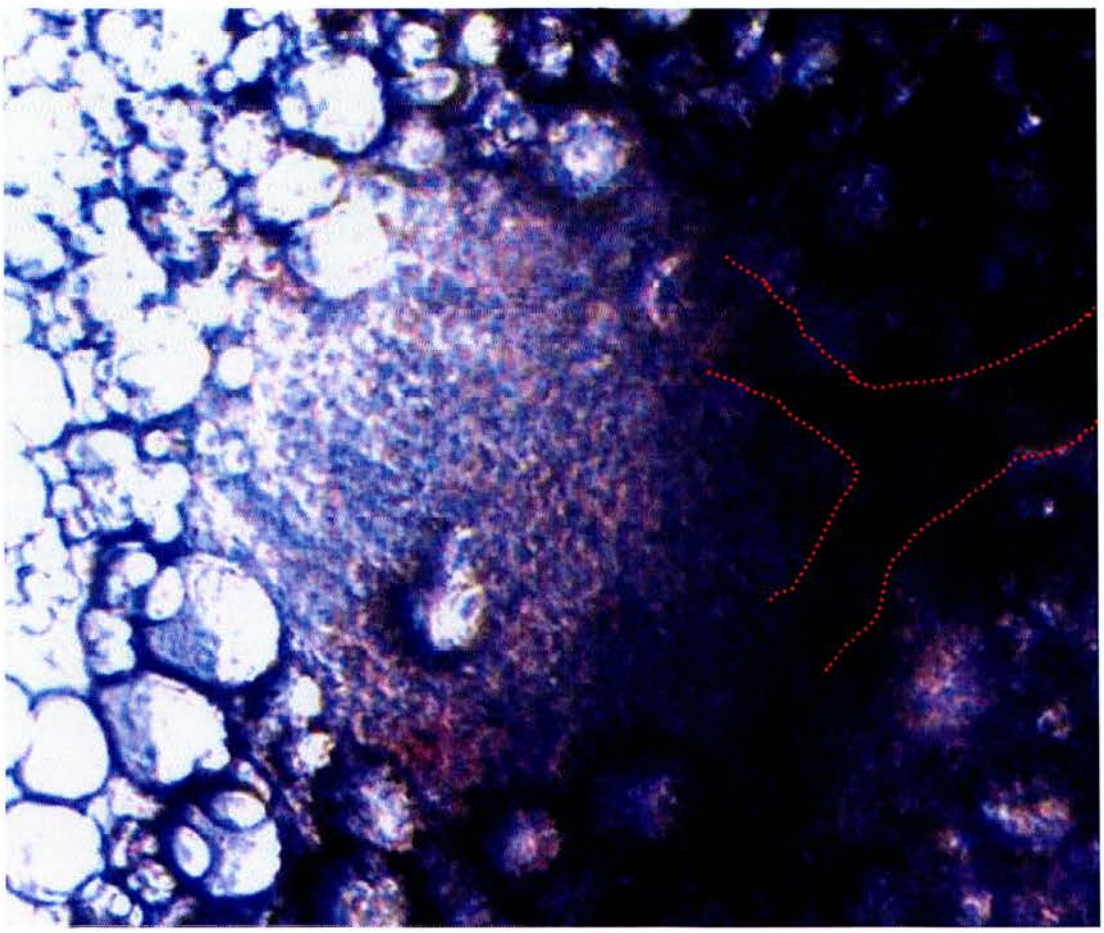

Central area shows finer, more granular cells corresponding to a milky spot. Surrounding larger cells are mostly adipocytes. Blood vessel entering milky spot at '2 o'clock' just visible (outlined with red lines). Magnification x20.

Figure 38. Unlabeled milky spot viewed under transmitted light microscopy

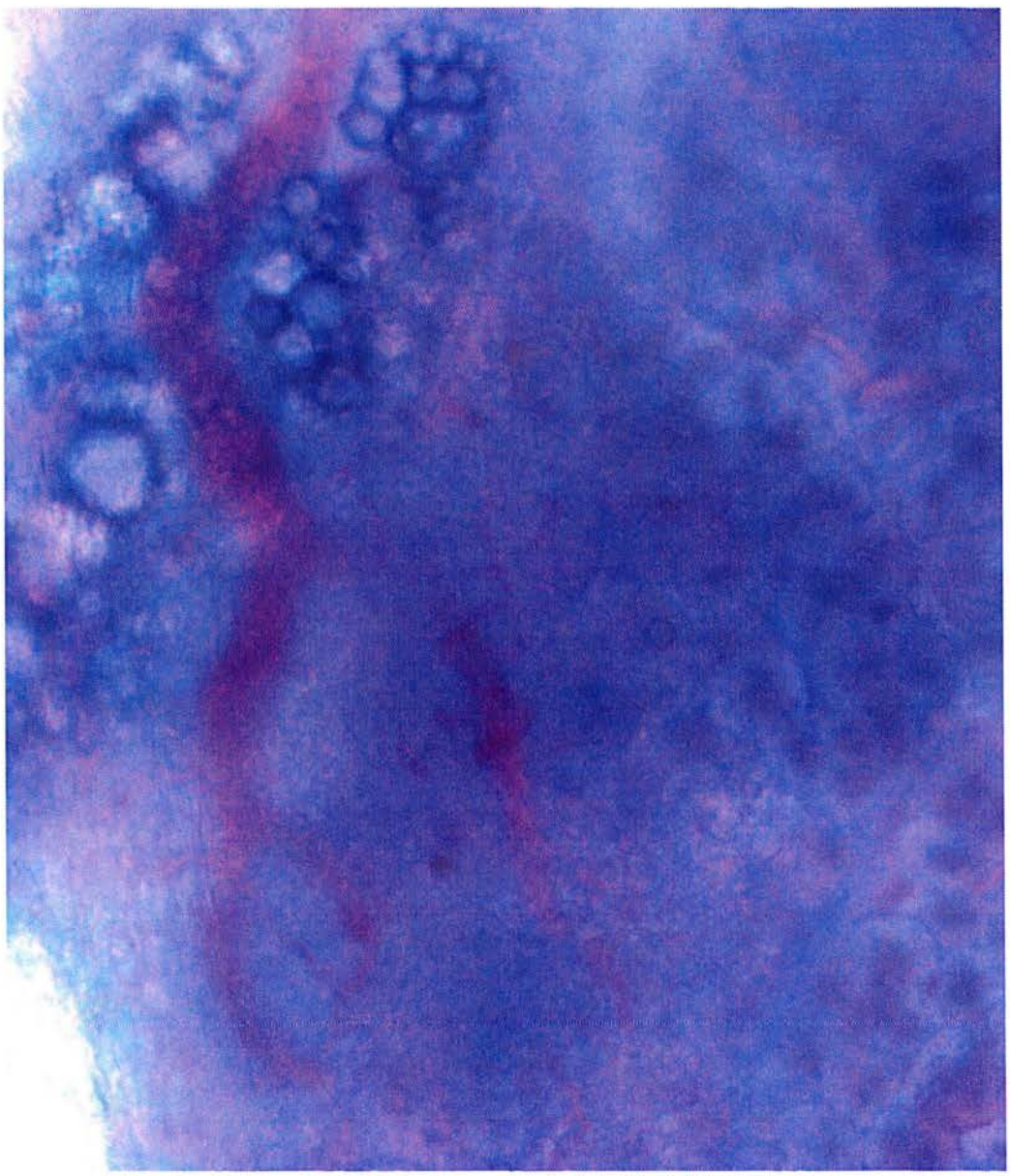

Adipocytes are clearly seen in the top left quadrant. A blood vessel runs from the top left quadrant and branches within a milky spot in the lower left quadrant. Note again the finer more granular appearance of the cells within the milky spot. Magnification x20.

The question of whether IP injected, CMFDA-labeled apoptotic cells were taken up by the omental milky spot Mφ was addressed next. Milky spots were highlighted by pre-labeled peritoneal Mφ with PKH-26 dye, as previously discussed. Next, 10^7 apoptotic thymocytes, double labeled with CMFDA-green and Hoescht 33342 were injected IP into C57BL/6 female mice. After 30 minutes, the mice were sacrificed and the omenta removed and examined under transmitted fluorescent microscopy. Fluorescent exposures were taken in both the blue and red transmitted channels and composite photomicrographs made. Representative images are shown (Figures 38 & 39).

Figure 39. Colocalisation of labeled apoptotic cells and Mφ within the omental milky spots (A)

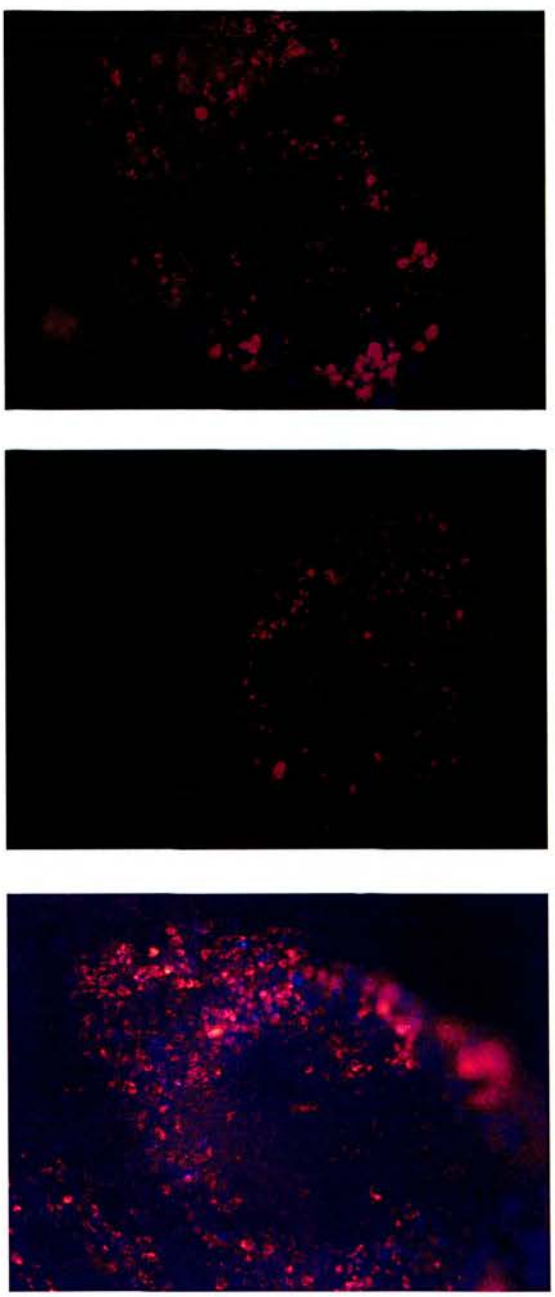

Three representative composite (red & blue channels merged) transmitted fluorescence photomicrographs of omental milky spots 30 minutes after the injection of Hoescht 333342 labeled apoptotic thymocytes. Resident peritoneal Mφ had been pre-labeled with PKH-26 fluorescent tracker dye (red). (x15)

Figure 40. Colocalisation of labeled apoptotic cells and Mφ within the omental milky spots (B)

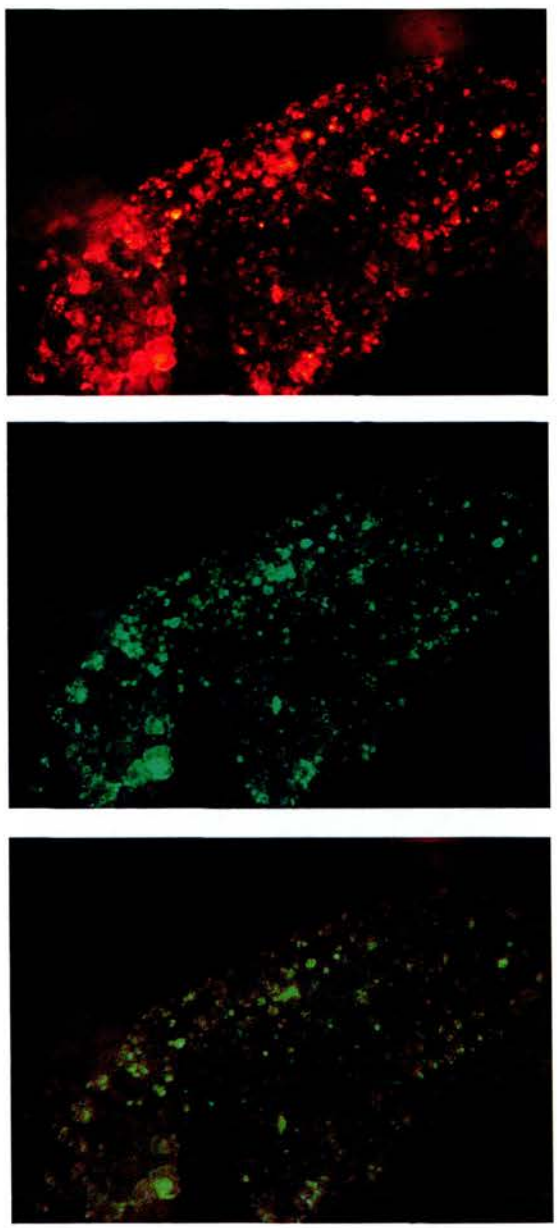

Fluorescent photomicrographs of milky spot 30 minutes after the IP injection of CMFDA green-labeled apoptotic thymocytes. Again, Mφ pre-labeled with PKH-26 red fluorescent dye. Individual red and green channel photos are shown (top and middle) plus composite image (bottom). The colocalisation of red and green labels give a yellow colour in composite picture. Nonetheless, some individual red and green labelled cells can be seen. (x15)

5.5 Omental Mφ phagocytose IP injected apoptotic cells

These observational studies strongly suggested that there was direct contact between apoptotic cells and Mφ and possibly phagocytosis of apoptotic thymocytes by Mφ. To test this further, CMFDA-green labeled apoptotic thymocytes were injected IP into groups of mice. After 30 minutes, omentectomies were performed and the omental lymphoid organs removed and digested as previously described. The omental cell suspension was then labeled with rat anti-mouse F4/80-PE/Cy5 Ab. The labeled cell suspension was then analysed by flow cytometry to assess firstly whether there was direct contact between the peritoneal Mφ and apoptotic cells and secondly whether unattached 'free' apoptotic cells were present within the omental lymphoid organ.

The FL-4 fluorescence was then analysed by flow cytometry and compared with unlabeled cells (Figure 41). A population of cells displayed a significant increase in FL4 fluorescence (red line). These fluorescent cells had the typical FSC/SSC characteristics of peritoneal Mφ. No such shift was seen in cells labeled with the isotype control (grey line) or unlabeled cells (black line).

The recovery process of omental Mφ was relatively inefficient and gating was quite stringent so only a relatively small number of omental Mφ were recovered. However, it was apparent that a significant proportion of the omental Mφ acquired FL-1 fluorescence following the injection of IP CMFDA-labeled apoptotic

thymocytes (Figure 41). It was not possible to assess this quantitatively but it appeared that the majority of omental Mφ had gained some FL-1 fluorescence after the IP injection of CMFDA-labeled apoptotic cells. Virtually no free FL-1+ cells were seen, suggesting that most of the IP injected apoptotic cells were either bound to or phagocytosed by omental Mφ.

Figure 41. Omental Mφ recovered by digestion are F4/80$^+$

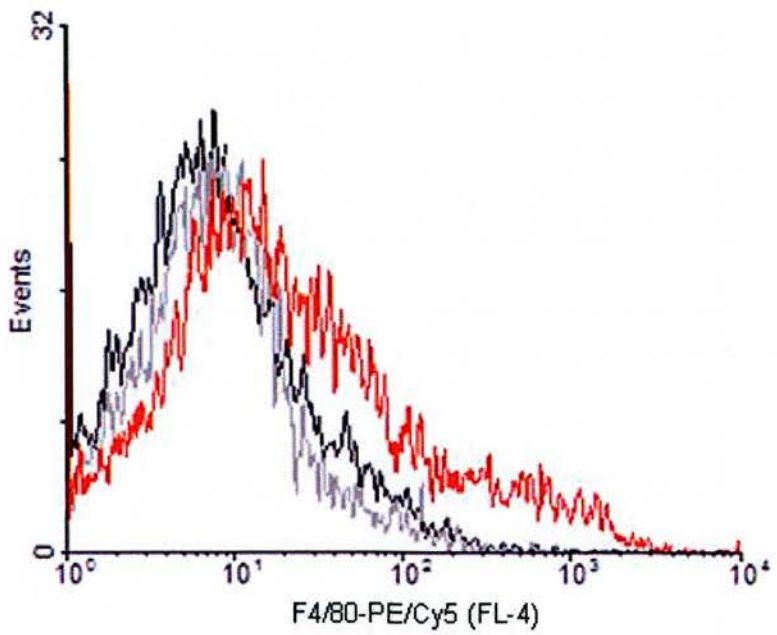

Black= unlabeled

Grey=Isotype control Ab

Red=F4/80-PE/Cy5 Ab

Y-axis= number of detected events; X-axis = log measurement of FL-4 fluorescence. Cell suspension recovered from the digested omenta labeled with rat anti-mouse F4/80-PE/Cy5 (red line), PE-Cy5-labeled isotype control antibody (grey line) unlabeled cells (black line). Representative image from N=3; 1 experiment.

Figure 42. Omental Mφ phagocytose CMFDA-green labeled apoptotic cells and acquire green fluorescence

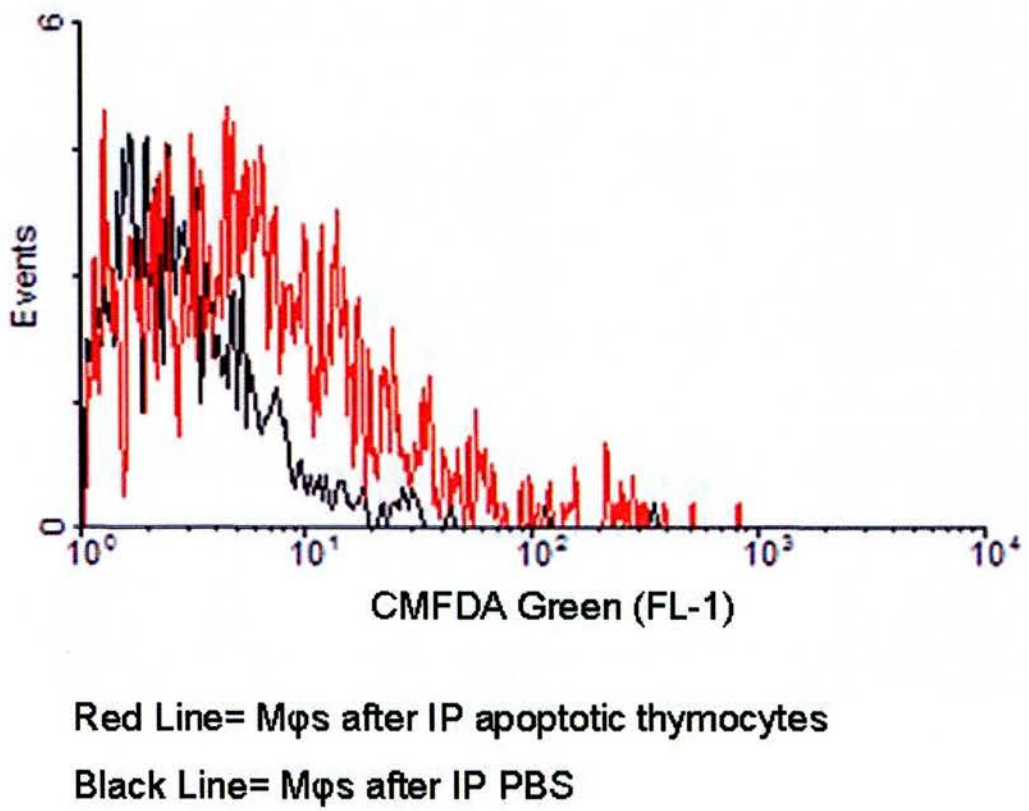

Flow cytometry FL-1 histogram of digested omental Mφ – identified by gating for F4/80-PE/Cy5-HI fluorescent cells (from figure 41). Red line represents FL-1 fluorescence of recovered omental Mφ 30 minutes after $5x10^6$ CMFDA+ apoptotic thymocytes. Black line represents FL-1 fluorescence of omental Mφ 30 minutes after IP PBS.

5.6 Peritoneal lavage technique samples 'free' intraperitoneal Mφ, not those within milky spots

The power of the intraperitoneal injection/lavage technique of instilling and sampling cells from the peritoneal cavity is that it is fast and minimally destructive. This allows for kinetic observations of the movement of peritoneal Mφ to be made over short and tightly-separated time intervals. However, a crucial problem is that it is unclear whether a peritoneal lavage recovers cells from the entire peritoneum, including the clusters of Mφ within omental milky spots or the non-milky spot populations of Mφ. Intuitively, one might imagine that the omental milky spot Mφ, being more organised, were less likely to be recovered by a lavage technique. This question has relevance for the interpretation of the data presented within this chapter and was addressed experimentally in the following way.

A group of 10 C57BL/6 mice were sacrificed and peritoneal lavage performed with a modification to the standard method. A small – approximately 3mm – incision was made in the peritoneal membrane in the left upper quadrant over the omental lymphoid organ. Then in 5 animals, the omental lymphoid organ was carefully externalised through this incision and the peritoneal membrane closed with a mosquito clip. In the remaining 5 animals, the incision was closed with the omentum remaining within the peritoneal cavity. With the clamp in place, all 10 animals then underwent a standard peritoneal lavage. The Mφ were then labeled with F4/80-PE and counted by flow cytometry using the standard method previously described.

The number of recovered peritoneal Mφ was virtually identical whether the lavage had been performed with the omentum inside or outside of the peritoneal cavity (Figure 43). Peritoneal lavage does not appear to remove Mφ from the omental lymphoid organ (omentum externalised Vs internalised – $6.29x10^5 \pm 4.43x10^4$ Mφ/ml Vs $6.19x10^5 \pm 8.90x10^4$ Mφ/ml, p=NS). This suggested that the peritoneal lavage technique selectively recovered non-omental 'free' peritoneal Mφ. A particularly interesting consequence of this result is that it suggests that during the MDR, non-adherent Mφ actively attach themselves to a structure or structures within the peritoneal cavity. The possibility that the MDR is merely omental Mφ becoming more adherent as a consequence of encountering apoptotic cells, is made less likely by this experiment.

Figure 43. The externalisation of the omentum has no effect on Mφ recovery by peritoneal lavage

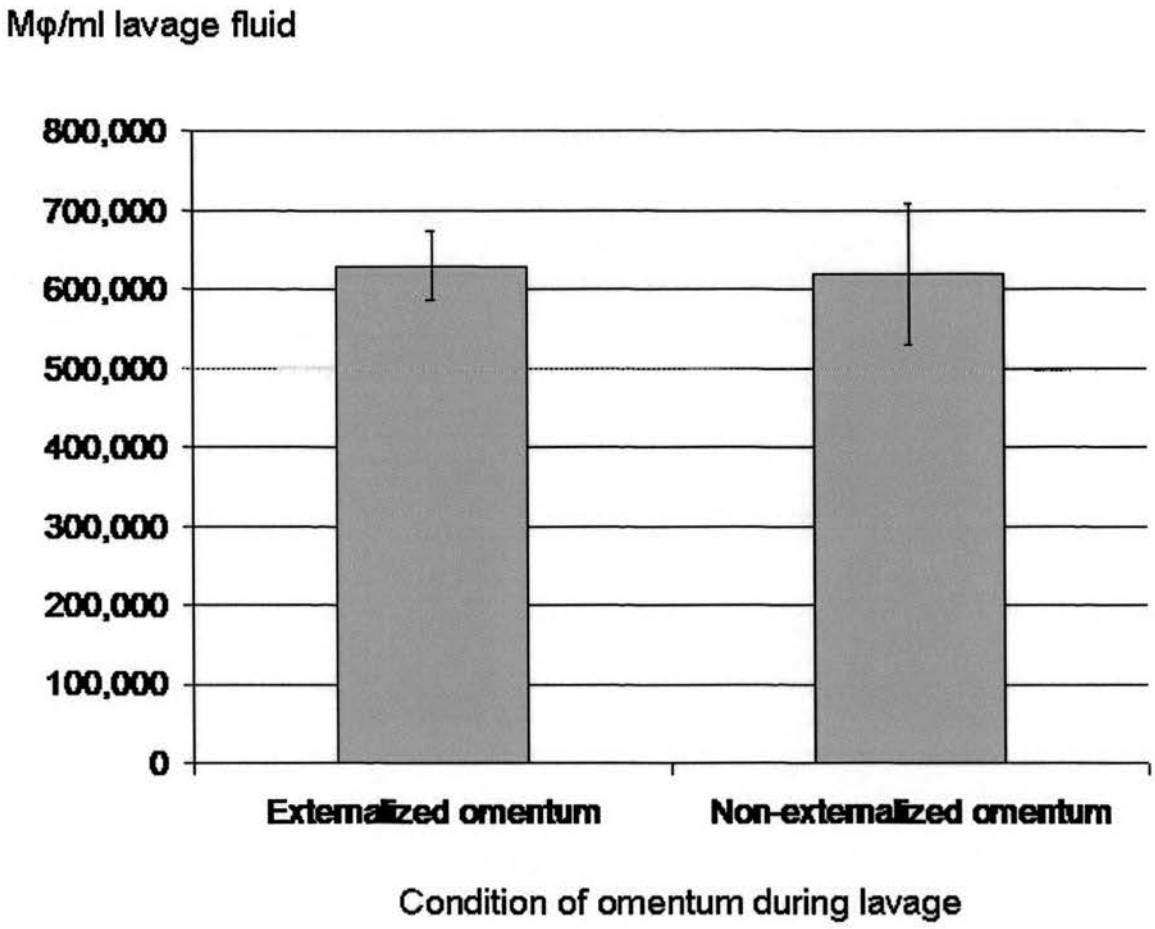

Y-axis = the number of peritoneal Mφ per ml of peritoneal lavage fluid; X-axis shows whether the omentum was within or outside the peritoneal cavity at the time the lavages were performed. N=5 per group; 2 experiments.

5.7 Peritoneal Mφ enter the omental lymphoid organ following IP apoptotic cells

It has already been shown that, following the IP administration of apoptotic cells, a rapid fall in the number of recoverable peritoneal Mφ was observed. The immediate fate of these Mφ was unknown but, given the previously proven role of milky spots in the emigration of inflammatory peritoneal Mφ (Bellingan et al., 2002), the possibility that these Mφ were attaching themselves to the omental lymphoid organ was investigated. Whilst it is relatively straightforward to label peritoneal Mφ with the PKH dyes (see Methods), there is no similar method to selectively label omental versus other intraperitoneal Mφ. The fate of intraperitoneal Mφ was thus determined by a combination of inferential and adoptive transfer experiments.

The first experiment aimed to see whether there was a change in the size of the omental Mφ population allowing the IP administration of apoptotic cells. If an increase in the number of omental Mφ was observed, then this could indicate that Mφ were being recruited to the omental lymphoid organ. Furthermore, if the entire peritoneal Mφ population was pre-labeled with PKH dye prior to the injection of apoptotic cells, any newly-arrived Mφ within the omentum could be identified as either intra- or extra-peritoneal in origin.

A further complication was the innate heterogeneity of omental lymphoid organs and differences in the amount of tissue recovered during dissection. There was

considerable variation in both of these parameters. This meant that in any experiment, the variation in the absolute number of Mφ recovered was considerable. Using the absolute number of Mφ as a means to measure relatively small changes in the omental Mφ population would be impractical. However, the ratio of B-lymphocytes to Mφ within uninflamed milky spots had been previously published (Dux et al., 1986, Goldsmith et al., 1990, Beelen et al., 1980) and seemed likely to be a more constant value than absolute numbers as far as comparisons between individual animals was concerned.

Preliminary experiments showed this to be the case. A group of C57BL/6 mice were sacrificed and omental dissection and digestion was performed. The recovered cell suspension was then labeled with rat-anti mouse B220-PE (to identify mature B-lymphocytes) and rat-anti mouse F4/80-PE/Cy5 to identify mature peritoneal Mφ. These cells were separately identified by flow cytometry and the number of B220-HI B-lymphocytes and F4/80-HI Mφ identified in each sample. The relative proportion of Mφ to B-lymphocytes was then calculated.

In a sample of 8 animals, the ratio of Mφ per B-lymphocyte recovered was 1.29 ± 0.20. This is a higher proportion of B-lymphocytes than was seen in previous published studies (approximately 2 Mφ per B-lymphocyte) and approximately opposite the ratio found within cells recovered from the peritoneal cavity. There may be a number of factors to explain these discrepancies. The seminal studies by Beelan and Dux (Beelen et al., 1980, Dux et al., 1986) relied upon electron

microscopy to identify the Mφ and lymphocyte populations within milky spots. Their inclusion criteria for 'macrophages' certainly included immature monocyte-derived Mφ, which are F4/80-LO or negative and thus would have been excluded from counting in this current study. Furthermore, the animals used in my experiment were younger and of a different sex and genetic strain to the ones used by Beelen and Dux. Whatever the discrepancies, the ratio of B-lymphocytes to Mφ within the omental lymphoid organs was quite constant and was used as the standard for measuring quantitative changes within the omental Mφ population.

C57BL/6 mice received 0.5 mls of PKH-26 red fluorescent dye as previously described. Then a group of 7 animals received an IP injection of $5x10^6$ CMFDA apoptotic thymocytes, made as previously described. A control group (N=7) of animals received an injection of 0.5 mls PBS. A second control group (N=3) received neither PKH-26 nor CMFDA green labeled apoptotic thymocytes and these animals provided tissue for flow cytometry fluorescent calibration.

The mice were sacrificed 30 minutes after receiving their IP injection of apoptotic thymocytes or PBS. Omental digestion and cell labeling was performed as previously described. The omental Mφ, which had been pre-labeled with PKH-26 red fluorescent dye were then labeled with rat anti-mouse F4/80-PE/Cy5 Ab and the B-lymphocytes with rat-anti mouse B220-PE Ab. Although the B220-PE and PKH-26 dye both fluoresce within the FL2 channel, previously published work and work done as part of this study had shown that a) the B-lymphocytes had clearly distinct

light scattering properties compared to Mφ and b) intra-peritoneal B-lymphocytes do not phagocytose the PKH dye *in vivo*. These facts made misidentification of either B-lymphocytes for PKH^+ Mφ or *vice versa* highly unlikely.

The group of mice that received IP apoptotic thymocytes demonstrated a significant increase in the ratio of Mφ:B-lymphocytes when compared to mice receiving PBS only (1.87±0.21 Vs 1.13±0.12, p=0.02 – Figure 42). Furthermore, flow cytometry dot plot analysis demonstrated that virtually all of the omental Mφ had taken up the PKH-26 dye, confirming their origin as intraperitoneal rather than extraperitoneal (Figure 43). Both of these observations supported the hypothesis that peritoneal Mφ were associating with the omental lymphoid organ during the MDR.

Figure 44. A proportional increase in Mφ within the omental lymphoid organ is seen following IP apoptotic thymocytes

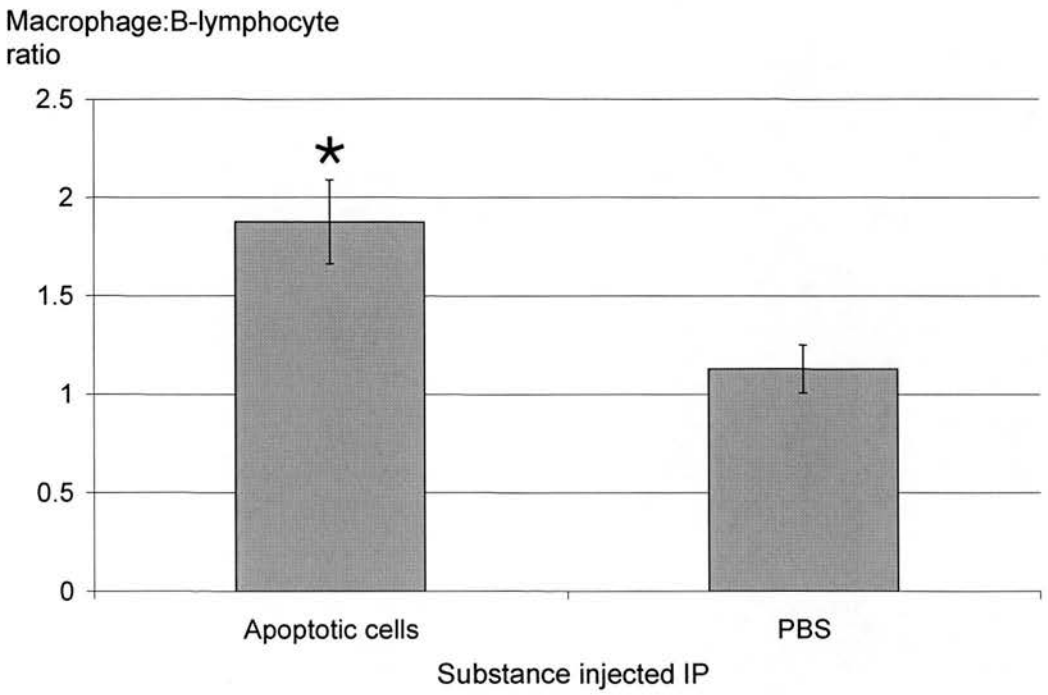

Y-axis = the ratio of Mφ:B-lymphocytes recovered by peritoneal lavage following IP injection; X-axis= the nature of the IP injected material. *A significantly higher ratio of Mφ: B-lymphocytes was seen in animals receiving IP apoptotic cells ($p=0.02$). N=6 per group; 2 experiments.

Figure 45. Intra-peritoneal Mφ enter the omental lymphoid organ after IP apoptotic cells

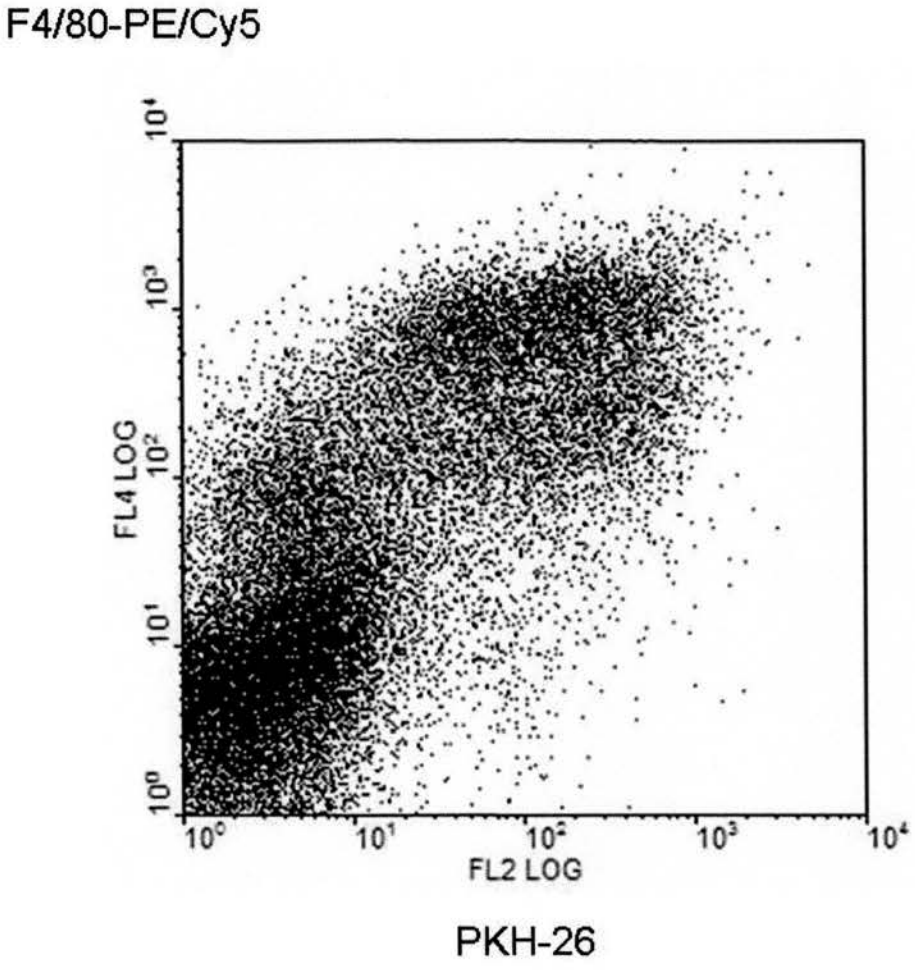

Flow cytometry plot of cells following enzymic dissociation of the omental lymphoid organ (B-lymphocytes excluded by selective gating). Y-axis shows fluorescent labeling with the rat-anti mouse F4/80-PE/Cy5 Ab in the FL4 channel. The X-axis shows fluorescent labeling with PKH-26 dye in the FL2 channel. Almost all of the F4/80-HI cells are also PKH-26 HI

5.8 Adoptively transferred peritoneal Mφ are selectively taken up by omental milky spots

Further evidence for the emigration of peritoneal Mφ to the omental milky spots after the IP injection of apoptotic cells was sought by means of adoptive transfer experiments. Peritoneal Mφ were labeled *in situ* within donor mice using the PKH-26 dye as previously described. After washing, $1x10^6$ donor peritoneal cells (61.9% Mφ) in 250µl of PBS were mixed at 4°C with $5x10^6$ Hoescht 333342 labeled apoptotic thymocytes in an equal volume of PBS. The mixture of apoptotic thymocytes and donor peritoneal cells was then injected IP into age and gender matched female C57BL/6 recipient animals. After 30 minutes the recipient animals were sacrificed and peritoneal lavage and omentectomy performed. Control animals received an IP injection of donor lavage cells mixed with 250µl of PBS. The recovered donor peritoneal Mφ were enumerated by flow cytometry using the previously described single platform flow cytometry counting method. The Mφ adherent to omental milky spots were counted manually using transmitted fluorescent microscopy to identify the red fluorescent adoptively transferred Mφ. Milky spots were identified by their characteristic appearance under transmitted white light microscopy (see earlier).

A significantly higher number of Mφ bound to the omental lymphoid organ milky spots when adoptively transferred with apoptotic cells compared to Mφ transferred

alone (46.3±7.54 Mφ/high power field Vs 9.65±1.89 Mφ/high power field, p=0.009 – Figure 46).

Figure 46. Apoptotic cells enhance the attachment of resident peritoneal Mφ to omental milky spots

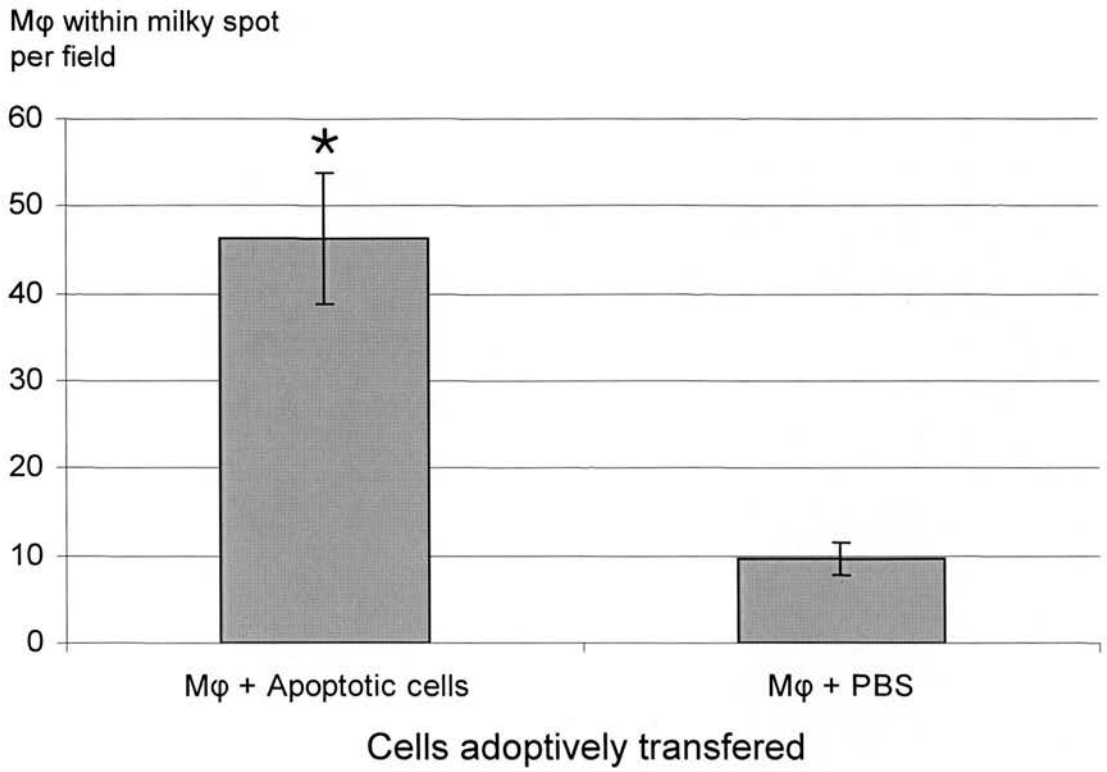

Y-axis = the number of adoptively transferred resident Mφ counted per field within milky spots. X-axis shows the nature of the adoptively transferred cells – Mφ transferred with or without apoptotic thymocytes. N=6 per group; 3 exeriments.

The experiment was repeated with inflammatory peritoneal Mφ harvested 4 days after an IP injection of 1ml of 3% brewers thioglycollate rather than resident non-inflammatory peritoneal Mφ. In a similar pattern to the resident Mφ, a significantly higher number of inflammatory Mφ adoptively transferred with apoptotic cells bound to the omental lymphoid organ milky spots compared to Mφ transferred alone (12.24±1.27 Mφ/field Vs 2.06±0.50 Mφ/field, p=0.003 – Figure 47).

Figure 47. Apoptotic cells enhance the attachment of inflammatory peritoneal Mφ to omental milky spots

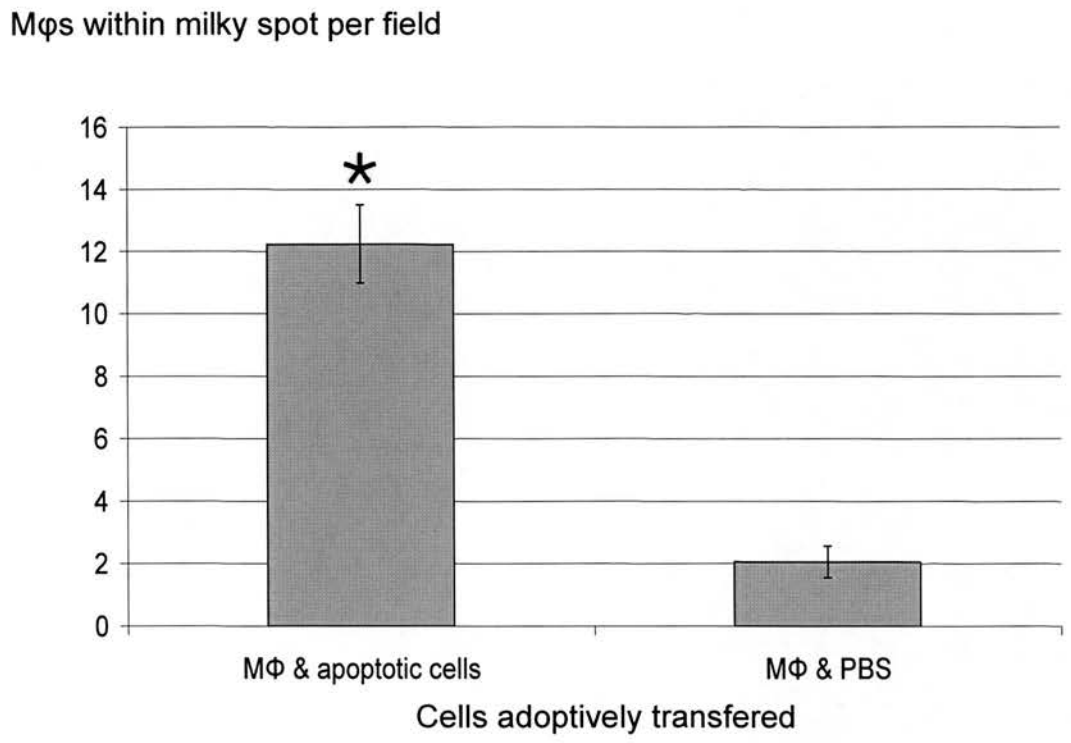

Y-axis = the mean number of adoptively transferred inflammatory Mφ counted per field within milky spots. X-axis shows the nature of the adoptively transferred cells – Mφ transferred with or without apoptotic thymocytes. N=5 per group; 2 experiments.

Figure 48. Representative images of adoptively transferred Mφ and labeled apoptotic cells binding to omental milky spots

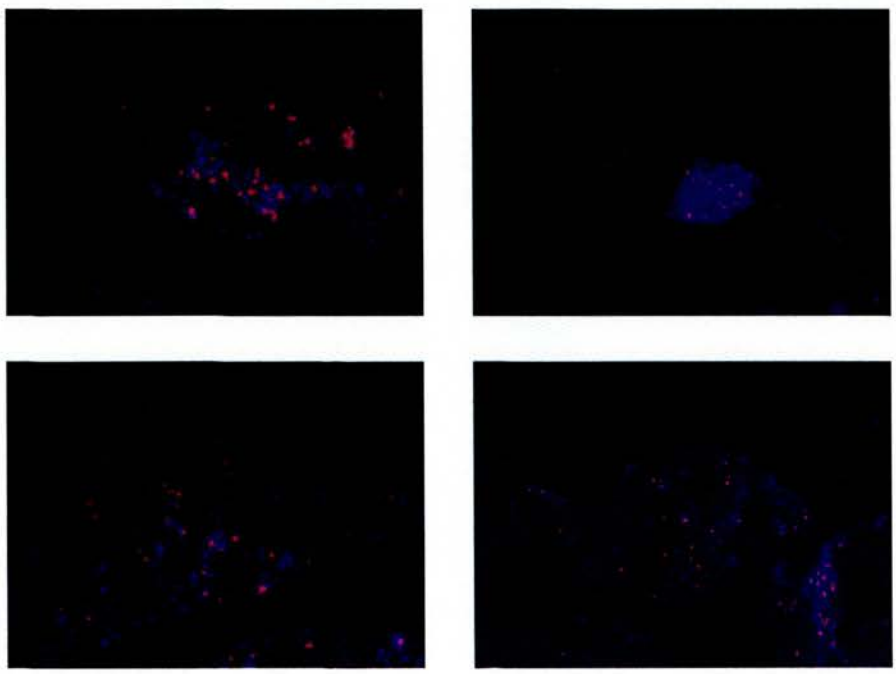

Four representative images of PKH-26 labeled adoptively transferred Mφ (red) and apoptotic thymocytes (blue) bound to omental milky spots. Magnification = x15.

5.9 The IP injection of apoptotic thymocytes promotes peritoneal Mφ emigration to parathymic lymph nodes

Bellingan has previously shown that, during the resolution phase of acute peritonitis, Mφ leave the peritoneal cavity and subsequently emigrate to draining lymph nodes (Bellingan et al., 1996). He focused on the intrathoracic parathymic lymph nodes, through which lymph from the peritoneal cavity passes en route to the thoracic duct. These lymph nodes are relatively easy to identify and dissect, particularly in the inflamed state (G Bellingan – personal communication). However, in his seminal paper in which he tracked the progress of inflammatory Mφ out of the peritoneal cavity over a 7 day period, he observed an abundance of Mφ within the omentum at a much earlier stage (4 hours) than they became apparent within the parathymic lymph nodes (24 – 72 hours) (Bellingan et al., 1996). Bellingan later identified milky spots as portals of emigration of peritoneal Mφ from the peritoneal cavity to the parathymic lymph nodes (Bellingan et al., 2002).

Bellingan used the sterile thioglycollate model of peritonitis for his Mφ emigration work and it is known that the IP injection of thioglycollate causes a very similar MDR to that which follows the injection of apoptotic thymocytes (Melnicoff et al., 1989). Taken together, these observations suggested that the MDR might be the first stage of a process of Mφ emigration from the peritoneal cavity to regional lymph nodes. It was therefore decided to test the hypothesis that the IP injection of

apoptotic cells would not only induce a rapid MDR but would also promote peritoneal Mφ emigration to regional lymph nodes.

12 C57BL/6 mice received an injection of PKH-26 dye as previously described. Four hours later, 6 mice received a further injection of $5x10^6$ CMFDA-labeled apoptotic thymocytes in 500μl PBS; the remaining 6 control animals received 500μl of PBS only. After 4 days, all the animals were sacrificed and the parathymic lymph nodes were recovered by careful dissection. The tissue was examined under fluorescent microscopy to confirm the presence of labeled peritoneal Mφ and then disaggregated and digested to liberate the Mφ within. The cell suspensions were examined by flow cytometry and the PKH-26 labeled Mφ were quantified as a percentage of all recovered cells.

A fairly small proportion of the cells recovered from the lymph node digestions were PKH-26+ peritoneal Mφ. Nonetheless, a significantly greater proportion of Mφ was recovered from animals that had received an IP injection of apoptotic thymocytes compared to the group receiving IP PBS only (3.58±0.51% Vs. 1.12±0.38%, N=6 per group, p=0.02 – Figure 49).

Figure 49. The IP injection of apoptotic thymocytes promotes resident Mφ emigration to parathymic lymph nodes

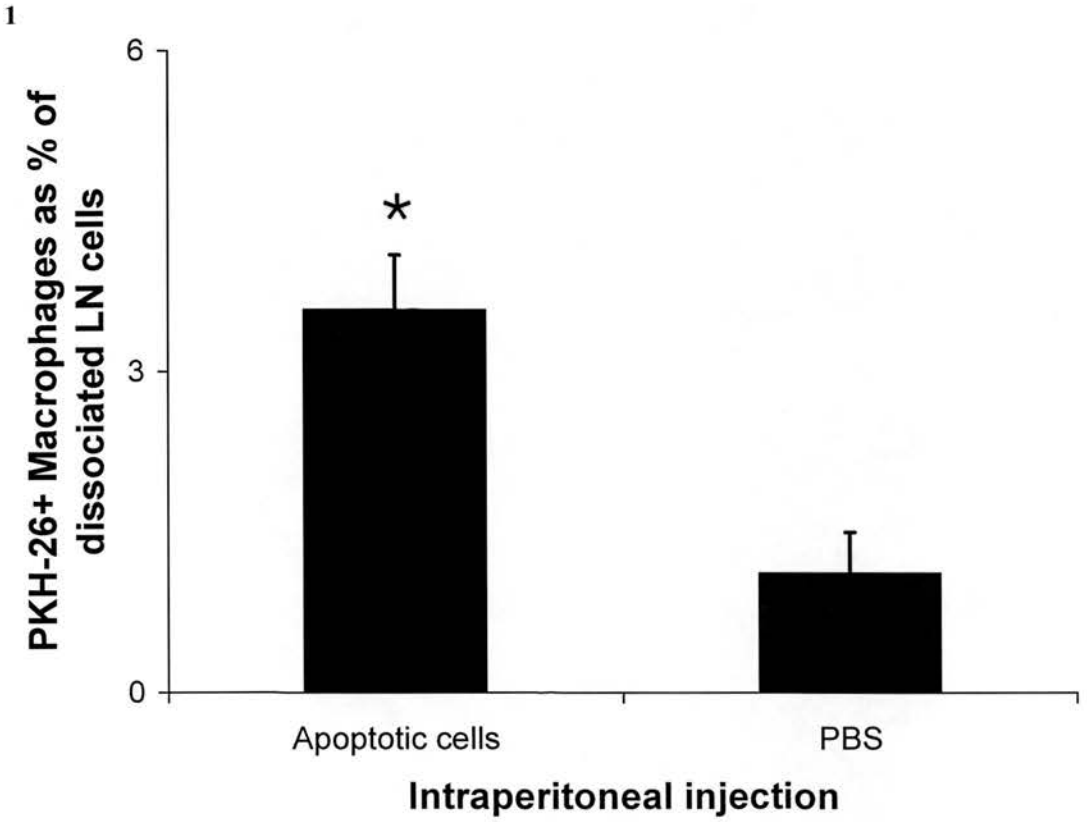

Y-axis = the proportion of PKH-26+ Mφ as a percentage of the total cell population recovered from the lymph node digestion. X-axis represents the IP injection received (either IP apoptotic thymocytes or IP PBS). *p=0.02. N=5 per group; 2 experiments.

5.10 Summary

- IP injected apoptotic cells rapidly concentrate within milky spots in the omental lymphoid organ
- Apoptotic cells within the omental milky spots have been phagocytosed by Mφ
- Peritoneal lavage samples extra-omental 'free' peritoneal Mφ, not those bound to milky spots
- Extra-omental Mφ enter the omental milky spots following the apoptotic cell induced MDR
- Both resident and inflammatory peritoneal Mφ enter omental milky spots when adoptively transferred with apoptotic cells
- Apoptotic cells promote the emigration of peritoneal Mφ to parathymic lymph nodes

6 CHAPTER 6 – RESULTS SECTION D

6.1 Introduction

The role of the omentum in the capture of free particles within the peritoneum *in vivo* was discussed in the Introduction. This activity is mediated by peritoneal Mφ of which there exists a 'free' population outside milky spots and a 'bound' population within milky spots. Evidence has been shown that some 'free' intraperitoneal Mφ bind to milky spots after interaction with apoptotic cells. Milky spots probably play a role in the initiation of secondary immune and inflammatory responses. The work presented in previous chapters has highlighted the consequences of interaction between instilled apoptotic cells and Mφ within the murine peritoneal cavity. There is considerable interest in *in vivo* assays of phagocytosis. The arrangement of the omentum, with 'naked' Mφ in direct contact with the peritoneal fluid is highly adapted for the phagocytosis of intraperitoneal particulate matter. Furthermore, it readily allows the passage of either white or fluorescent light, making it very amenable to microscopic study. In this chapter, specific mechanisms of apoptotic cell uptake by the omentum are investigated. The interactions of other particles (e.g. viable, non-apoptotic cells and fixed killed bacteria) with the omentum are also investigated.

6.2 *Free intraperitoneal apoptotic cells, rather than viable non-apoptotic cells, are preferentially bound to Mφ within the omental milky spots*

The omental lymphoid organ is ideally suited for the removal of particulate matter from within the peritoneal cavity. This has been shown clearly by the speed, efficiency and specificity of peritoneal apoptotic cell clearance. However, it is possible that the capture and subsequent phagocytosis of IP injected thymocytes was not a consequence of their being apoptotic. Thymocytes are, after all, immature T-lymphocytes which have the capacity to interact with Mφ in the context of antigen presentation within the immune response.

To ensure that omental Mφ were selectively binding to IP apoptotic cells I set up a competition assay. Equal numbers of apoptotic and non-apoptotic viable thymocytes were made using protocols described in the Methods section. The viable (5% apoptotic cells) and apoptotic thymocytes (85% apoptotic cells) were differentially labeled with CMFDA green and Hoescht 333342. Prior to labeling, the percentage apoptosis was measured in representative samples of cells using Hoescht 333342 and assessing nuclear morphology. A 50:50 mixture of $1x10^7$ viable and apoptotic cells ($5x10^6$ cells of each type) was injected IP into 5 C57BL/6 mice. After 30 minutes the mice were sacrificed and the omental lymphoid organs dissected and examined under light microscopy. 6 images from different regions of the omental lymphoid organ were taken in both the green, blue and orange channels allowing the apoptotic

and viable cells to be identified. The number of viable and apoptotic cells bound to omental milky spots within each image were then quantified.

The overwhelming majority of thymocytes which bound to the omental milky spots were apoptotic rather than viable (93.89 ± 1.74% Vs 6.11 ± 1.73%, apoptotic thymocytes Vs viable thymocytes, p=0.000006 – Figure 50). This data strongly supported the hypothesis that the apoptotic thymocytes are captured within the peritoneal cavity in preference to viable cells and thence taken up by milky spots. Apoptosis, or more probably the presence of 'eat me' signals on the cell surface, seemed to be a requirement for cell capture and phagocytosis by the omental milky spots.

There are important caveats to this data, which implies that a small number of viable, non-apoptotic cells may be captured. *In vivo*, potentially autoreactive thymocytes are deleted by apoptosis to prevent their development into mature T-cells. Furthermore, the extraction process requires the application of mechanical stress which is likely to induce apoptosis in some thymocytes. As a result, approximately 5% of the so-called 'viable' thymocytes instilled IP may in fact have been apoptotic and this may account for some of the 'viable' cells tethering to milky spots.

Figure 50. Apoptotic, rather than viable cells, preferentially localise to omental milky spots

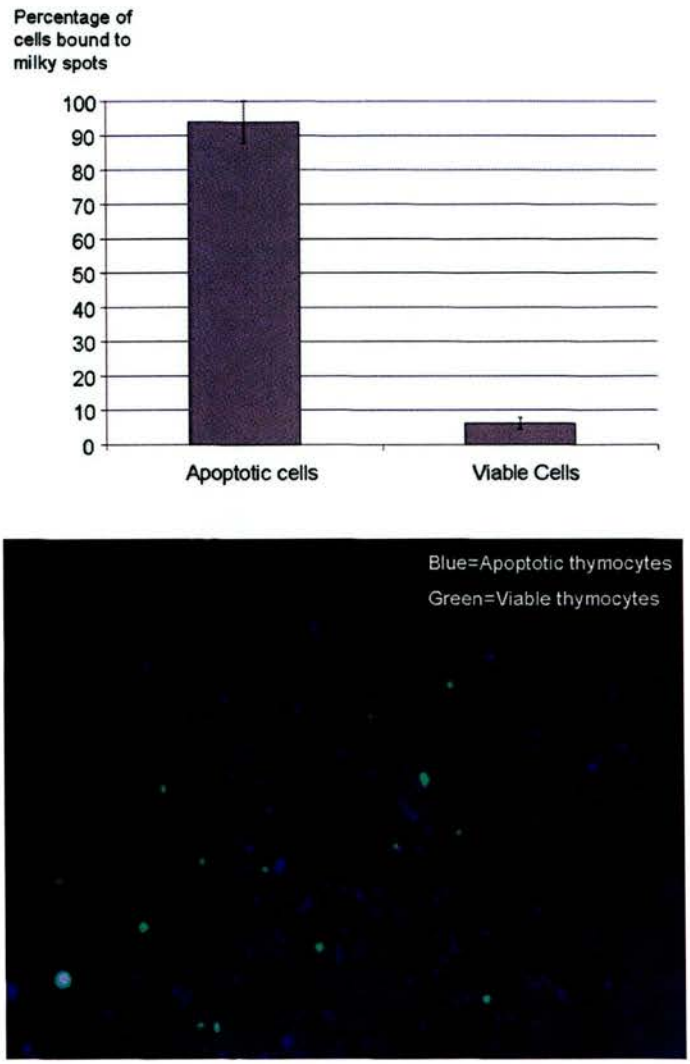

Top panel - Y-axis shows the percentage of thymocytes that bound to the milky spots that were either from the viable or apoptotic cell preparation. X-axis shows the nature of the bound cell – either an apoptotic thymocyte or viable thymocyte. N=4; 1 experiment.

Bottom panel – representative image showing green viable cells and blue Hoescht 333342 labeled apoptotic cells (magnification x50)

6.3 *Apoptotic thymocytes prepared from C1q +/+ mice preferentially localise to milky spots compared with apoptotic thymocytes from C1qa -/- donors*

A number of receptor-ligand pairings are known to mediate the recognition and phagocytosis of apoptotic cells by phagocytes (see Introduction). The relevance of these pairings *in vivo* in mammals is less well understood and is the subject of much scientific interest. C1q is known to be an important bridging molecule between the apoptotic cell and Mφ and its absence is associated with defective phagocytosis of apoptotic cells *in vivo* and autoimmunity (Botto et al., 1998, Taylor et al., 2000). It was therefore decided to see whether apoptotic cells opsonised in serum containing C1q would localise to the OLO in preference to those not opsonised with C1q.

Apoptotic murine thymocytes, derived from C1qa -/- mice, labeled with either CMFDA green or CMFDA red cell tracker dye, were prepared as previously outlined. The red apoptotic thymocytes were then incubated in serum from C57BL/6 mice whilst the green thymocytes were incubated in serum from age and sex matched C1qa -/- mice, which completely lacked C1q. After appropriate washing steps to remove any residual serum, an equal '50:50' suspension of green and red apoptotic thymocytes was prepared at a final concentration of $1x10^7$cells/ml in PBS. 0.5 mls of this suspension was injected IP into recipient C1qa -/- mice. After 30 minutes the OLOs were recovered by careful dissection and the number of red and green

apoptotic thymocytes attached to milky spots was counted by fluorescence microscopy.

Apoptotic thymocytes opsonised in C1q replete C57BL/6 serum localised to OLO milky spots in clear preference to those opsonised in C1q deficient serum from C1qa -/- mice. 78.48 ± 1.3 % of captured apoptotic thymocytes had been opsonised in C57BL/6 serum whilst the remaining 28.52 ± 1.3% had been opsonised in C1qa -/- serum ($p=0.0000054$, $N=4$ – Figure 51). This result was repeated when the cell tracker dyes were used in the opposite combination. This suggested that, not only was the localisation of cells to OLO milky spots the result of the cells being apoptotic, but the presence of C1q on the surface of the apoptotic cells further enhanced the localisation to OLO milky spots.

Figure 51. Opsonisation with C1q replete serum preferentially increases the localisation of apoptotic cells to omental milky spots

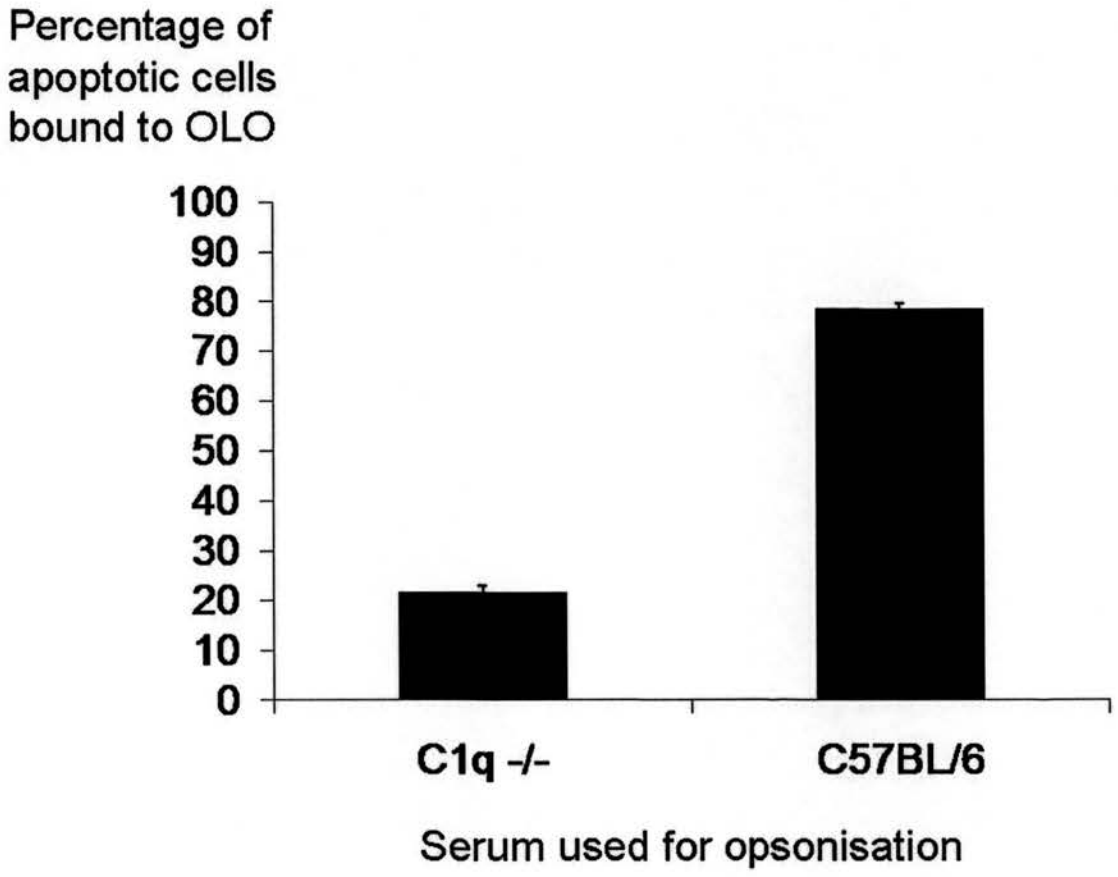

Y-axis = the percentage of differentially labeled cells counted on the OLO; X-axis indicates the nature of the opsonising serum used for each cell type. N=5; 1 experiment.

6.4 Viable thymocytes lacking CD31 localise to omental milky spot more readily than those expressing CD31

It has been shown previously that the antibody mediated blockade of CD31 inhibits the detachment of viable cells from phagocytes *in vitro* (Brown et al., 2002). This phenomenon has not, however, been demonstrated *in vivo*. CD31 is expressed by thymocytes and thymocytes completely lacking CD31 are available in the form of tissue harvested from CD31 knockout mice (CD31 -/-). A variant of the competition assays described above was used to determine whether the presence of CD31 influenced the proportion of viable thymocytes captured by intraperitoneal Mφ.

Viable, non-apoptotic thymocytes were extracted from CD31 -/- and CD31 +/+ controls (all females, less than 12 weeks old) as previously described. The CD31 -/- and +/+ thymocytes were then labeled with CMFDA green and red respectively and after appropriate washing to avoid contamination, a 50:50 mixture of green and red labeled cells was made at a final concentration of $1x10^7$ cells/ml. 0.5mls of this mixture was then injected IP into recipient CD31 +/+ mice. 30 minutes after the IP injection, the mice were sacrificed, OLOs recovered by careful dissection and the labeled cells that were attached to the OLO counted by fluorescence microscopy.

The number of viable thymocytes attached to the OLO was considerably lower than would have expected for IP injected apoptotic thymocytes. Nonetheless, it was clear that CD31 -/- viable thymocytes were preferentially bound to the OLO milky spots in

place of CD31 +/+ cells (percentage of CD31 -/- Vs CD31 +/+ thymocytes attached to the OLO respectively 69.48 ± 1.07% Vs 31.52 ± 1.07%, p= 0.00056, N=5 – Figure 52). This result was repeated when the cell tracker dyes were used in the opposite combination. These data supported the previous observation of Brown et al. that CD31 has a role in mediating the detachment of viable cells from phagocytes.

Figure 52. CD31 -/- viable thymocytes preferentially bind to OLO milky spots compared to CD31 +/+ thymocytes

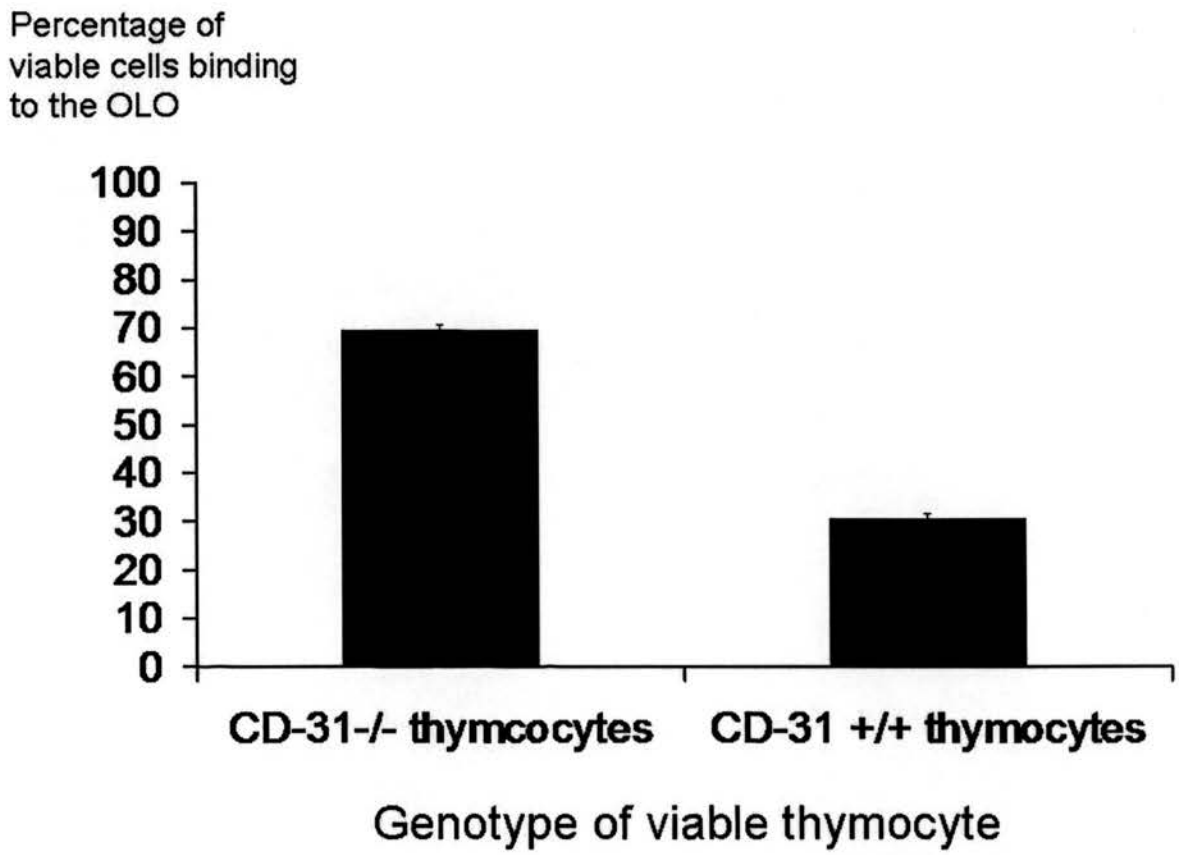

Y-axis = the percentage of differentially labeled cells counted on the OLO; X-axis = the genotype of the IP injected apoptotic cells. N=6 per group; 1 experiment.

6.5 *The Mφ phagocytosis of killed and fixed Staphylococcal aureus bacteria and their transportation to the omental milky spots*

Mφ are known to phagocytose bacteria *in vivo*, thus aiding the resolution of bacterial infection. Specific interactions between bacterial surface molecules and receptors on Mφ mediate the phagocytosis of bacteria in a similar way to the phagocytosis of apoptotic cells (see chapter 1). The possibility of using the omentum to study the mechanisms and consequences of the phagocytosis of bacteria *in vivo* was explored in some preliminary experiments discussed below.

The bacteria used for the following experiment were heat killed *Staphylococcus aureus*, Wood strain without protein A, labeled with Alexa 488 green cell tracker dye. These were bought commercially (Molecular Probes Catalog # S23371) and resuspended in PBS to a concentration of $5x10^6$ bacteria/ml according to the manufacturer's instructions. $1x10^6$ bacteria were injected IP into recipient C57BL/6 mice which were sacrificed after 30 minutes. Their omenta were dissected and examined under fluorescent microscopy as previously described. Many fluorescent bacteria were seen within milky spots. The omenta were then mechanically disaggregated and digested using the previously described methods. The resultant cell suspensions were then washed twice in PBS, labeled with F4/80-PE cell tracker dye as outlined previously. When examined by flow cytometry and fluorescent microscopy, it was apparent that the IP injected bacteria had been phagocytosed by omental Mφ (figures 52 and 53).

Figure 53. Phagocytosed fluorescently labeled S. aureus bacteria within Mφ recovered from omental milky spots (A)

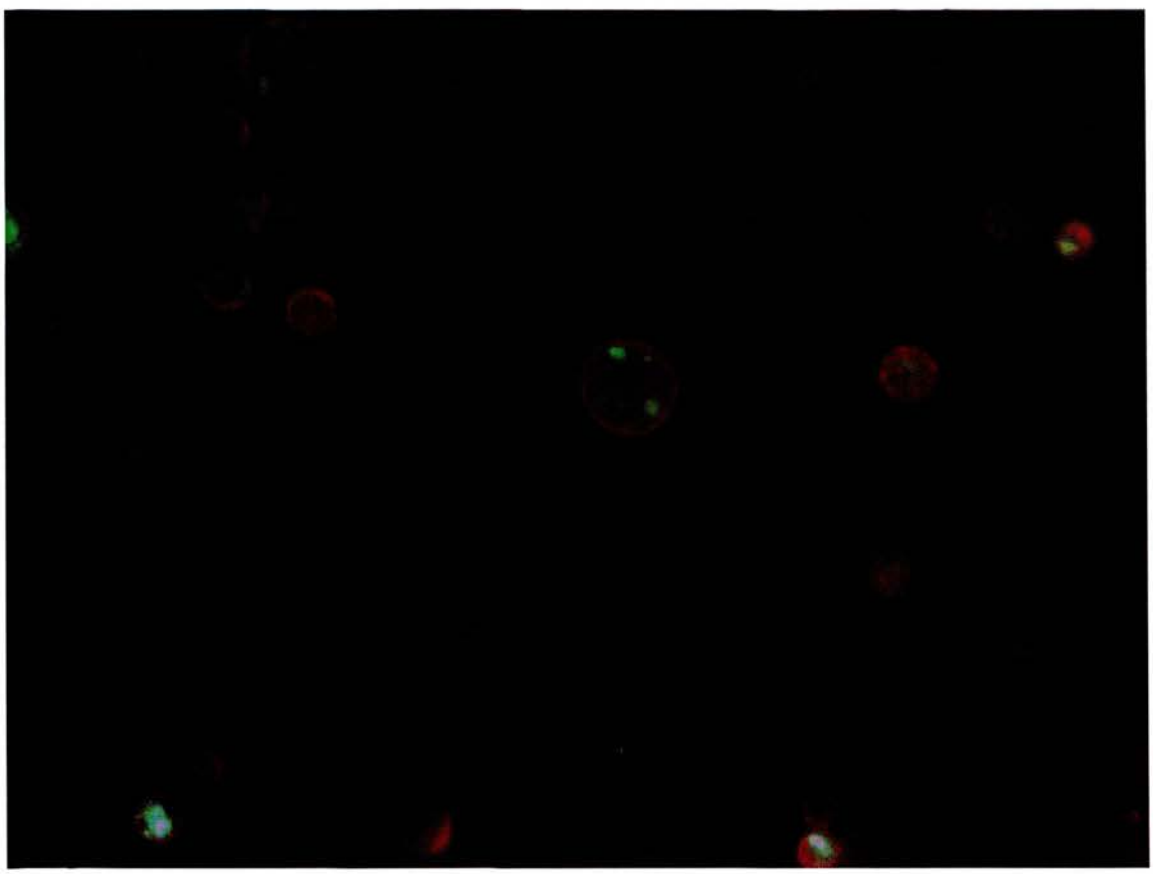

Fluorescence photomicrograph of omental Mφ (F4/80-PE – red) recovered 30 minutes after the IP injection of heat-killed *S. aureus* bactera (Alexa 488 – green). Green fluorescent bacteria may be clearly seen within Mφ phagolysosomes. Magnification x 400

Figure 54. Phagocytosed fluorescently labeled S. aureus bacteria within Mφ recovered from omental milky spots

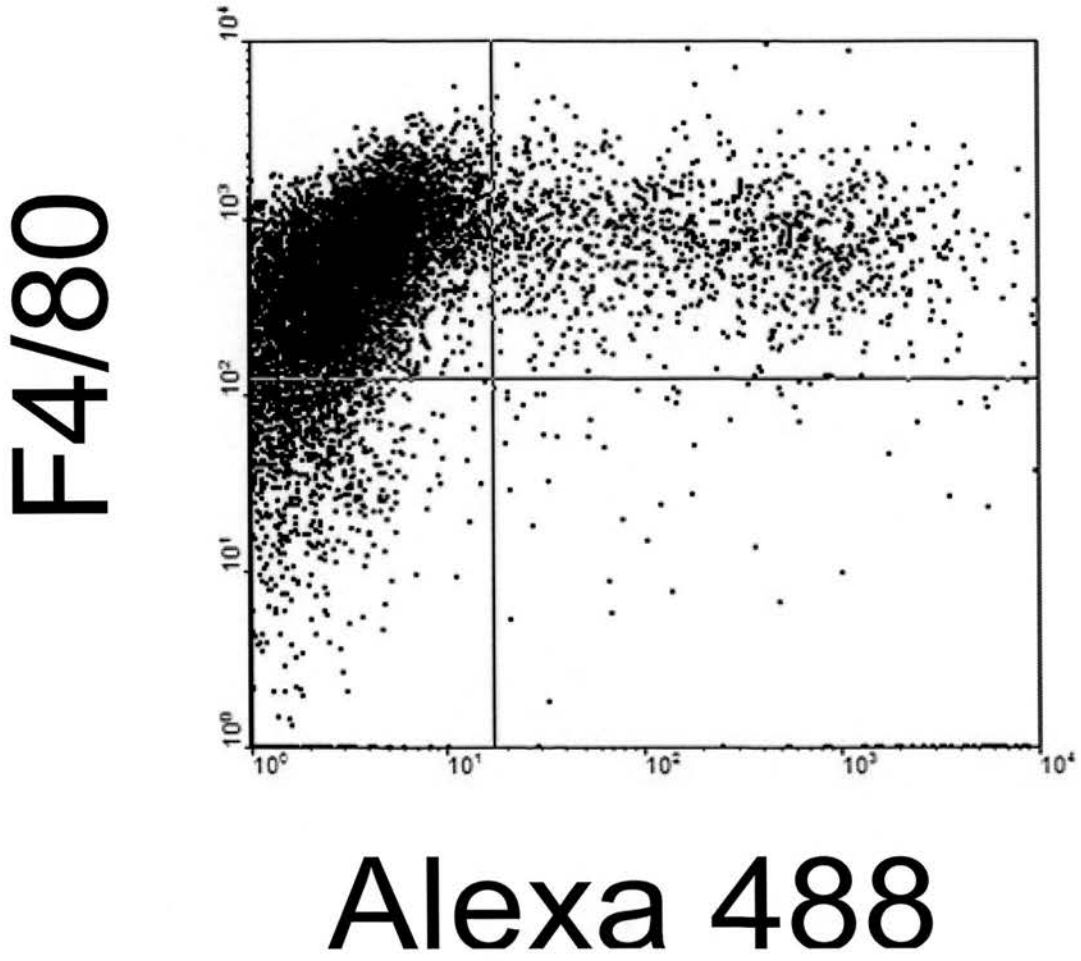

Flow cytometry dot plot. Y-axis = F4/80-PE (FL2); X-axis = Alexa 488 (FL1). F4/80-HI Mφ population has acquired FL1 labeling indicating that Mφ have phagocytosed $FL1^+$ bacteria.

6.6 *IP injection of S. aureus, but not apoptotic cells, causes PMN recruitment to the omentum*

The omentum is thought to be the major site of PMN recruitment during peritonitis. Significant recruitment of PMNs following the IP injection of AC had not been seen but it seemed likely that this would follow IP bacteria. To compare the relative potential for omental PMN recruitment of bacteria and AC, the following experiment was performed. C57BL/6 mice received an IP injection of either a) $1x10^6$ heat killed *S. aureus* (Alexa 488 labeled), b) $5x10^6$ apoptotic thymocytes or c) 0.5ml PBS. Animals from each group were sacrificed at 24 and 48 hours and their omenta digested. PMNs within the cell suspension were identified by labeling with rat-anti-mouse GR1. The labeled samples were analysed by flow cytometry and the number of GR1-HI PMNs expressed as a percentage of total recoverable cells.

A very large recruitment of PMNs to the omentum was apparent 24 hours after IP *S. aureus* injection (Figure 55). This was still apparent after 48 hours but to a lesser degree. Neither the injection of AC or PBS caused a significant recruitment of PMNs to the omentum.

Figure 55. IP S. aureus injection causes PMN recruitment to the omentum

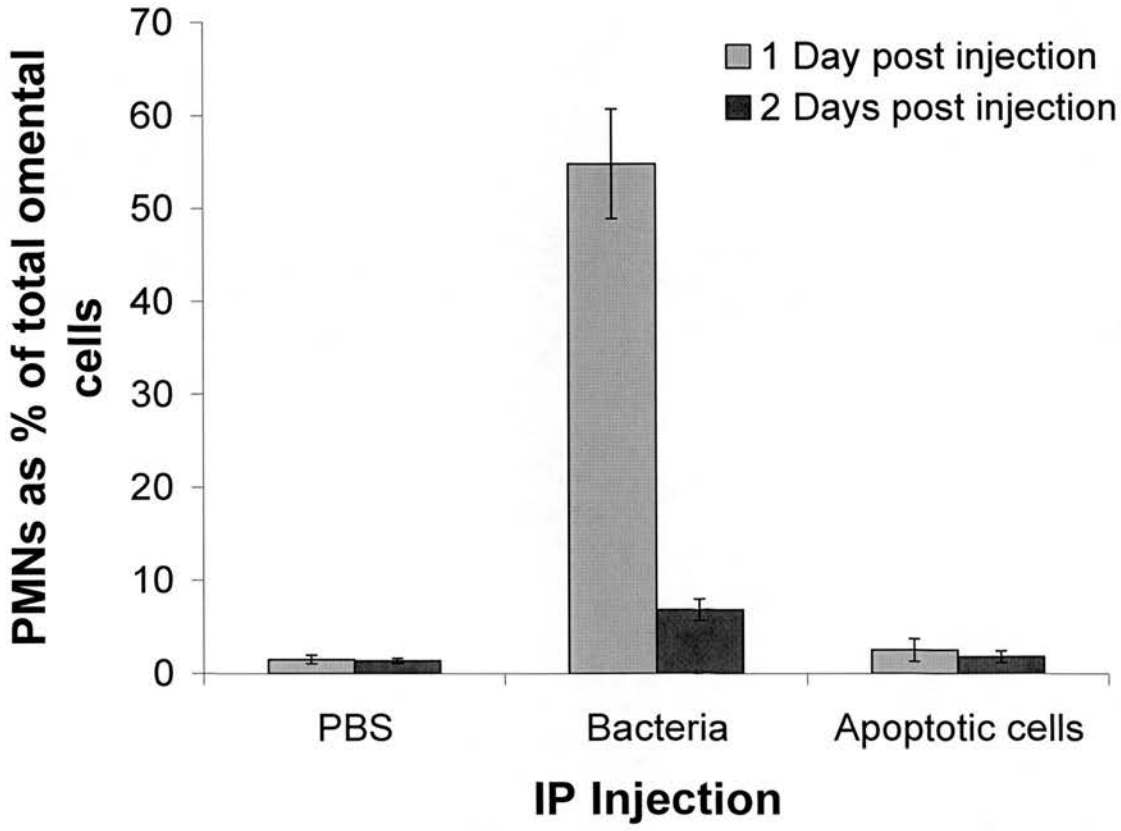

Y-axis = GR1-HI PMNs recovered from digested omenta expressed as the percentage of total omental cells within the cell suspension. X-axis= IP injection given to groups of mice

6.7 Summary

- Omental milky spots preferentially bound apoptotic, rather than viable thymocytes
- Omental milky spots prefertially bound apoptotic cells opsonised in C1qa +/+ serum, rather than C1qa -/- serum
- Viable, non-apoptotic thymocytes lacking CD31 localised to omental milky spots more readily than those expressing CD31
- IP injected heat-killed and fixed S. aureus bacteria also localize to omental milky spots
- IP injection of heat-killed and fixed S. aureus bacteria causes PMN recruitment to the omental lymphoid organ; apoptotic cells do not

7 CHAPTER 7 – DISCUSSION

7.1 IP injected apoptotic cells cause a MDR

The Mφ disappearance reaction (MDR) was first described over 40 years ago (Nelson, 1963) but remains something of an immunological mystery to this day. The MDR typically follows injurious, pro-inflammatory insults to the peritoneal cavity. This study reports that IP instilled apoptotic cells can induce a MDR.

There are several pieces of evidence indicating that apoptotic cells trigger a MDR involving resident peritoneal Mφ. IP injected apoptotic thymocytes induce a profound and rapid loss of lavageable resident peritoneal Mφ. This occurs simultaneously with the loss of apoptotic cells due to their clearance by phagocytic resident Mφ. The MDR is seen following IP administration of apoptotic murine thymocytes and apoptotic Jurkat cells. Control injections in which the peritoneal membrane was merely breached or PBS was injected IP did not induce a MDR. The MDR induced by apoptotic thymocytes is not confined to the C57BL/6 strain (in which most experiments were performed) but was also seen in Balb/c mice. The co-injection of polymyxin B with apoptotic cells had no effect on the MDR, suggesting that contaminating LPS was not causing the MDR. Furthermore, the MDR seen in LPS-resistant CD14 -/- mice after IP apoptotic cells was of identical size to that seen in LPS-sensitive control Balb/c mice.

Unexpectedly, IP injected Flowcheck beads also induced a MDR, albeit one of smaller magnitude than that induced by apoptotic cells. The only published data

regarding IP synthetic beads on the size of the resident Mφ population was by Haskill and Becker who used tiny fluorescent spheres to label the resident peritoneal Mφ population prior to the induction of a MDR (Haskill and Becker, 1985). These beads were phagocytosed by Mφ but did not induce a MDR, though one did subsequently occur after IP administration of *C. parvum* bacteria. Nonetheless, the induction of a MDR and other inflammatory responses by inorganic material is not unprecedented. A pleural leukocyte disappearance reaction followed the intrapleural instillation of ground glass (Sultan et al., 1978). Inorganic particulate matter such as carbon particles or titanium dioxide is phagocytosed by alveolar Mφ causing their activation (Renwick et al., 2004). Furthermore, urate crystals, when phagocytosed by Mφ with subtly different maturation states, induce different inflammatory responses from the phagocytosing Mφ (Yagnik et al., 2000). It is impossible to properly compare the spheres used by Haskill and Becker and Flowcheck microspheres but it is almost certain that they will differ significantly. Haskill and Becker's work suggests that phagocytosis of beads does not always induce a MDR. They did not examine their peritoneal lavages until 96 hours after IP beads during which time Mφ may have disappeared and then reappeared. However, the presence of a similar number of Mφ at the 96 hour time point suggests that a MDR did not occur.

The same authors identified clumps of Mφ held together by fibrinous strands following the MDR (Haskill and Becker, 1985). Three days later, resident Mφ began to reappear in the peritoneal fluid and elevated levels of plasminogen activating

factor (PAF) were also noted within the peritoneal cavity, suggesting that fibrin degradation was occurring (Haskill and Becker, 1985). Leak et al. also observed that resident Mφ reappeared 72 hours post-MDR together with evidence of fibrinolysis in peritoneal lavage fluid (Leak, 1983). A MDR directly induced by thrombin has also been reported (Jokay and Karczag, 1973). These data, taken as a whole, suggest that activation of the coagulation cascade and fibrin deposition can account for some descriptions of the MDR.

The MDR induced by apoptotic cells appears to be faster than others reported elsewhere. Melnicoff reported a MDR induced by the IP injection of brewers thioglycollate (Melnicoff et al., 1989). A MDR was observed in 20% of mice at 30 minutes and in all mice by 60 minutes. This seems to be slower than the MDR induced by IP administration of AC. No other published report of the MDR examined time points below 30 minutes. However, a complete disappearance of Mφ was almost always observed in other published studies.

The rapidity and magnitude of the MDR suggests that direct contact with the provoking agent may not be necessary to trigger an MDR. Secondary amplification mechanisms may trigger the disappearance after an initial contact with the primary agent. Such signals could be mediated by cells other than Mφ, such as peritoneal mesothelial cells, known to mediate peritoneal inflammation by cytokine secretion (Topley, 1995). Peritoneal lavage supernatant transfer experiments from donor animals receiving apoptotic cells to naïve recipients might shed light upon this.

There have been no reported studies showing a MDR following the instillation of noxious material in humans though one observational study provides indirect evidence for this (personal communication, Professor Simon Davies, Keele University). A longitudinal study of peritonitis in patients on peritoneal dialysis involved patients retaining daily samples of peritoneal dialysis fluid. The study aimed to examine the microbiological and leukocyte profiles of the peritoneal dialysis fluid immediately before and after the clinical manifestation of peritonitis. The investigators were surprised to observe a fall in the number of resident peritoneal Mφ in the hours before peritonitis became clinically apparent.
This observation was not explained but, in retrospect, it is tempting to conclude that a MDR involving resident peritoneal Mφ occurred.

Another possibility worthy of consideration is that apoptotic cells may have played a significant role in previous published reports of MDRs. It should be remembered that many reports of MDRs were published in the period 1960-90. Apopsosis was only discovered in 1972 (Kerr et al., 1972) and its fundamental and wide-reaching importance as a biological processes only truly appreciated in the late 1980s. Furthermore, practical, straightforward tests to identify apoptotic cells were not available during the period in which much of the pioneering work on the MDR was published. It is entirely possible that previous investigators were either unaware of or unable to identify apoptotic cells as part of their investigations of the MDR.

There is certainly reason to believe that many of the agents historically used to induce MDRs could have themselves lead to apoptosis of cells within the peritoneal cavity. Firstly, apoptosis is now recognized to be the predominant mode of death for PMNs after the first phase of acute inflammation (Haslett, 1999, Haslett et al., 1994, Haslett et al., 1991) and it is generally accepted that these cells are removed from inflamed tissue by phagocytic Mφ (Savill, 1992, Savill and Fadok, 2000). It is possible that these apoptotic PMNs induce a MDR; it is certainly clear that the period in which these cells are dying is associated with rapid trafficking of Mφ (Melnicoff et al., 1989). However infectious pathogens can themselves induce apoptosis in host cells and these too could stimulate a MDR. Mycobacterium bovis is known to induce the MDR in Guinea pigs (Gillissen and Bubenzer, 1970) and it also induces apoptosis of Mφ as part of its pathogenic behaviour (Fratazzi et al., 2000). Similar behaviour has been described in other Mycobacteria including Mycobacterium avium (Allen et al., 2001). Group B streptococci also induce Mφ apoptosis (Ullet and Adderson, 2003) and a MDR (Bultmann et al., 1971).

Non-leukocyte cells within the peritoneal cavity are also prone to inflammation-dependent apoptosis. Peritoneal mesothelial cells become susceptible to Fas-mediated apoptosis in the presence of high levels of TNF-α (Chen et al., 2003). It is entirely possible that apoptosis of peritoneal mesothelial cells occurs during peritonitis and that these may induce a secondary MDR. However, such a possibility has not yet been investigated.

7.2 Mechanism of the AC-induced MDR

This present study also investigated possible mechanisms mediating an apoptotic cell induced MDR. The MDR was initially observed in apoptotic cells injected in PBS lacking Ca^{2+} and Mg^{2+}. When apoptotic cells were injected in a Ca^{2+} and Mg^{2+} containing PBS solution, no difference in the magnitude of the MDR was seen. However, apoptotic cells injected in PBS containing EDTA triggered a significantly larger MDR than EDTA-free controls. A lesser degree of apoptotic cell phagocytosis was also observed in those mice receiving EDTA. EDTA has been added to peritoneal lavage solutions, the purpose being to increase the recovery of Mφ by disabling Ca^{2+}-dependent Mφ adhesion mechanisms (Taylor et al., 2000). It seems likely that EDTA induced a large reduction in the cation concentration within the peritoneal fluid which may have disrupted integrin-mediated phagocytosis of apoptotic cells. Nonetheless, these data suggest that the MDR is not critically dependent on the presence of extracellular divalent cations.

The Arg-Gly-Asp (RGD) motif mediates cell adhesion to several extracellular matrix components (including those involving integrins) as well as cell-cell interactions (Yamada, 1997). The addition of RGD peptide to IP injected suspension of apoptotic thymocytes reduced the apoptotic cell-induced MDR. However a proportionate decrease in the clearance of the apoptotic cells was also observed. Integrins bearing the RGD motif are known to be involved in the phagocytosis of apoptotic cells (Savill et al., 1990). Bellingan has shown that thioglycollate-elicited Mφ binding to

milky spots was inhibited by the action of RGDS and antibodies blocking VLA-4 and VLA-5 integrins (Bellingan et al., 2002). Furthermore, the action of phagocytosing apoptotic cells modulates the expression of integrins on the phagocytic Mφ (albeit to decrease their expression) (Erwig et al., 1998). For his binding experiments to milky spots, Bellingan used a ring clamp system to minimise the volume of distribution of his antibodies (Bellingan et al., 2002). In this present study, the phagocytosis of apoptotic cells was believed to be a prerequisite for the binding of Mφ to milky spots. IP injection of bulk antibody had been shown to modulate Mφ emigration to parathymic lymph nodes (Bellingan et al., 2002) and future work may use this strategy to examine Mφ behaviour following the uptake of apoptotic cells including the interaction with the omentum.

IP hyaluronidase reduced the apoptotic cell-induced MDR without affecting the phagocytosis of apoptotic cells. Hyaluronic acid is a disaccharide polymer composed of D-glucuronic acid and D-N-acetylglucosamine (Alberts, 1994). It is an important component of extracellular matrix with roles in solute and water movement across the peritoneal membrane and in cell migration (Wright and Day, 2005, Edward et al., 2005). Mφ and other cells bear CD44 which has hyaluronic acid as its main ligand. CD44 is also known to be involved in the phagocytosis of apoptotic human PMNs (Hart et al., 1997). IP injected hyaluronidase is known to break down intraperitoneal hyaluronic acid (Shannon and Love, 1980). Furthermore hyaluronic acid has previously been shown to play a role in the MDR. The BCG-induced MDR observed in mice was almost completely abolished by the IP co-

administration of hyaluronidase (Shannon et al., 1980). Moreover, when Mφ reappeared following the BCG-induced MDR, peritoneal hyaluronic acid levels fell compared to the time of MDR induction (Shannon et al., 1980). There is also some evidence to suggest that peritoneal Mφ from C3H/Hej mice, which do not undergo a BCG-induced MDR, have a lower capacity to bind hyaluronic acid than the C57BL/6 strain, in which an MDR is seen (Shannon and Love, 1980). No data has previously been published linking CD44 to the MDR.

This present study also demonstrated that unfractionated heparin reduced the apoptotic cell induced MDR without reducing the phagocytosis of apoptotic cells. The coagulation cascade has been implicated in other examples of the MDR. The first instance of this is the intrapleural MDR induced by the injection of ground glass (Sultan et al., 1978). As previously discussed, the pleural and peritoneal cavities have many similarities and Mφ disappearance reactions occur in both. The MDR observed by Sultan et al. was inhibited by both heparin and warfarin. The coincidence of a reduced MDR in two structurally unrelated anticoagulant agents strongly implicated the coagulation cascade in the ground glass MDR. Mφ clumps encased in fibrin were also observed following a MDR (Sultan et al., 1978), a finding reported in other examples of the MDR (Nelson and Boyden, 1963, Haskill and Becker, 1985).

Heparin may also disrupt the MDR independently of its actions on coagulation. Heparin is known to disrupt the diapedesis of extravasating T-lymphocytes, probably

by binding to polysaccharide receptors (Gorski et al., 1991). Furthermore, heparin is known to bind to Mφ-borne receptors for L-Selectin, a molecule which again might conceivably be involved in the MDR (Nelson et al., 1995).

The role of other types of leukocytes in the MDR was investigated by Barth (Barth et al., 1995). Leukocyte precursors in murine bone marrow were selectively depleted using Sr^{89}. Barth et al showed that the MDR induced by *P. acnes* could still occur, even in the absence of significantly reduced numbers of circulating monocytes, lymphocytes or leukocytes. However, it would be a mistake to take this as evidence that the MDR is never mediated by other leukocytes. Sonoszaki and Ochiya showed that T-lymphocytes, depleted of Mφ, from sensitised donors could passively transfer the MDR to naïve recipient mice (Sonozaki and Cohen, 1971, Ochiya et al., 1982). Furthermore, cyclosporine inhibits the MDR induced by muramyl dipeptide (Matsushima and Baba, 1990). This finding might now be reinterpreted as not necessarily implicating T-cells in the MDR.

7.3 Fate of the 'disappeared' Mφ

In these studies IP apoptotic cells triggers a MDR followed by a specific binding of Mφ to omental milky spots. The evidence for this came from three key observations. Firstly, 'free' apoptotic cells bind to and are phagocytosed by Mφ within peritoneal fluid. After the MDR, these apoptotic cells are seen in high concentrations and are, once again, bound to or phagocytosed by Mφ. Secondly, the omentum appeared to

become 'enriched' with Mφ following the MDR. Thirdly, adoptively transferred Mφ (resident or inflammatory Mφ) bound to omental milky spots when transferred with apoptotic cells. It was not possible to determine what proportion of the 'disappeared' peritoneal Mφ bound to omental milky spots. The peritoneal membrane has a relatively high surface area. Its strong adherence to underlying structures and tendency to fold when dissected meant that examination of the entire peritoneal membrane was practically impossible. However, few if any Mφ were seen away from milky spots following the MDR.

Bellingan identified milky spots as sites to which inflammatory peritoneal Mφ selectively attach themselves (Bellingan et al., 2002, Bellingan et al., 1996). Thioglycollate-elicited Mφ labeled with PKH-26 dye left the peritoneal cavity during the resolution phase of inflammation and migrated to the parathymic lymph nodes (Bellingan et al., 1996). A thorough survey of the abdominal contents identified the milky spots as sites in which peritoneal Mφ congregated. The highest concentration of Mφ was found in the omentum and, though not published in the original paper, the author has confirmed that the locality of these Mφ was within the omental milky spots (G. Bellingan - personal communication).

Other reports suggest a different fate for the disappeared Mφ, not necessarily involving the milky spots. The first report of the MDR described the finding of clumps of Mφ within peritoneal lavage fluid (Nelson and Boyden, 1963). Electron microscopy showed Mφ in very close association without obvious fibrinous material

holding them together. From the modern perspective, this suggests the involvement of cell-membrane adhesion molecules, such as integrins and their ligands. Other authors also found Mφ clumped within peritoneal fluid. Sultan et al. studied the MDR that occurs in the pleural cavity of rats (a structure which shares many features with the peritoneal cavity, including milky spots) (Sultan et al., 1978). Clumps of Mφ encased in fibrin were recovered following a MDR induced by intrapleural ground glass. Haskill and Becker also observed clumping of Mφ on the peritoneal membrane following a MDR and also the reappearance of 'disappeared' Mφ after approximately 3 days (Haskill and Becker, 1985).

It was not possible to track the Mφ that disappeared after IP apoptotic cell injection for a time period beyond 24 hours for several reasons. Firstly, phagocytosed microspheres would have allowed prolonged tracking but may have compromised the phagocytic ability of Mφ and possibly induced a MDR themselves. Secondly, phagocytosed apoptotic cells and their associated CMFDA marker are rapidly degraded within the Mφ phagolysosome and hence cannot be identified after 5-7 hours (personal communication – J Gilmore). Another possibility was to label apoptotic cells with a pH sensitive dye that would signal the entry of an apoptotic cell into an acidic phagolysosome. Preliminary enquiries to appropriate suppliers suggested that such dyes would not persist for the period of time required for a more lengthy study. This, plus time and resource constraints, meant that studies on pH-sensitive dyes were not undertaken.

It may be that several variations of the MDR exist, some involving the milky spots and others not. The production of fibrin is a well-recognised and frequent complication of peritonitis is clinical practice (Dunn et al., 1984, Hau and Simmons, 1978, Muntean, 1987, Nadig et al., 1997). Even here the milky spots may be playing a role by encouraging the extravasation of coagulation factors during peritonitis (Cranshaw and Leak, 1990).

7.4 Link between phagocytosis and the MDR

This study showed that the phagocytosis of apoptotic thymocytes, injected IP, was very rapid and resulted in a simultaneous disappearance of resident peritoneal Mφ. Flow cytometry of recovered peritoneal lavage cells clearly showed that apoptotic cells were being phagocytosed. Apoptotic cells were concentrated within omental milky spots. When Mφ were digested from the omentum after the apoptotic cell-induced MDR, it was clear that these Mφ had also phagocytosed apoptotic cells.

The question of whether the apoptotic cell-induced MDR actually required phagocytosis of apoptotic cells was addressed by examining the MDR in C1qa -/- mice. These mice have a well-characterised defect in the phagocytosis of apoptotic cells (Taylor et al., 2000). C1q is not thought to play a direct role in Mφ adhesion or emigration. Both the phagocytosis of apoptotic cells and the MDR were both diminished in C1qa -/- mice, implying a direct causal link between the first process and the second.

The MDR is no doubt mediated by molecules involved in Mφ adhesion, as discussed earlier. Many adhesion molecules including integrins and ICAMs are involved in both phagocytosis of apoptotic cells and Mφ adhesion (Gregory et al., 1998, Moffatt et al., 1999, Savill et al., 1990). Indeed, it is known that alterations in the extracellular matrix environment can decrease the ability of Mφ to phagocytose apoptotic cells, probably by sequestrating Mφ receptors that would normally engage the apoptotic cell on ECM proteins (Kirkham et al., 2004, McCutcheon et al., 1998). The ligation of integrin receptors downregulates Mφ phagocytic ability (Erwig et al., 1999). The phagocytosis of Mycobacterium tuberculosis is known to increase the adhesiveness of human Mφ via the increased expression of LFA-1 and ICAM-1 (DesJardin et al., 2002). However, there appears to have been no specific studies of changes in Mφ adhesion following the phagocytosis of apoptotic cells.

7.5 Mφ may emigrate to lymph nodes following the MDR

Resident peritoneal Mφ appeared to emigrate to parathymic lymph nodes following the IP administration of apoptotic cells. PKH-26 labeled cells, of peritoneal origin, appeared in parathymic lymph nodes several days after the IP injection of apoptotic cells (unlabeled). In this study, and previously published work (Melnicoff et al., 1988b) 99% of PKH-HI cells within the peritoneal cavity are resident Mφ. It is possible that the PKH-26 dye was carried to parathymic lymph nodes by peritoneal

dendritic cells, rather than Mφ. However, few if any $CD11c^+$ dendritic cells are identified within the quiescent peritoneal cavity. In control animals receiving PKH-26 but no apoptotic cells, PKH-26 fluorescence was nonetheless identified within parathymic lymph nodes. This probably indicates that resident peritoneal Mφ migrate to regional lymph nodes as part of their normal life cycle, though this has not been shown definitively. Nonetheless, a significantly greater proportion of PKH-26+ cells were found in the parathymic lymph nodes after IP apoptotic cells.

Bellingan found that the attachment of inflammatory peritoneal Mφ to milky spots was partially mediated by VLA-4 and VLA-5 integrins (Bellingan et al., 2002). Furthermore, these same anti-VLA-4 and anti-VLA-5 blocking antibodies also inhibited emigration of peritoneal Mφ to parathymic lymph nodes (Bellingan et al., 2002). These data suggested that the emigration of Mφ from the peritoneal cavity involved an initial binding of Mφ to milky spots followed by emigration to lymph nodes. Blocking this initial binding to milky spots appeared to delay the entire emigratory process. Mandache et al. made similar observations in rats (Mandache et al., 1985). They injected rats with *C. parvum*, excised their omenta at a variety of time points and examined the milky spots by electron microscopy. Within 30 minutes, layers of Mφ were seen overlying the surface of milky spots. After 24 hours, resident Mφ were found in the deeper layers of the milky spot and after four days within regional lymph nodes.

There is no published evidence that the phagocytosis of apoptotic cells promotes the emigration of Mφ to draining lymph nodes though circumstantial evidence suggests that it might. Huynh demonstrated that the instillation of intra-tracheal apoptotic cells enhanced the resolution of experimental pneumonia via the release of TGF-β (Huynh et al., 2002). A dramatic decrease in the number of inflammatory Mφ was observed during this resolution phase. It could be that the production of anti-inflammatory cytokines mediated the emigration of resident peritoneal Mφ to lymph nodes, though TGF-β production following the phagocytosis of apoptotic cells by quiescent Mφ is not well established.

Dendritic cell (DC) migration to lymph nodes is an important part of their function as antigen presenting cells (Janeway, 2001a). Hirao and colleagues showed that dendritic cells co-cultured with apoptotic tumour cells altered their expression of chemokine receptors, upregulating CCR7 and downregulating CCR1 (Hirao et al., 2000). The presence of the CCR7 ligands, macrophage inflammatory protein 3b and secondary lymphoid-tissue chemokine significantly increased the migration of DCs co-cultured with apoptotic cells in an *in vitro* migration assay. Furthermore, increased expression of CCR7 *in vivo* resulted in increased emigration of DCs to lymph nodes *in vivo* (in the presence of apoptotic tumour cells). Similar studies on Mφ have not been published.

7.6 Novel uses for the omentum to explore Mφ behaviour and function

IP injected apoptotic cells are rapidly taken up by the murine omental milky spots partly by free peritoneal Mφ which phagocytose apoptotic cells before themselves attaching to milky spots. However, Mφ already resident within the milky spots will almost certainly capture and phagocytose passing free apoptotic cells within the peritoneal cavity. The architecture of the milky spot places fully mature resident peritoneal Mφ, with the greatest capacity for phagocytosis, at the outermost layer in direct contact with the peritoneal fluid. This allows mature Mφ to constantly sample peritoneal fluid and capture passing particulate matter, including apoptotic cells and bacteria.

These features were exploited in various competition assays. In these assays, a 50:50 mixtures of differentially labeled cells with differing properties were injected and the number of each cell type that ultimately became attached to milky spots was counted by fluorescence microscopy. The power of injecting a mixture of cells was that uncontrollable variables – cell leakage, size and cellularity of the omental lymphoid organ, cell pooling within the peritoneal cavity etc.- were identical for both types of injected cell. This vastly reduced the errors in comparative measurements compared with injecting homgenous pools of cells into separate groups of recipients.

As proof of this principle, a 50:50 mixture of differentially labeled apoptotic and viable thymocytes was injected IP. The hypothesis was that both peritoneal and omental milky spot Mφ would preferentially bind apoptotic, rather than viable, thymocytes. This was indeed the case. However, the difference was large – about 20 fold – and highly statistically significant despite injections only being given to 3 animals. The reason for this highly significant result was the extremely consistent ratio of viable:live cells attached to milky spots.

The next test for this system was to inject a mixture of apoptotic thymocytes derived from C1qa -/- mice; 50% were opsonised in serum from C1q +/+ mice and 50% were opsonised in C1qa -/- serum. Thus, 50% of the administered apoptotic thymocytes would have C1q bound to their cell surface. The hypothesis was that C1q-opsonised thymocytes would have a greater probability of being phagocytosed by peritoneal and milky spot Mφ and this indeed was the case. As with viable and apoptotic cells, the difference was large – about 4 fold in favour of C1q opsonised cells – and highly significant.

Although the issue of whether the milky spot Mφ had actually phagocytosed apoptotic cells in this particular experiment was not directly assessed, previous experiments had shown that apoptotic cells injected IP are phagocytosed by Mφ within this time interval. This type of competition experiment could therefore be considered a 'phagocytosis assay', notwithstanding the absence of direct observation of phagocytosed apoptotic cells within milky spot Mφ. Various *in vivo* other

phagocytosis assays do not include the direct observation of apoptotic cells within Mφ, in particular those which rely on the persistence of apoptotic cells as evidence for defective phagocytosis (Scott et al., 2001, Robson et al., 2001, Platt et al., 1996).

This system is potentially a very powerful one for identifying factors on the apoptotic cell surface that are thought to mediate the phagocytosis of the cell by Mφ. The production of paired data and reduction in uncontrolled variability offers far more robust data than injecting cells into different groups of animals. 'Refinement and reduction' are key principles in the development of *in vivo* experiments, especially given concern amongst the lay public about the use of animals in experimentation.

The final application of the competition assay in this study switched from apoptotic to viable cells. Brown et al. had shown that CD31 mediates the repulsion of Mφ and viable cells *in vitro*. Using a flow cell system to apply shear stress, at room temperature viable leukocytes became attached to Mφ but detached at 37°C. When CD31 was either blocked with antibody or not expressed, this detachment was inhibited. This observation suggested that, *in vivo*, CD31 may act as a 'badge' to inform Mφ to disregard them as a possible 'phagocytic meal'. This hypothesis had not been tested *in vivo* and the paired competition assay was an ideal tool for this purpose. The observation that viable thymocytes from CD31 -/- mice were significantly more likely to be captured by omental milky spots than CD31 +/+ thymocytes supported Brown's *in vitro* observation.

7.7 Why should apoptotic cells induce a MDR?

The consensus view is that the MDR is an immune response to injurious stimuli (Barth et al., 1995). This raises the question of why might the immune system regard apoptotic cells as a potentially injurious stimulus? The first danger posed by apoptotic cells is the possibility of triggering autoimmunity. During the process of apoptosis, many intra-cellular components, normally invisible to the immune system – proteins, DNA, phospholipids etc. - are expressed at the cell surface (Savill and Fadok, 2000). In some cases – e.g. phosphatidylserine - these substances have a clear role in allowing the phagocyte to recognise, attach to and ultimately phagocytose the apoptotic cell (Fadok et al., 1992b). The proteins and nucleic acids expressed on the surface during apoptosis are usually modified by enzymic degradation during the apoptotic programme. This processing produces 'altered self' which can provoke autoantibody production (Kinoshita et al., 1999, Cline and Radic, 2004, Rosen and Casciola-Rosen, 1999).

It is not only the potential for autoantibody production that gives apoptotic cells their injurious potential. Apoptotic cells can secrete chemokines that recruit both Mφ and PMNs. This was demonstrated most elegantly in experiments utilising a vascular smooth muscle cell line designed to undergo apoptosis via the over-expression of FADD under a Tet-off control (Schaub et al., 2000, Bowen-Pope and Schaub, 2001). The apoptotic smooth muscle cells expressed high levels of IL-8 (neutrophil chemokine) and MCP-1, a Mφ chemokine *in vitro*. When seeded within the

vasculature of rats, the mass apoptosis of these cells resulted in significant local inflammation and Mφ recruitment.

More recent work has identified other chemoattractants produced during apoptosis. *In vivo*, tumours such as Burkitt's lymphoma are characterized by large numbers of infiltrating Mφ which clear apoptotic tumour cells. It has been shown *in vitro* that apoptosis of Burkitt's lymphoma cells leads to the chemotaxis of Mφ (Truman et al., 2004). Recently a chemoattractant has been identified that is produced during apoptosis which might explain how professional phagocytes find distant apoptotic cells (Lauber et al., 2003). Lauber induced apoptosis in a variety of different tumour cell lines in vitro and showed that this lead to the chemoattraction of various types of monocyte-Mφ cells (Lauber et al., 2003). Furthermore, the supernatant from these cultured apoptotic cells also induced transmigration of monocyte-Mφs. Whilst the phenomenon was not restricted to apoptosis induced in a single cell type, it was notably not seen in MCF7 cells (Lauber et al., 2003).

Unlike the other apoptotic cell types tested by Lauber, the MCF7 cell line did not express caspase-3. Lauber showed that restoring the production of caspase-3 in MCF7 cells also restored their ability to produce a chemoattractant supernatant during apoptosis (Lauber et al., 2003). Further investigations showed that the chemotactic agent within this supernatant was lysophosphatidylcholine, produced by an as-yet imperfectly understood mechanism involving the activation of caspase-3 and calcium-independent phospholipase A_2 (Lauber et al., 2003).

Lysophosphatidylcholine has also been identified as a membrane bound 'eat me' signal on apoptotic cells (Kim et al., 2002). Kim et al. also showed that membrane-bound lysophosphatidylcholine on apoptotic cells is recognized by IgM natural antibodies which recruit C1q, a molecule known to mediate the phagocytosis of apoptotic cells (Kim et al., 2002, Taylor et al., 2000). Whether the same mechanisms are responsible for the production of bound and secreted lysophosphatidylcholine is unknown as are the inflammatory consequences of lysophosphatidylcholine secretion.

7.8 Apoptotic cells and bacteria – amplification of the 'danger signal'?

Despite triggering a MDR, IP apoptotic cells do not appear to promote acute inflammation, as judged by the recruitment of PMNs. Mφ play a pivotal role in the recruitment of PMNs to the peritoneum through the induction of CXC chemokine production (Cailhier et al., 2005). It is not clear whether the omentum produces these chemokines, and this would be an interesting area for future study. It seems highly likely that one purpose of the MDR is to allow activated Mφ the opportunity to present danger signals to the site of peritoneal leukocyte trafficking – i.e. omental milky spots. Although the phagocytosis of apoptotic cells itself is generally deemed a non-inflammatory process, there is some evidence that the phagocytosis of apoptotic cells can, in certain circumstances, augment an inflammatory response (Lucas et al., 2003). It would be interesting to study the effects of co-administration

of apoptotic cells and bacteria, on both the MDR and inflammatory cell trafficking. The presence of apoptotic cells and large number of bacteria may result in an amplification of the 'danger signal'. On the other hand, the phagocytosis of apoptotic cells may reprogram some Mφ from a pro- to anti-inflammatory phenotype and reduce the subsequent level of peritoneal inflammation. The ratio of apoptotic cells: bacteria is likely to be critical to the outcome of such experiments.

7.9 Further definition of the mechanism driving the MDR

This study offered some insights into the mechanism driving the apoptotic cell induced MDR but did not fully define it. The MDR has been shown to be enhanced by hyaluronidase and inhibited by EDTA and unfractionated heparin. Both the MDR and apoptotic cell clearance were inhibited by RGDS peptide, which blocks the activity of certain integrins.

CD44 is the major receptor on Mφ for hyaluronic acid and a possible role in the MDR merits further investigation, possibly utilising CD44 knockout mice. One of the problems with knockout animals in general is the uncertainty as to what compensatory phenotypical changes may have occurred in the genetically modified animal. Thus, instilling anti-CD44 antibodies or Fab fragments may also help to clarify this.

The role of integrins should be more fully explored. IP RGD inhibited both phagocytosis and the MDR. However, this shone little light on the exact mechanism governing the MDR as RGD block a wide variety of integrins. It might be possible to define integrins involved in phagocytosis from others involved in the adhesion and disappearance of Mφ by the use of specific antibodies or Fab fragments. Alternatively, adoptive transfer of Mφ lacking specific integrins from genetically modified mice or cell lines could be used. Other molecules involved in cell adhesion, including members of the ICAM and VCAM families, which are again highly expressed in milky spots (Cui et al., 2002), could be included in such a study.

The role of chemokines was not examined in this study. The omentum is known to secrete large amounts of chemokines, including SDF-1α (Pinho Mde et al., 2002), and it is conceivable that these play a role in the MDR. Again, this could be studied by testing the MDR in knockout mice lacking genes encoding chemokines or chemokine receptors. Again, antibody blocking strategies could also be considered. Such materials were not available to me during the period of this study. However, a simple test screening test could be performed using IP instilled pertussis toxin, a general inhibitor of the action of chemokines.

The effect of heparin on the MDR is both intriguing and challenging. It is well-recognised clinically that peritonitis is complicated by the production of fibrin and hence intraperitoneal heparin is often used to prevent this (Johnson and Feehally, 2003). The coagulation cascade is complex with many components. An initial first

step to identifying clotting factors that might be involved in the MDR could include a comparative trial of warfarin and heparin to see whether the MDR was mediated by the intrinsic or extrinsic coagulation pathway. However, as previously mentioned, heparin has effects other than those on coagulation which might be of relevance to the MDR, including inhibition of selectins (Nelson et al., 1995). Selectins are another possible family of molecules that may play a role in the MDR and would be candidates for investigation. Recently-published work has also demonstrated that chemerin, an agonist of CMKLR1 which is activated by the coagulation cascade, can direct the migration of dendritic cells to sites of injury in which bleeding has occurred (Zabel et al., 2005a). It may be that this, or other chemokine pathways associated with haemorrhage, are being disabled by heparin and chemerin is another interesting candidate as a mediator of the apoptotic cell-induced MDR.

7.10 Further definition of the role of CD31 in Mφ-viable cell interactions

The observation that viable non-apoptotic thymocytes lacking CD31 were more likely to become attached to milky spots that viable non-apoptotic CD31 +/+ thymocytes was interesting and novel. CD31 is not expressed on all cell types and it was assumed that binding occurred in a homophilic manner between the thymocyte and milky spot Mφ. This could be proven by either confocal microscopy or by flow cytometry of digested omental cells.

Brown and colleagues showed that certain cytoplasmic tail mutations in CD31 removed the ability of Mφ and viable leukocytes to detach under shear stress e.g. a double tyrosine to phenylalanine mutant of the ITIM motif within the cytoplasmic tail of CD31 (Brown et al., 2002). This region is known to be involved in intracellular signalling pathways (Reedquist et al., 2000) and integrin activation (Newton et al., 1997). A number of cell lines expressing CD31 molecules with various tail mutations have been produced (S. Brown – personal communication). The competition assay described within this thesis could be used to determine whether some or all play a role in the detachment of viable cells from Mφ.

7.11 The omentum for investigation of leukocyte trafficking in vivo

The murine omentum is in many ways an ideal organ for examining the trafficking of leukocytes *in vivo*. Milky spots are well established as the sites of leukocyte recruitment to the omentum and, in the case of Mφ, the site of emigration too. Milky spots have a clear morphology that allows them to be identified with light microscopy or by simple staining, such as PKH-26 or even intraperitoneal carbon particles. They are highly reactive to intraperitoneal inflammatory stimuli with the number and cellularity of milky spots increasing dramatically during inflammation. Furthermore, the position of the omentum within the abdominal cavity allows it to be readily accessed and externalised. Whilst this study only attempted to do this post-mortum, it is quite possible that intravital microscopy could be performed on the omentum using similar technology to that applied to the murine mesentery (Little et al., 2005).

Furthermore, the presence of lymphatic vessels within omental milky spots makes the omentum an attractive target for studying leukocyte emigration from the peritoneal cavity, again using intravital microscopy. An intriguing if highly speculative possible consequence of the MDR is the relationship with lymphangiogenesis. Twenty years ago, a study of the behaviour of murine omental milky spots following stimulation with sheep erythrocytes noted that Mφ bound to milky spots and nearby peritoneal membrane formed clumps similar to those described in other studies (Dux et al., 1986). Several days later, tubular structures

were seen in association with these clumps and it was speculated that these might be newly developing lymphatic vessels whose production was stimulated by the attached peritoneal Mφ. At the time, the technology to identify these as lymphatic vessels within the peritoneal membrane did not exist. However, it has recently been shown that Mφ can themselves transdifferentiate into lymphatic endothelial cells during corneal inflammation (Maruyama et al., 2005). Furthermore, *in vitro* peritoneal Mφ can form tube like structures and express markers typically found on lymphatic endothelial cells including Prox-1 and LYVE-1 (Maruyama et al., 2005). Once again, the accessibility of the omentum for intra-vital microscopy makes it an ideal place to study lymphangiogenesis. Indeed, generations of surgeons have exploited the omentum for its apparent ability to encourage revascularisation following surgery, including procedures beyond the abdominal cavity (Shrager et al., 2003, Goldsmith, 2004) Indeed, a novel if controversial therapy for Alzheimers dementia involving transplantation of omentum within the brain is currently the subject of clinical trials within the USA (Goldsmith, 2004). It is known that the omentum contains high levels of VEGF (Zhang et al., 1997, Sigrist et al., 2003, Williams et al., 1989) and the mechanisms governing its action within the omentum would be a fascinating subject for investigation.

7.12 Future work

The data presented within this thesis identifies a novel process by which apoptotic cells within the peritoneal cavity induce a MDR. This MDR is not induced by live cells and is not restricted to particular type of apoptotic cell. Resident and inflammatory Mφ localize to the milky spots of the omentum and may then migrate to regional lymph nodes. Future work arising from this thesis should focus on three main areas. Firstly, the mechanism by which apoptotic cells induce the attachment of Mφ to milky spots, secondly the mechanism governing the emigration of Mφ from the peritoneal cavity to regional lymph nodes and thirdly the generalisability of the the apoptotic cell-induced MDR.

This mechanism governing the binding of Mφ to milky spots is clearly one that can be rapidly activated given the short time interval between the IP injection of apoptotic cells and the MDR. Attachment and recognition molecules on the Mφ and target sites of milky spots are unlikely to be synthesized *de novo* during the MDR but are far more likely to be pre-formed and activated at the initiation of the MDR. Integrins are attractive candidate molecules for such a mechanism and should be investigated. Data presented in this thesis demonstrates that RGD peptide does indeed inhibit the MDR but this could have been explained by RGD-dependent inhibition of phagocytosis of apoptotic cells. Further work should focus on more precise interuption of integrin function that avoids inhibition of phagocytosis. Such a experiments could involve the adoptive transfer of genetically modified Mφ (either

mature peritoneal Mφ or via bone marrow transplant) that fail to express defined integrins. A good starting candidate would be β_1 integrins such as VLA-4 or VLA-5 already implicated in inflammatory Mφ adhesion to milky spots (Bellingan et al., 2002). Another strategy could be to employ blocking antibodies or fAb fragments against target integrins though the large quantity of antibody needed for effective blockade of the whole peritoneal cavity could be a significant practical problem.

The role of the coagulation system in the apoptotic cell-induced MDR also merits further investigation. The coagulation cascade is rapidly activated during injury – physical and inflammatory – and certainly is capable of inducing the apoptotic cell-induced MDR. Further evidence for a role for the coagulation system in the apoptotic cell induced MDR could be obtained by using warfarin to disable coagulation. Then more defined experiments could be performed to investigate the role of individual components of the coagulation cascade in the apoptotic cell-induced MDR. Potential candidates for investigation could include factor XIIa and plasmin, serine proteases that activate both the coagulation cascade and chemerin, a ligand for the G-protein-coupled receptor CMKLR1 present on dendritic cells and Mφ. Chemerin recruits circulating antigen presenting cells to sites of injury following activation by the coagulation cascade (Zabel et al., 2005b, Zabel et al., 2005a). Inhibitors of chemerin and genetic knockout mice are available and could be tested as inhibitors of the apoptotic cell-induced MDR.

The process by which Mφ leave the omentum and emigrate to regional lymph nodes appears to be slower than the immediate Mφ disappearance reaction but nevertheless there could still be shared mechanistic elements. For example, Bellingan demonstrated that β_1 integrins were involved in both the initial rapid binding of Mφ to peritoneal milky spots and their subsequent emigration, despite the fact that the first process occurred over minutes and the second over days (Bellingan et al., 2002). Therefore future work should examine a role for integrins not only in the immediate MDR but also in subsequent emigration of peritoneal Mφ to draining lymph nodes.

Chemokines are likely to play a role in the emigration of Mφ to draining lymph nodes. Recent work showed that the expression of CCR7 on dendritic cells was increased following contact with apoptotic tumour cells resulting in emigration of dendritic cells to draining lymph nodes (Hirao et al., 2000). It is quite possible that a similar mechanism governs the emigration of Mφ from the peritoneal cavity following the MDR. The hypothesis that chemokines were involved in the emigration of peritoneal Mφ by using pertussis toxin as a general inhibitor of chemokines. The specific role of CCR7 could be investigated by measuring its expression on Mφ that have phagocytosed apoptotic cells. CCR7 knockout mice do exist and these might be used in experiments to determine the role of CCR7 in Mφ emigration to lymph nodes *in vivo*.

It is important to determine whether the MDR and subsequent Mφ emigration to lymph nodes are peculiar to the peritoneal cavity or more generalisable phenomena.

To determine which is the case, it should first be established whether the apoptotic cell-induced MDR occurs other coelomic cavities. This could be done by recreating the apoptotic cell transfer experiments described in this thesis. Further work could investigate whether apoptotic cells induce a MDR in solid organs. In such cases in would not be practical to directly inject apoptotic but these could be generated in situ for example by ultraviolet irradiation of the skin or systemic administration of dexamethasone to induce the apoptosis of thymocytes.

8 REFERENCES

Agalar, F., Sayek, I., Cakmakci, M., Hascelik, G. and Abbasoglu, O. (1997) *Eur J Surg,* **163,** 605-9.

Akakura, S., Singh, S., Spataro, M., Akakura, R., Kim, J. I., Albert, M. L. and Birge, R. B. (2004) *Exp Cell Res,* **292,** 403-16.

Albert, M. L., Sauter, B. and Bhardwaj, N. (1998) *Nature,* **392,** 86-9.

Alberts, B. (1994) *Molecular biology of the cell,* Garland Pub., New York.

Albina, J. E. and Reichner, J. S. (1998) *Cancer Metastasis Rev,* **17,** 39-53.

Allen, S., Sotos, J., Sylte, M. J. and Czuprynski, C. J. (2001) *Clin Diagn Lab Immunol,* **8,** 460-4.

Ambroze, W. L., Jr., Wolff, B. G., Kelly, K. A., Beart, R. W., Jr., Dozois, R. R. and Ilstrup, D. M. (1991) *Dis Colon Rectum,* **34,** 563-5.

Barth, M. W., Hendrzak, J. A., Melnicoff, M. J. and Morahan, P. S. (1995) *J Leukoc Biol,* **57,** 361-7.

BCSH (1997) In *Clin Lab Haematol*, Vol. 19, pp. 231-41.

Becq, F., Hamon, Y., Bajetto, A., Gola, M., Verrier, B. and Chimini, G. (1997) *J Biol Chem,* **272,** 2695-9.

Beelen, R. H., Eestermans, I. L., Dopp, E. A. and Dijkstra, C. D. (1988) *Adv Exp Med Biol,* **237,** 745-50.

Beelen, R. H., Fluitsma, D. M. and Hoefsmit, E. C. (1980) *J Reticuloendothel Soc,* **28,** 585-99.

Bell, C. G. (1993) *Biochem Soc Trans,* **21 (Pt 3),** 288S.

Bellingan, G. J., Caldwell, H., Howie, S. E., Dransfield, I. and Haslett, C. (1996) *J Immunol,* **157,** 2577-85.

Bellingan, G. J., Xu, P., Cooksley, H., Cauldwell, H., Shock, A., Bottoms, S., Haslett, C., Mutsaers, S. E. and Laurent, G. J. (2002) *J Exp Med,* **196,** 1515-21.

Blander, J. M. and Medzhitov, R. (2004) *Science,* **304,** 1014-8.

Boes, M. (2000) *Mol Immunol,* **37,** 1141-9.

Border, W. A. and Noble, N. A. (1994) *N Engl J Med,* **331,** 1286-92.

Bose, J., Gruber, A. D., Helming, L., Schiebe, S., Wegener, I., Hafner, M., Beales, M., Kontgen, F. and Lengeling, A. (2004) *J Biol,* **3,** 15.

Botto, M., Dell'Agnola, C., Bygrave, A. E., Thompson, E. M., Cook, H. T., Petry, F., Loos, M., Pandolfi, P. P. and Walport, M. J. (1998) *Nat Genet,* **19,** 56-9.

Botto, M. and Walport, M. J. (2002) *Immunobiology,* **205,** 395-406.

Bowen-Pope, D. F. and Schaub, F. J. (2001) *Trends Cardiovasc Med,* **11,** 42-5.

Bretscher, M. S. (1972) *Nat New Biol,* **236,** 11-2.

Brown, S., Heinisch, I., Ross, E., Shaw, K., Buckley, C. D. and Savill, J. (2002) *Nature,* **418,** 200-3.

Bultmann, B., Bigazzi, P. L., Heymer, B. and Haferkamp, O. (1971) *Z Immunitatsforsch Exp Klin Immunol,* **142,** 267-75.

Cailhier, J. F., Partolina, M., Vuthoori, S., Wu, S., Ko, K., Watson, S., Savill, J., Hughes, J. and Lang, R. A. (2005) *J Immunol,* **174,** 2336-42.

Casciola-Rosen, L. A., Anhalt, G. and Rosen, A. (1994) *J Exp Med,* **179,** 1317-30.

Castellano, F., Chavrier, P. and Caron, E. (2001) *Semin Immunol,* **13,** 347-55.

Chen, J. Y., Chi, C. W., Chen, H. L., Wan, C. P., Yang, W. C. and Yang, A. H. (2003) *Nephrol Dial Transplant,* **18,** 1741-7.

Chow, J. C., Young, D. W., Golenbock, D. T., Christ, W. J. and Gusovsky, F. (1999) *J Biol Chem,* **274,** 10689-92.

Cikala, M., Alexandrova, O., David, C. N., Proschel, M., Stiening, B., Cramer, P. and Bottger, A. (2004) *BMC Cell Biol,* **5,** 26.

Cline, A. M. and Radic, M. Z. (2004) *Clin Immunol,* **112,** 175-82.

Cranshaw, M. L. and Leak, L. V. (1990) *Arch Histol Cytol,* **53 Suppl,** 165-77.

Cui, L., Johkura, K., Liang, Y., Teng, R., Ogiwara, N., Okouchi, Y., Asanuma, K. and Sasaki, K. (2002) *Cell Tissue Res,* **310,** 321-30.

Cui, P., Qin, B., Liu, N., Pan, G. and Pei, D. (2004) *Exp Cell Res,* **293,** 154-63.

Danilevicius, Z. (1973) *Jama,* **223,** 434-5.

DesJardin, L. E., Kaufman, T. M., Potts, B., Kutzbach, B., Yi, H. and Schlesinger, L. S. (2002) *Microbiology,* **148,** 3161-71.

Devitt, A., Moffatt, O. D., Raykundalia, C., Capra, J. D., Simmons, D. L. and Gregory, C. D. (1998) *Nature,* **392,** 505-9.

Devitt, A., Parker, K. G., Ogden, C. A., Oldreive, C., Clay, M. F., Melville, L. A., Bellamy, C. O., Lacy-Hulbert, A., Gangloff, S. C., Goyert, S. M. and Gregory, C. D. (2004) *J Cell Biol,* **167,** 1161-70.

Devitt, A., Pierce, S., Oldreive, C., Shingler, W. H. and Gregory, C. D. (2003) *Cell Death Differ,* **10,** 371-82.

Doherty, N. S., Griffiths, R. J., Hakkinen, J. P., Scampoli, D. N. and Milici, A. J. (1995) *Inflamm Res,* **44,** 169-77.

D'Silva, H., Yoshida, T. and Cohen, S. (1983) *J Exp Pathol,* **1,** 61-9.

Duffield, J. S., Forbes, S. J., Constandinou, C. M., Clay, S., Partolina, M., Vuthoori, S., Wu, S., Lang, R. and Iredale, J. P. (2005) *J Clin Invest,* **115,** 56-65.

Dunn, D. L., Rotstein, O. D. and Simmons, R. L. (1984) *Arch Surg,* **119,** 139-44.

Dux, K., Rouse, R. V. and Kyewski, B. (1986) *Eur J Immunol,* **16,** 1029-32.

Edward, M., Gillan, C., Micha, D. and Tammi, R. H. (2005) *Carcinogenesis,* **26,** 1215-23.

Ekre, H. P., Naparstek, Y., Lider, O., Hyden, P., Hagermark, O., Nilsson, T., Vlodavsky, I. and Cohen, I. (1992) *Adv Exp Med Biol,* **313,** 329-40.

Ellis, H. M. and Horvitz, H. R. (1986) *Cell,* **44,** 817-29.

Ellis, R. E., Jacobson, D. M. and Horvitz, H. R. (1991) *Genetics,* **129,** 79-94.

Enari, M., Sakahira, H., Yokoyama, H., Okawa, K., Iwamatsu, A. and Nagata, S. (1998) *Nature,* **391,** 43-50.

Erwig, L. P., Gordon, S., Walsh, G. M. and Rees, A. J. (1999) *Blood,* **93,** 1406-12.

Erwig, L. P., Kluth, D. C., Walsh, G. M. and Rees, A. J. (1998) *J Immunol,* **161,** 1983-8.

Fadok, V. A., Bratton, D. L., Konowal, A., Freed, P. W., Westcott, J. Y. and Henson, P. M. (1998) *J Clin Invest,* **101,** 890-8.

Fadok, V. A., Bratton, D. L., Rose, D. M., Pearson, A., Ezekewitz, R. A. and Henson, P. M. (2000) *Nature,* **405,** 85-90.

Fadok, V. A., Savill, J. S., Haslett, C., Bratton, D. L., Doherty, D. E., Campbell, P. A. and Henson, P. M. (1992a) *J Immunol,* **149,** 4029-35.

Fadok, V. A., Voelker, D. R., Campbell, P. A., Bratton, D. L., Cohen, J. J., Noble, P. W., Riches, D. W. and Henson, P. M. (1993) *Chest,* **103,** 102S.

Fadok, V. A., Voelker, D. R., Campbell, P. A., Cohen, J. J., Bratton, D. L. and Henson, P. M. (1992b) *J Immunol,* **148,** 2207-16.

Faull, R. J. (2000) *Semin Dial,* **13,** 47-53.

Florey, H., Walker, J. and Carleton, H. (1926) *J Path Bacteriol,* 97-106.

Fratazzi, C., Manjunath, N., Arbeit, R. D., Carini, C., Gerken, T. A., Ardman, B., Remold-O'Donnell, E. and Remold, H. G. (2000) *J Exp Med,* **192,** 183-92.

Fukatsu, K., Saito, H., Han, I., Yasuhara, H., Lin, M. T., Inoue, T., Furukawa, S., Inaba, T., Hashiguchi, Y., Matsuda, T. and Muto, T. (1996) *J Am Coll Surg,* **183,** 450-6.

Garin, J., Diez, R., Kieffer, S., Dermine, J. F., Duclos, S., Gagnon, E., Sadoul, R., Rondeau, C. and Desjardins, M. (2001) *J Cell Biol,* **152,** 165-80.

Gillissen, G. and Bubenzer, B. (1970) *Experientia,* **26,** 781-2.

Goldsmith, H., S., Surgical Rehabilitation, F. and National Organization of, D. (1990) Springer.

Goldsmith, H. S. (2004) *Neurol Res,* **26,** 586-93.

Gorski, A., Wasik, M., Nowaczyk, M. and Korczak-Kowalska, G. (1991) *Faseb J,* **5,** 2287-91.

Gregory, C. D. and Devitt, A. (1999) *Apoptosis,* **4,** 11-20.

Gregory, C. D., Devitt, A. and Moffatt, O. (1998) *Biochem Soc Trans,* **26,** 644-9.

Hanayama, R., Tanaka, M., Miwa, K., Shinohara, A., Iwamatsu, A. and Nagata, S. (2002) *Nature,* **417,** 182-7.

Hart, S. P., Dougherty, G. J., Haslett, C. and Dransfield, I. (1997) *J Immunol,* **159,** 919-25.

Haskill, S. and Becker, S. (1985) *Cell Immunol,* **90,** 179-89.

Haslett, C. (1999) *Am J Respir Crit Care Med,* **160,** S5-11.

Haslett, C., Lee, A., Savill, J. S., Meagher, L. and Whyte, M. K. (1991) *Chest,* **99,** 6S.

Haslett, C., Savill, J. S., Whyte, M. K., Stern, M., Dransfield, I. and Meagher, L. C. (1994) *Philos Trans R Soc Lond B Biol Sci,* **345,** 327-33.

Hau, T. and Simmons, R. L. (1978) *Ann Surg,* **187,** 294-8.

Haziot, A., Ferrero, E., Lin, X. Y., Stewart, C. L. and Goyert, S. M. (1995) *Prog Clin Biol Res,* **392,** 349-51.

Hengartner, M. O. (2000) *Nature,* **407,** 770-6.

Hewitson, K. S., McNeill, L. A., Riordan, M. V., Tian, Y. M., Bullock, A. N., Welford, R. W., Elkins, J. M., Oldham, N. J., Bhattacharya, S., Gleadle, J. M., Ratcliffe, P. J., Pugh, C. W. and Schofield, C. J. (2002) *J Biol Chem,* **277,** 26351-5.

Hirao, M., Onai, N., Hiroishi, K., Watkins, S. C., Matsushima, K., Robbins, P. D., Lotze, M. T. and Tahara, H. (2000) *Cancer Res,* **60,** 2209-17.

Hoffmann, P. R., deCathelineau, A. M., Ogden, C. A., Leverrier, Y., Bratton, D. L., Daleke, D. L., Ridley, A. J., Fadok, V. A. and Henson, P. M. (2001) *J Cell Biol,* **155,** 649-59.

Hong, J. R., Lin, G. H., Lin, C. J., Wang, W. P., Lee, C. C., Lin, T. L. and Wu, J. L. (2004) *Development,* **131,** 5417-27.

Horvitz, H. R. (2003) *Chembiochem,* **4,** 697-711.

Huang, F. P., Platt, N., Wykes, M., Major, J. R., Powell, T. J., Jenkins, C. D. and MacPherson, G. G. (2000) *J Exp Med,* **191,** 435-44.

Huynh, M. L., Fadok, V. A. and Henson, P. M. (2002) *J Clin Invest,* **109,** 41-50.

Iger, Y., Lock, R. A., van der Meij, J. C. and Wendelaar Bonga, S. E. (1994) *Arch Environ Contam Toxicol,* **26,** 342-50.

Jacobs, D. M. and Morrison, D. C. (1977) *J Immunol,* **118,** 21-7.

Jandl James, H. (1996) *Blood : textbook of hematology,* Little, Brown, London.

Janeway, C., A. (2001a) *Chapter 1 : Basic Concepts in Immunology in Immunobiology 5 : the immune system in health and disease,* Garland ; Edinburgh : Churchill Livingstone, New York.

Janeway, C., A. (2001b) *Chapter 2 : Innate Immunity in Immunobiology 5 : the immune system in health and disease,* Garland ; Edinburgh : Churchill Livingstone, New York.

Janeway, C., A. (2001c) *Immunobiology 5 : the immune system in health and disease,* Garland ; Edinburgh : Churchill Livingstone, New York.

Johnson, R. J. and Feehally, J. (2003) Mosby, Edinburgh, pp. xvii, 1229.

Jokay, I. and Karczag, E. (1973) *Experientia,* **29,** 334-5.

Kasaian, M. T. and Casali, P. (1993) *Autoimmunity,* **15,** 315-29.

Kawasaki, K., Akashi, S., Shimazu, R., Yoshida, T., Miyake, K. and Nishijima, M. (2000) *J Biol Chem,* **275,** 2251-4.

Kerr, J. F., Harmon, B. and Searle, J. (1974) *J Cell Sci,* **14,** 571-85.

Kerr, J. F., Wyllie, A. H. and Currie, A. R. (1972) *Br J Cancer,* **26,** 239-57.

Kim, S. J., Gershov, D., Ma, X., Brot, N. and Elkon, K. B. (2002) *J Exp Med,* **196,** 655-65.

Kinoshita, G., Purcell, A. W., Keech, C. L., Farris, A. D., McCluskey, J. and Gordon, T. P. (1999) *Clin Exp Immunol,* **115,** 268-74.

Kirkham, P. A., Spooner, G., Rahman, I. and Rossi, A. G. (2004) *Biochem Biophys Res Commun,* **318,** 32-7.

Kishimoto, T., Kikutani, H., Vom dem Borne, A. E. G. K., Goyert, S., Mason, D., Miyasaka, M., Moretta, L., Okumura, K., Shaw, S., Springer, S., Sugarmura, T. and Zola, H. (1997) *Leukocyte Typing VI,* Garland Publishing Inc., New York and London.

Koenen, H. J., Smit, M. J., Simmelink, M. M., Schuurman, B., Beelen, R. H. and Meijer, S. (1996) *Cancer Immunol Immunother,* **42,** 310-6.

Konturek, S. J., Brzozowski, T., Majka, I., Pawlik, W. and Stachura, J. (1994) *Dig Dis Sci,* **39,** 1064-71.

Koopman, G., Reutelingsperger, C. P., Kuijten, G. A., Keehnen, R. M., Pals, S. T. and van Oers, M. H. (1994) *Blood,* **84,** 1415-20.

Korb, L. C. and Ahearn, J. M. (1997) *J Immunol,* **158,** 4525-8.

Krahling, S., Callahan, M. K., Williamson, P. and Schlegel, R. A. (1999) *Cell Death Differ,* **6,** 183-9.

Krist, L. F., Eestermans, I. L., Steenbergen, J. J., Hoefsmit, E. C., Cuesta, M. A., Meyer, S. and Beelen, R. H. (1995) *Anat Rec,* **241,** 163-74.

Krist, L. F., Koenen, H., Calame, W., van der Harten, J. J., van der Linden, J. C., Eestermans, I. L., Meyer, S. and Beelen, R. H. (1997) *Anat Rec,* **249,** 399-404.

Kunisaki, Y., Masuko, S., Noda, M., Inayoshi, A., Sanui, T., Harada, M., Sasazuki, T. and Fukui, Y. (2004) *Blood,* **103,** 3362-4.

Lan, H. Y., Mitsuhashi, H., Ng, Y. Y., Nikolic-Paterson, D. J., Yang, N., Mu, W. and Atkins, R. C. (1997) *Am J Pathol,* **151,** 531-8.

Lauber, K., Bohn, E., Krober, S. M., Xiao, Y. J., Blumenthal, S. G., Lindemann, R. K., Marini, P., Wiedig, C., Zobywalski, A., Baksh, S., Xu, Y., Autenrieth, I. B., Schulze-Osthoff, K., Belka, C., Stuhler, G. and Wesselborg, S. (2003) *Cell,* **113,** 717-30.

Leak, L. V. (1983) *Lab Invest,* **48,** 479-91.

Lemaitre, B., Nicolas, E., Michaut, L., Reichhart, J. M. and Hoffmann, J. A. (1996) *Cell,* **86,** 973-83.

Lenzi, H. L., Oliveira, D. N., Pelajo-Machado, M., Borojevic, R. and Lenzi, J. A. (1996) *Braz J Med Biol Res,* **29,** 19-24.

Letterio, J. J. and Roberts, A. B. (1998) *Annu Rev Immunol,* **16,** 137-61.

Little, M. A., Pusey, C. D. and Nourshargh, S. (2005) *Clin Nephrol,* **64,** 465-70.

Loghmani, F., Mohammed, K. A., Nasreen, N., Van Horn, R. D., Hardwick, J. A., Sanders, K. L. and Antony, V. B. (2002) *Inflammation,* **26,** 73-82.

Lucas, M., Stuart, L. M., Savill, J. and Lacy-Hulbert, A. (2003) *J Immunol,* **171,** 2610-5.

Ma, L., Chan, K. W., Trendell-Smith, N. J., Wu, A., Tian, L., Lam, A. C., Chan, A. K., Lo, C. K., Chik, S., Ko, K. H., To, C. K., Kam, S. K., Li, X. S., Yang, C. H., Leung, S. Y., Ng, M. H., Stott, D. I., MacPherson, G. G. and Huang, F. P. (2005) *Eur J Immunol,* **35,** 3364-75.

Mandache, E., Moldoveanu, E. and Savi, G. (1985) *Morphol Embryol (Bucur),* **31,** 137-42.

Maruyama, K., Ii, M., Cursiefen, C., Jackson, D. G., Keino, H., Tomita, M., Van Rooijen, N., Takenaka, H., D'Amore, P. A., Stein-Streilein, J., Losordo, D. W. and Streilein, J. W. (2005) *J Clin Invest,* **115,** 2363-72.

Matsushima, Y. and Baba, T. (1990) *J Exp Pathol,* **5,** 39-48.

McCutcheon, J. C., Hart, S. P., Canning, M., Ross, K., Humphries, M. J. and Dransfield, I. (1998) *J Leukoc Biol,* **64,** 600-7.

Medzhitov, R., Preston-Hurlburt, P. and Janeway, C. A., Jr. (1997) *Nature,* **388,** 394-7.

Melnicoff, M. J., Horan, P. K., Breslin, E. W. and Morahan, P. S. (1988a) *J Leukoc Biol,* **44,** 367-75.

Melnicoff, M. J., Horan, P. K. and Morahan, P. S. (1989) *Cell Immunol,* **118,** 178-91.

Melnicoff, M. J., Morahan, P. S., Jensen, B. D., Breslin, E. W. and Horan, P. K. (1988b) *J Leukoc Biol,* **43,** 387-97.

Mevorach, D., Mascarenhas, J. O., Gershov, D. and Elkon, K. B. (1998) *J Exp Med,* **188,** 2313-20.

Mironov, V. A., Gusev, S. A. and Baradi, A. F. (1979) *Cell Tissue Res,* **201,** 327-30.

Miura, M., Zhu, H., Rotello, R., Hartwieg, E. A. and Yuan, J. (1993) *Cell,* **75,** 653-60.

Moffat, C. F., McLean, M. W., Long, W. F. and Williamson, F. B. (1991) *Eur J Biochem,* **197,** 449-59.

Moffatt, O. D., Devitt, A., Bell, E. D., Simmons, D. L. and Gregory, C. D. (1999) *J Immunol,* **162,** 6800-10.

Muntean, V. E. (1987) *Ann Surg,* **206,** 681-2.

Mutsaers, S. E. and Wilkosz, S. (2007) *Cancer Treat Res,* **134,** 1-19.

Nadig, C., Binswanger, U. and von Felten, A. (1997) *Perit Dial Int,* **17,** 493-6.

Nelson, D. S. (1963) *Lancet,* **2,** 175-6.

Nelson, D. S. and Boyden, S. V. (1963) *Immunology,* **6,** 264-75.

Nelson, R. M., Venot, A., Bevilacqua, M. P., Linhardt, R. J. and Stamenkovic, I. (1995) *Annu Rev Cell Dev Biol,* **11,** 601-31.

Newton, J. P., Buckley, C. D., Jones, E. Y. and Simmons, D. L. (1997) *J Biol Chem,* **272,** 20555-63.

Nicholson, J. K., Stein, D., Mui, T., Mack, R., Hubbard, M. and Denny, T. (1997) *Clin Diagn Lab Immunol,* **4,** 309-13.

Ochiya, T., Baba, T., Mizushima, A., Onozaki, K. and Yaoita, H. (1982) *Cell Immunol,* **71,** 346-52.

Ochiya, T., Baba, T., Onozaki, K., Yaoita, H., Uyeno, K. and Hashimoto, T. (1983) *Cell Immunol,* **81,** 134-43.

Ogden, C. A., deCathelineau, A., Hoffmann, P. R., Bratton, D., Ghebrehiwet, B., Fadok, V. A. and Henson, P. M. (2001) *J Exp Med,* **194,** 781-95.

Oka, K., Sawamura, T., Kikuta, K., Itokawa, S., Kume, N., Kita, T. and Masaki, T. (1998) *Proc Natl Acad Sci U S A,* **95,** 9535-40.

Paik, Y. H., Schwabe, R. F., Bataller, R., Russo, M. P., Jobin, C. and Brenner, D. A. (2003) *Hepatology,* **37,** 1043-55.

Pereira Ade, D., Aguas, A. P., Oliveira, M. J., Cabral, J. M. and Grande, N. R. (1994) *J Anat,* **185 (Pt 3),** 471-9.

Petry, F., McClive, P. J., Botto, M., Morley, B. J., Morahan, G. and Loos, M. (1996) *Immunogenetics,* **43,** 370-6.

Pinho Mde, F., Hurtado, S. P., El-Cheikh, M. C., Rossi, M. I., Dutra, H. S. and Borojevic, R. (2002) *Cell Tissue Res,* **308,** 87-96.

Platt, N., Suzuki, H., Kodama, T. and Gordon, S. (2000) *J Immunol,* **164,** 4861-7.

Platt, N., Suzuki, H., Kurihara, Y., Kodama, T. and Gordon, S. (1996) *Proc Natl Acad Sci U S A,* **93,** 12456-60.

Poltorak, A., Smirnova, I., He, X., Liu, M. Y., Van Huffel, C., McNally, O., Birdwell, D., Alejos, E., Silva, M., Du, X., Thompson, P., Chan, E. K., Ledesma, J., Roe, B., Clifton, S., Vogel, S. N. and Beutler, B. (1998) *Blood Cells Mol Dis,* **24,** 340-55.

Pozzi, L. A., Maciaszek, J. W. and Rock, K. L. (2005) *J Immunol,* **175,** 2071-81.

Reddien, P. W. and Horvitz, H. R. (2000) *Nat Cell Biol,* **2,** 131-6.

Reedquist, K. A., Ross, E., Koop, E. A., Wolthuis, R. M., Zwartkruis, F. J., van Kooyk, Y., Salmon, M., Buckley, C. D. and Bos, J. L. (2000) *J Cell Biol,* **148,** 1151-8.

Renwick, L. C., Brown, D., Clouter, A. and Donaldson, K. (2004) *Occup Environ Med,* **61,** 442-7.

Robson, M. G., Cook, H. T., Botto, M., Taylor, P. R., Busso, N., Salvi, R., Pusey, C. D., Walport, M. J. and Davies, K. A. (2001) *J Immunol,* **166,** 6820-8.

Rosen, A. and Casciola-Rosen, L. (1999) *Cell Death Differ,* **6,** 6-12.

Rothenberg, R. and Rosenblatt, P. (1942) *Arch Surg,* 418-421.

Rovere, P., Manfredi, A. A., Vallinoto, C., Zimmermann, V. S., Fascio, U., Balestrieri, G., Ricciardi-Castagnoli, P., Rugarli, C., Tincani, A. and Sabbadini, M. G. (1998) *J Autoimmun,* **11,** 403-11.

Savill, J. (1992) *Clin Sci (Lond),* **83,** 649-55.

Savill, J., Dransfield, I., Hogg, N. and Haslett, C. (1990) *Nature,* **343,** 170-3.

Savill, J. and Fadok, V. (2000) *Nature,* **407,** 784-8.

Savill, J., Hogg, N., Ren, Y. and Haslett, C. (1992) *J Clin Invest,* **90,** 1513-22.

Schaub, F. J., Han, D. K., Liles, W. C., Adams, L. D., Coats, S. A., Ramachandran, R. K., Seifert, R. A., Schwartz, S. M. and Bowen-Pope, D. F. (2000) *Nat Med,* **6,** 790-6.

Schimke, R., Bernstein, B. and Ambrosius, H. (1977) *Allerg Immunol (Leipz),* **23,** 34-42.

Scott, R. S., McMahon, E. J., Pop, S. M., Reap, E. A., Caricchio, R., Cohen, P. L., Earp, H. S. and Matsushima, G. K. (2001) *Nature,* **411,** 207-11.

Shannon, B. T. and Love, S. H. (1980) *Immunol Commun,* **9,** 735-46.

Shannon, B. T., Love, S. H. and Myrvik, Q. N. (1980) *Immunol Commun,* **9,** 357-70.

Shapiro, S. D. (1999) *Thromb Haemost,* **82,** 846-9.

Shimotsuma, M., Shields, J. W., Simpson-Morgan, M. W., Sakuyama, A., Shirasu, M., Hagiwara, A. and Takahashi, T. (1993) *Lymphology,* **26,** 90-101.

Shrager, J. B., Wain, J. C., Wright, C. D., Donahue, D. M., Vlahakes, G. J., Moncure, A. C., Grillo, H. C. and Mathisen, D. J. (2003) *J Thorac Cardiovasc Surg,* **125,** 526-32.

Sigrist, S., Mechine-Neuville, A., Mandes, K., Calenda, V., Legeay, G., Bellocq, J. P., Pinget, M. and Kessler, L. (2003) *J Vasc Res,* **40,** 359-67.

Sipka, S., Boldogh, I. and Szilagyi, T. (1977) *Acta Allergol,* **32,** 3-7.

Sonozaki, H. and Cohen, S. (1971) *J Immunol,* **106,** 1404-6.

Stuart, L. M., Lucas, M., Simpson, C., Lamb, J., Savill, J. and Lacy-Hulbert, A. (2002) *J Immunol,* **168,** 1627-35.

Sultan, A. M., Dunn, C. J., Mimms, P. C., Giroud, J. P. and Willoughby, D. A. (1978) *J Pathol,* **126,** 221-30.

Surh, C. D. and Sprent, J. (1994) *Nature,* **372,** 100-3.

Taguchi, T., Mitcham, J. L., Dower, S. K., Sims, J. E. and Testa, J. R. (1996) *Genomics,* **32,** 486-8.

Taylor, P. R., Carugati, A., Fadok, V. A., Cook, H. T., Andrews, M., Carroll, M. C., Savill, J. S., Henson, P. M., Botto, M. and Walport, M. J. (2000) *J Exp Med,* **192,** 359-66.

Tomazic, V., Bigazzi, P. E. and Rose, N. R. (1977) *Immunol Commun,* **6,** 49-62.

Topley, N. (1995) *Perit Dial Int,* **15,** 116-7.

Topley, N., Jorres, A., Luttmann, W., Petersen, M. M., Lang, M. J., Thierauch, K. H., Muller, C., Coles, G. A., Davies, M. and Williams, J. D. (1993) *Kidney Int,* **43,** 226-33.

Truman, L. A., Ogden, C. A., Howie, S. E. and Gregory, C. D. (2004) *Immunobiology,* **209,** 21-30.

Ullet, G. and Adderson, E. (2003) *Abstr Intersci Conf Antimicrob Agents Chemother Intersci Conf Antimicrob Agents Chemother.,* **43,** B-1049.

Vaananen, H. K., Zhao, H., Mulari, M. and Halleen, J. M. (2000) *J Cell Sci,* **113 (Pt 3),** 377-81.

van den Eijnde, S. M., Boshart, L., Baehrecke, E. H., De Zeeuw, C. I., Reutelingsperger, C. P. and Vermeij-Keers, C. (1998) *Apoptosis,* **3,** 9-16.

Voll, R. E., Herrmann, M., Roth, E. A., Stach, C., Kalden, J. R. and Girkontaite, I. (1997) *Nature,* **390,** 350-1.

von Recklinghausen, F. (1863) *Virchows Arch Pathol Anat,* 157-166.

Wang, X., Wu, Y. C., Fadok, V. A., Lee, M. C., Gengyo-Ando, K., Cheng, L. C., Ledwich, D., Hsu, P. K., Chen, J. Y., Chou, B. K., Henson, P., Mitani, S. and Xue, D. (2003) *Science,* **302,** 1563-6.

Whyte, M. K., Meagher, L. C., MacDermot, J. and Haslett, C. (1993) *J Immunol,* **150,** 5124-34.

Williams, R. J., Robertson, D. and Davies, A. J. (1989) *Histochem J,* **21,** 271-8.

Witowski, J., Thiel, A., Dechend, R., Dunkel, K., Fouquet, N., Bender, T. O., Langrehr, J. M., Gahl, G. M., Frei, U. and Jorres, A. (2001) *Am J Pathol,* **158,** 1441-50.

Wright, A. J. and Day, A. J. (2005) *Adv Exp Med Biol,* **564,** 57-69.

Wu, Y. C. and Horvitz, H. R. (1998a) *Cell,* **93,** 951-60.

Wu, Y. C. and Horvitz, H. R. (1998b) *Nature,* **392,** 501-4.

Wu, Y. C., Tsai, M. C., Cheng, L. C., Chou, C. J. and Weng, N. Y. (2001) *Dev Cell,* **1,** 491-502.

Wyllie, A. H. (1980) *Nature,* **284,** 555-6.

Yagnik, D. R., Hillyer, P., Marshall, D., Smythe, C. D., Krausz, T., Haskard, D. O. and Landis, R. C. (2000) *Arthritis Rheum,* **43,** 1779-89.

Yamada, T. (1997) *Tanpakushitsu Kakusan Koso,* **42,** 31-41.

Zabel, B. A., Allen, S. J., Kulig, P., Allen, J. A., Cichy, J., Handel, T. M. and Butcher, E. C. (2005a) *J Biol Chem,* **280,** 34661-6.

Zabel, B. A., Silverio, A. M. and Butcher, E. C. (2005b) *J Immunol,* **174,** 244-51.

Zakeri, Z. F. and Ahuja, H. S. (1994) *Biochem Cell Biol,* **72,** 603-13.

Zhang, Q. X., Magovern, C. J., Mack, C. A., Budenbender, K. T., Ko, W. and Rosengart, T. K. (1997) *J Surg Res,* **67,** 147-54.

Zhu, H., Naito, M., Umezu, H., Moriyama, H., Takatsuka, H., Takahashi, K. and Shultz, L. D. (1997) *J Leukoc Biol,* **61,** 436-44.